NASA Technical Memorandum 86476

Research and Technology

1984 Annual Report of the Marshall Space Flight Center

NOVEMBER 1984

NASA

NASA Technical Memorandum 86476

Research and Technology

1984 *Annual Report of the* *Marshall Space Flight Center*

Compiled by
Research and Technology Office

Edited by
Tauna W. Moorehead

George C. Marshall Space Flight Center
Marshall Space Flight Center, Alabama

TABLE OF CONTENTS

TABLE OF CONTENTS (concluded)

LIST OF ILLUSTRATIONS

ILLUSTRATIONS (continued)

ILLUSTRATIONS (continued)

ILLUSTRATIONS (concluded)

TECHNICAL MEMORANDUM

RESEARCH AND TECHNOLOGY,
1984 ANNUAL REPORT OF THE MARSHALL SPACE FLIGHT CENTER

INTRODUCTION

The product of a research and technology program is knowledge. The input to the program is the dedicated effort of highly qualified people, utilizing specialized equipment and facilities, doing theoretical, analytical, and experimental work.

This report describes the accomplishments of the Marshall Space Flight Center (MSFC) research and technology program for FY-84. The successful flight of OAST-1 and the repair of the Solar Maximum Mission satellite, enabling the acquisition of new information whose analysis is just beginning, highlight these accomplishments. There are others too numerous to mention here.

This report is presented in three sections--Advanced Studies, Research, and Technology--with the Advanced Studies section providing the background for the requirements under which the R&T programs are conducted.

The names, organizational symbols, and telephone numbers of the contributors to the report as well as publications generated during the reporting period are included at the end of the respective topics. The individuals identified herein welcome direct requests for additional information.

ADVANCED STUDIES

SPACE STATION

NASA spent 2.5 years initiating a careful definition process for a Space Station so that an informed decision could be made on whether or not the Space Station should be the next major step for the U.S. space program. In May 1982, the NASA Administrator established the NASA Space Station Task Force reporting to the NASA Associate Deputy Administrator. This activity was a NASA-wide effort involving all NASA Centers and Headquarters.

The primary activities were system and subsystem trade studies to assist the task force in defining an overall Space Station architecture that can be conceptualized as a cluster in space. The cluster includes both manned and unmanned elements. The manned base consists of habitat modules, logistics modules, resource subsystems providing electrical power and thermal functions, and laboratory modules in which to conduct experiments and other development activities. Airlocks will be provided for any required extravehicular activity (EVA), and docking ports will be provided on modules for receiving transportation elements, supplies, and inhabitants. The unmanned elements perform various functions in the infrastructure, such as science and Earth observations or materials processing. The manned and unmanned elements are complemented by other functions and capabilities, such as the ability to perform EVA and to deploy and retrieve free flyers with the use of an Orbital Maneuvering Vehicle (OMV). The Space Station may be used to support high-energy orbits, including geosynchronous placement and retrieval and planetary injection.

The Johnson Space Center was selected as the lead center for Space Station program development, and an activity was initiated to support the Request for Proposal (RFP) preparation, develop a reference configuration, and provide supporting data. This was a NASA-wide effort involving all NASA Centers and Headquarters. The reference configuration, called the Power Tower, is presented in Figure 1.

Early in 1984, MSFC was assigned the lead center role in the advanced development area of attitude control/stabilization, onboard propulsion, and space mechanisms. The center was later assigned the lead role for structures which was combined with the mechanisms activities. MSFC has a supporting role in advanced development for those disciplines where the lead is at another center. These areas include thermal control, environmental control and life support, electrical power, communications, data handling, and human productivity. These advanced development assignments include the focusing of the Office of Aeronautics and Space Technology (OAST) generic technology, developing test components, and developing and operating ground test beds and flight experiments.

Advanced development plans were developed in FY-84 to outline the component development and tests needed to bring the technology to a point where it could be selected by a Phase C/D contractor.
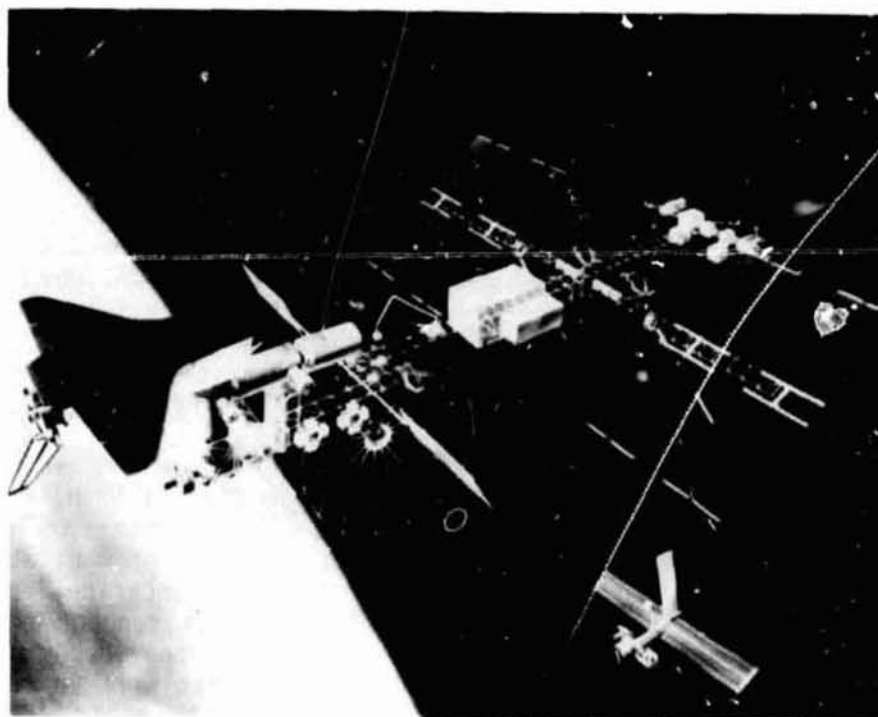
Figure 1. Space Station Concept.

MSFC developed plans for a guidance, navigation, and control (GN&C) test bed to demonstrate the adequacy of advanced technology hardware and software to perform GN&C functions and to promote reliability and long life for the Space Station.

Advanced development plans were developed for propulsion, including studies, analyses, design, fabrication, and test of propellant thermal conditioners; waste heat simulators; accumulators; gaseous hydrogen thrusters for advanced oxygen/hydrogen; and gaseous hydrogen propulsion systems applicable to the Space Station.

The advanced development activity for structures and mechanisms has been defined to include structures and environmental protection, materials, and prototype hardware including rotating joints, berthing systems, mobile manipulators, latches, damping techniques, and erectable and deployable beams.

Control Moment Gyroscope (CMG) life tests of bearing and slip rings were continued to support CMG design modification. The CMG spin bearing life test has now successfully completed 22,000 hours of testing, and the CMG slip ring life test successfully accumulated over 20,000 hours. Outgassing tests continue to indicate that the seals which were added to prevent excessive lubricant outgassing are fully effective. A math model for a CMG hybrid simulation system was used to simulate Space Station motion and inertial properties.

MSFC also continued advanced development activities in related areas. The Electrical Power System (EPS) testing was continued to determine the performance of high-voltage electrical power systems using programmable power processors and the operation and charge control of high-voltage NiCd batteries. Two 88-cell, 55-Ah batteries are being tested to investigate charge control techniques in an effort to achieve optimum performance under low-Earth orbit conditions and to investigate the effects of high-rate pulse discharge demands on the batteries. One battery has accumulated 10,780 orbital cycles and is presently being reconfigured for further testing, while the second battery has accumulated 10,200 cycles and is still undergoing testing. (C. Gregg/PM01/205-453-0541)

SPACE STATION TECHNOLOGY

This system analysis was focused on the definition of technology appropriate for the early Space Station. Rationale for technology selection included improvement in life cycle cost, performance, mass, volume, complexity, and growth potential. Specific areas of the Space Station selected for study, characterized broadly in Figure 2, were the data management, subsystem autonomous control, attitude control, and thermal management.

Figure 2. Space Station Technology.

In the data management area, system requirements, architecture, and software were addressed. Architecture analysis included preliminary definition of the network interface module, and software analysis centered on characteristics of the network operating system. For attitude control, a typical Space Station configuration was modeled with a candidate two-axis, double-gimbaled, parallel-mounted CMG system. Simulations using this model were conducted to determine the quality and extent of control provided.

Results were analyzed from these simulations and recommendations made as to appropriate methods of damping for system motions outside the control of the CMG's. Two-phase systems definition and options, bus characteristics, and control features were specific areas of analysis in thermal management. A comparison of single- and two-phase systems was also included. Ammonia and water were studied as working fluids. For the technology selected in each area of study, a plan for resolution was prepared which included test requirements, facility needs, schedules, costs, and manpower. Study results are provided in "Space Station Systems Technology," Vols. I-III, Boeing Aerospace Company Document No. D180-27935, February 1984. (R. Nixon/PD21/205-453-4165)

THE HUMAN ROLE IN SPACE

Appropriate roles for humans and automation and combinations of the two were examined. This contracted activity focused on the perspective of human roles in contrast with the perspective of automation. Manned space flight experiences were analyzed and compared with established human capabilities and limitations in the space environment. Contemporary and future manned missions were examined to provide typical tasks that are recurring in typical manned missions. Categories of human involvement for each task were established. The categories ranged from total human involvement to total automation. Viable combinations of human and automation involvement in each task were formulated, and relationships for performance, technological risk, and task implementation costs were established. Costs were based on support requirements for alternative ways of performing each task. Compensation was included for overlapping support requirements for groups of similar tasks. The findings are documented in an arrangement which permits rapid analysis of man/machine roles and are especially applicable to the preliminary design phase of projects when decision making is particularly difficult and involves far-reaching effects. Finally, requirements were identified for new technologies which enhance human capabilities. Also, specific guidelines and criteria regarding human roles for advanced missions were developed. This contract, which was funded jointly by the Office of Aeronautics and Space Technology and the Office of Space Flight, was performed by McDonnell Douglas Aerospace Corporation. (S. Hall/PD24/205-453-4196)

AFT CARGO CARRIER (ACC)

The ACC is being studied as a potential improvement to the Space Transportation System (STS). Its applications include large-diameter payloads for DOD, large Orbital Transfer Vehicles (OTV's), transport to Low-Earth Orbit (LEO) of Large-Diameter Reflector (LDR) subassemblies, propellant scavenging tanks for OTV/Space Station, and additional Payload Assist Module-deployed payloads at reduced user charge. The ACC can be used to augment the capability of the STS for carrying payloads to LEO and Geosynchronous Orbit (GEO) (Figure 3).

During FY-84, the 6.4-percent acoustic tests of the STS with ACC were completed. When data review is complete, these tests will determine the external acoustic and over-pressure environment in the vicinity of the ACC during the lift-off phase. Other tests were conducted of the acoustic

transmission of ACC test panels (approximately 5 by 7 feet) in a special test chamber which allowed the gas on each side of the panel to be varied as the acoustic levels and frequencies were varied. Results showed that when the inside of the ACC is purged with the helium at low pressures (<1 psig), acoustic levels reaching the payload are significantly reduced. The ACC acoustic environment can be made equal to that in the Orbiter payload bay. (J. E. Hughes/PS03/205-453-0162)
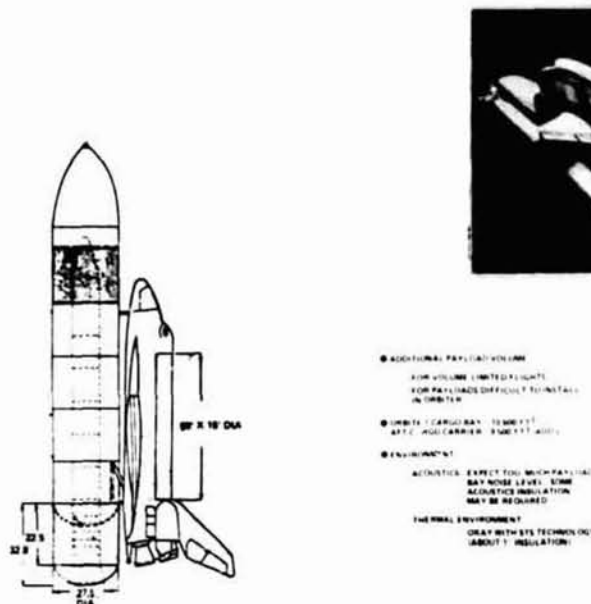
Figure 3. Aft Cargo Carrier (ACC).

PROPELLANT SCAVENGING

The results of a study to investigate the feasibility and requirements to scavenge propellant from the shuttle External Tank (ET) and feedlines at the completion of a shuttle mission will be included in final reports to be published in November 1984. The study estimated that approximately 2.5 million pounds of propellant will be available for scavenging over a 10-year period (1991-2000) based on the current mission model. The study considered a number of scavenging concepts; two concepts were selected for more detailed investigation: (1) propellant collected in tanks located in the Aft Cargo Carrier (ACC) and the tanks delivered from Low-Earth Orbit (LEO) to Space Station orbit via an Orbital Maneuvering Vehicle (OMV), and (2) propellant collected in tanks located in the ACC and delivered from LEO to Space Station orbit with an integral propulsion system. The systems will be designed to be returned to Earth via the shuttle cargo bay.

Technologies required to transfer cryogenic propellants from the ET into the transfer tanks and from the transfer tanks into the orbital holding/storage tank at the Space Station vicinity under zero gravity will

7

need to be developed. Gauging the amount of cryogenic propellant in a tank
in a zero-gravity environment is also a technology that requires develop-
ment.

Plans are to continue the evaluation of the selected scavenging
concepts/systems in 1985 to investigate scavenging tanks and other hardware
recycling techniques and interfaces and to enhance cost estimates. (M. A.
Page/PS03/205-453-0162)

GEOSTATIONARY PLATFORM

Past conceptual studies have indicated that a single shuttle-launched
experimental platform is needed in the early 1990's to enable operational
geostationary platforms. This platform would demonstrate an integrated
system of communications and platform technologies.

Current studies are evaluating the implications of the anticipated
availability of a Low-Earth Orbit (LEO) Space Station and of updated projec-
tions of Geosynchronous Orbit (GEO) Orbital Maneuvering Vehicles (OMV's) and
LEO-GEO transfer vehicles. Although these studies have just begun, an ex-
perimental geostationary platform, such as shown in Figure 4, might also
serve to demonstrate Space Station, OMV, and Orbital Transfer Vehicle (OTV)
capabilities. Future redefinition to incorporate these roles is antici-
pated.

Figure 4. Geostationary Platform.

Regardless of the final form the experimental geostationary platform
takes, the technologies that would be demonstrated by such a platform in-
clude deployable structures and structural mechanisms; active stabilization
of large space structures; a high efficiency ac power system; LEO-to-GEO

8

transfer of deployed structures; automated unmanned servicing at GEO; platform intermodule docking; an integrated attitude control system for docked platform modules; multibeam antennas; scanning beam antennas; accurate beam pointing; interplatform links; onboard communication switching and processing; a platform communications controller/processor; link performance enhancement techniques; effective isotropic radiated high power and small Earth station antennas; dual polarization Ka-band; and use of high-power, long-life, traveling-wave tube amplifiers.   (R. Durrett/PS04/205-453-2792)

Publication:

Ramler, J., and R. Durrett, "NASA's Geostationary Communications Platform Program," Paper No. AIAA-84-0702 in Proceedings of the 10th AIAA Communications Satellite Systems Conference (Orlando, Florida, March 19-22, 1984; AIAA: New York, 1984, pp. 613-623).

STRUCTURAL ASSEMBLY DEMONSTRATION EXPERIMENT (SADE)

SADE is a proposed 1987 shuttle flight experiment that will demonstrate that relatively complex structural systems can be built in space.   Two ground tests series were completed in MSFC's Neutral Buoyancy Simulator in 1984.   The SADE structure was assembled in almost its full flight configuration, permitting a functional evaluation of all basic hardware elements; i.e., connectors, latches, moving structural members, etc.   All assembly procedures were verified, and a preliminary assessment of flight-realistic timelines was obtained.   The assembly time varied from about 50 minutes for the first run to about 25 minutes for the seventh run.   The corresponding disassembly time range was 20 to 40 minutes.   A quick-look test report was published by the Massachusetts Institute of Technology in August 1984. Figure 5 depicts the SADE concept.   (J. Harrison/PS04/205-453-2795)

Figure 5.   Structural Assembly Demonstration Experiment (SADE).

SOLAR ARRAY FLIGHT EXPERIMENT VOLT II

The proposed VOLT II flight experiment will refly the solar array equipment (with some modifications/additions) from the OAST-1 experiment. The OAST-1 flight primarily evaluated the dynamics/mechanics of the large lightweight solar array and deployment boom operation, while the proposed VOLT II experiment will add additional active solar electric panels (to self-generate voltages above 400 Vdc) and diagnostic instrumentation so that the interactions of the Earth's plasma with a large, high-voltage (>100 Vdc) solar array can be fully evaluated in operational system configurations. Solar array design considerations currently limit operational voltages (and thus effectively spacecraft distribution voltages) to below $\sim$100 Vdc due to potential insulation breakdown/current leakage resulting from interactions with the Earth's plasma. The size of the array is increased, and the weight of conductor wire is also increased in the array and in the Spacecraft Distribution System due to lower operating voltages.

The proposed VOLT II experiment offers unique potential opportunities for low cost by using previously flown and available equipment (with modifications for plasma instrumentation and additional active solar collectors), and protoflight system configurations. Plans for potential involvement of the science community in the proposed flight experiment have been defined and coordinated with NASA Headquarters. (R. L. Middleton/PS04/205-453-2792)

Publication:

Carruth, M. R., and C. K. Purvis, "Space Test Program of High Voltage Solar Array/Space Plasma Interactions," USAF Spacecraft Interactions Technology Conference, Air Force Academy, Colorado, October 4, 1983.

DEPLOYABLE ANTENNA FLIGHT EXPERIMENT

Flight test definition/planning was continued in FY-84 together with initiation of test hardware designs for aperture deployment/retraction ground tests. These follow-on activities augment the parallel system definition studies during FY-80 through FY-83 on a 50-meter antenna (Orbiter-attached) flight test. Candidate configurations analyzed for flight testing are depicted in Figure 6. The baseline 50-meter antenna test program addresses prevailing needs for large space sensor capabilities on future applications of microwave radiometry, multibeam communications, spaceborne radar, and radio astronomy. The flight test article is configured as a reusable test bed which utilizes a lightweight precision structure for large, phased-array apertures as well as parabolic reflector apertures. This structure systems test will validate the integrated performance of several component technology thrusts undergoing development and test by NASA and DOD (precision structural joints, lens/array membrane, large deployable mast, large mesh apertures, antenna feed systems, etc.). Developed flight hardware, such as the flight support system developed for the Multimission Modular Spacecraft (MMS), is used for structural integration with the Orbiter.

Current program activities are focused on development of smaller test article designs for structural ground test which can also be utilized for subsequent flight tests. Test article designs initiated in FY-84 are based

on radiating membrane configurations developed during recent Defense Advanced Research Projects Agency (DARPA)/USAF technology programs. The structural deployment/retraction validation tests are being pursued as a cooperative NASA/DOD test program to support large spaceborne radar sensors and other applications. (W. Thompson/PS04/205-453-2792)
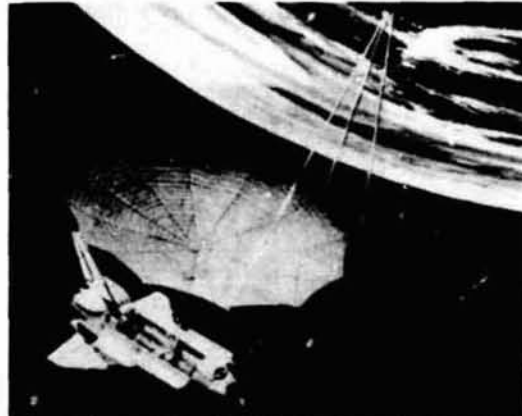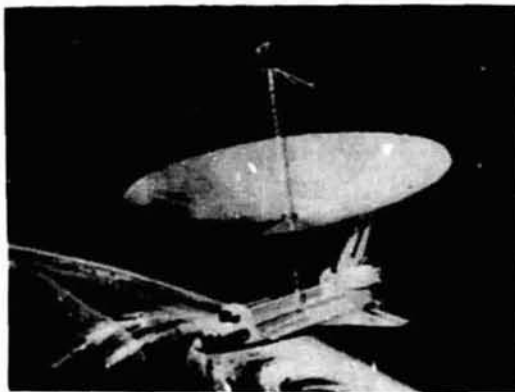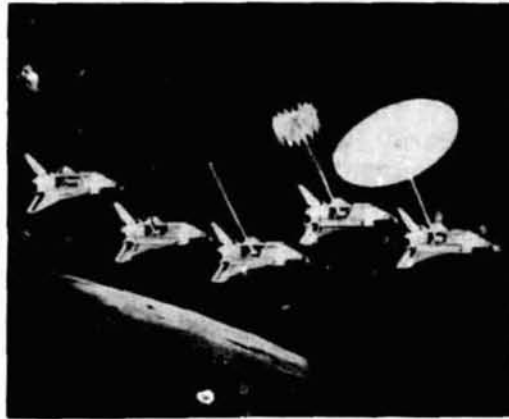
Figure 6. Deployable Antenna Flight Experiment.

ORBITAL MANEUVERING VEHICLE (OMV)

The space shuttle provides an efficient method of delivering and re-trieving spacecraft to and from low-Earth orbit. The efficiency of the shuttle can be enhanced by using a minispace tug called OMV which has been studied at MSFC for several years. The OMV will operate in orbits higher than the shuttle parking orbit and may also be used in geosynchronous orbits when delivered by high-energy upper stages such as the Transfer Orbit Stage (TOS), Centaur, and Orbital Transfer Vehicles (OTV's). This system is closely associated with the original Teleoperator Retrieval System (TRS), which was developed earlier to reboost/deboost the Skylab.

In-house and contracted conceptual (Phase A) studies were concluded in October 1983. These studies led to the conceptual definition of a highly efficient vehicle which can be used for a wide range of services. A representative configuration shown in Figure 7 depicts the use of the vehicle to support the delivery, retrieval, reboost, viewing, and servicing of free-flying satellites. In addition, the OMV vehicle will be available for assembly and buildup of the initial Space Station and will provide augmentation and enhancement to the Space Station. Many specific configurations are being studied, but the vehicle can generally be described as a relatively thin wafer, approximately 3 to 4 feet thick and approximately 15 feet in diameter. This configuration allows it to be directly mounted to the shuttle longerons and keel without the use of a cradle and thereby maximizes the shuttle payload manifesting flexibility. The OMV will be controlled initially from the ground and later from the Space Station when it becomes operational.

Many advanced missions are visualized beyond the missions shown in Figure 7. The OMV can support on-orbit refueling and servicing functions by the addition of mission kits consisting of refueling modules and manipulator/servicer systems capable of module exchange. In addition, specialized docking systems and/or end effectors will make it possible to collect debris and retrieve tumbling spacecraft.
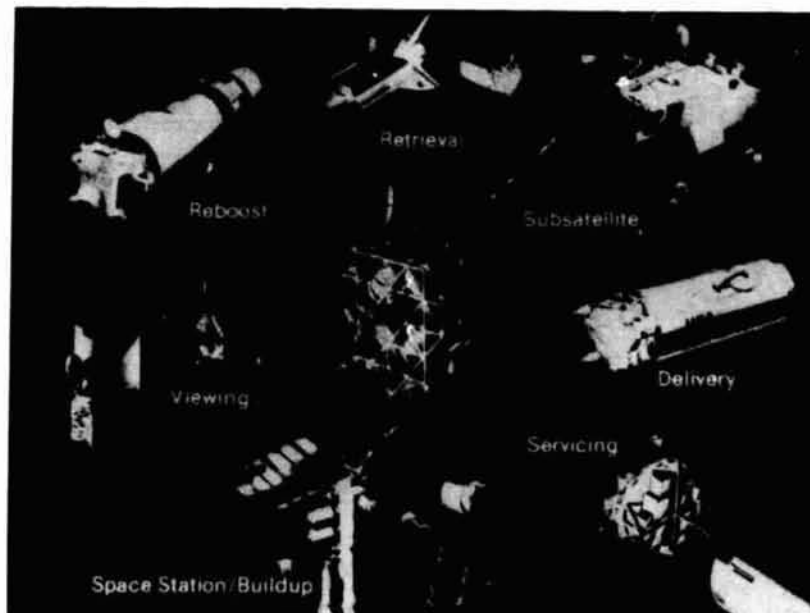
Figure 7. OMV Operational Missions.

The Request for Proposal (RFP) for OMV Phase B studies was released in January 1984. Contracts for three 12-month Phase B studies were awarded in August 1984 to Martin Marietta, LTV, and TRW. These activities are being supported by concentrated supporting development activities in the rendez-vous and docking simulation areas, including the design, testing, and evaluation of various docking interfaces and docking/rendezvous aids. Particular

emphasis is being placed on man/machine system controls and rendezvous and docking sensors. These activities utilize the simulation capabilities of the Docking Dynamic Simulator (six degrees of freedom), the OMV Flat Floor Simulator Facility, and the Target Motion Simulator, and are further supported by several industrial facilities. (W. Huber/PF14/205-453-5311)

ORBITAL TRANSFER VEHICLE (OTV)

Martin Marietta Aerospace Corporation and Boeing Aerospace Company were awarded contracts in July 1984 to perform parallel 15-month concept definition studies of Orbital Transfer Vehicles (OTV's). These studies are jointly funded by the Advanced Programs Office of the Office of Space Flight and the Space Station Program Office. The studies will investigate alternative OTV concepts and conduct program-level trade studies which will allow focusing the OTV program toward future development. The studies will also define potential Space Station accommodations, hardware elements, resources, and interfaces necessary to support a space-based OTV fleet. A representative space-based OTV concept is shown in Figure 8.
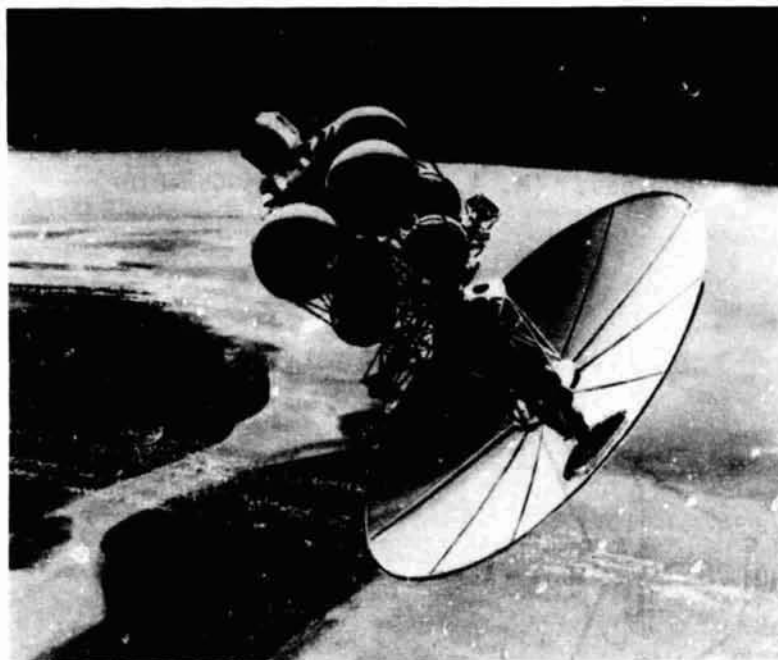
Figure 8. Orbital Transfer Vehicle.

A study completed by General Dynamics/Convair defines the test bed role of an early manned Space Station in the context of technology development and demonstration for space-based OTV servicing. This study resulted in an integrated OTV servicing technology development plan that addresses the requirements for ground analysis and testing, shuttle sortie missions, and Space Station technology development missions in several technology discipline areas and provides schedule and funding estimates.

13

Technology studies aimed at improving the performance of cryogenic stages have been underway for several years and involve advanced engine studies, cryogenic propellant management breadboard testing, and aero-assist system technology and flight experiment definition. A reference OTV mission model has been developed that covers fiscal years 1993 through 2010. (D. Saxton/PS03/205-453-0162)

ADVANCED TRANSPORTATION SYSTEMS

Studies of Shuttle-Derived Vehicles (SDV's) (Figure 9) continued to investigate means to utilize Shuttle components to configure unmanned vehicles that have increased payload weight and size capabilities. Emphasis has been on configurations that have capabilities to evolve to a Heavy Lift Launch Vehicle (HLLV). The two configurations with intermediate payload capability (80,000-160,000 pounds) are the side-mount concept with the Orbiter replaced with a cargo carrier and propulsion/avionics module; and the in-line concept with the Orbiter removed, the Space Shuttle Main Engine (SSME) placed under the External Tank (ET), and the payload placed above the ET. Each concept has been studied with expendable and reusable propulsion systems. A vehicle with expendable propulsion systems could be developed in approximately 4 years and serve as a complementary cargo vehicle to the shuttle. This vehicle could evolve to a vehicle with the reusable propulsion system which would be more economical.

Studies have also been performed to configure an HLLV with a payload range of 200,000 to 500,000 pounds. These concepts evolved from the SDV and employed liquid boosters with hydrocarbon booster engines and third stages with lox/hydrogen engines. (M. A. Page/PS03/205-453-0162)
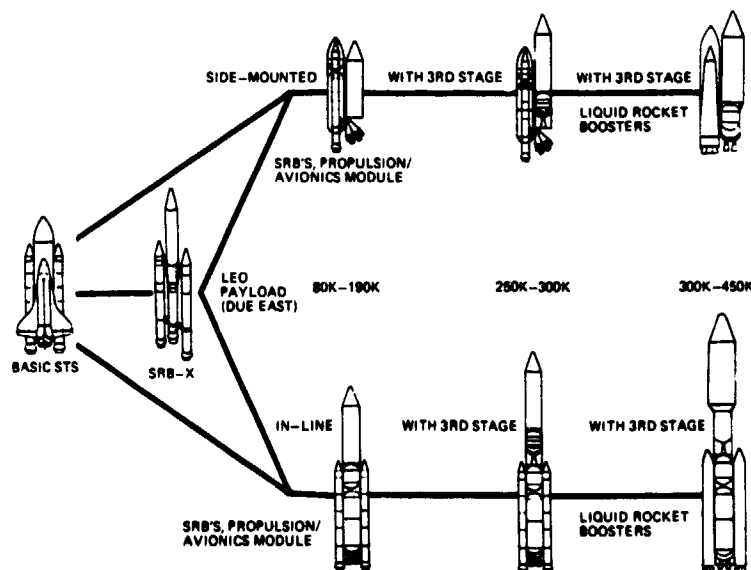
Figure 9. Shuttle-Derived Vehicles.

TETHER APPLICATIONS IN SPACE

Research and development efforts over the past several years have re-sulted in the implementation of a tethered satellite system to investigate electrodynamic power and force generation, as well as upper atmospheric phenomena.

As an outgrowth of investigations of tethers in space, a large number and variety of other tether applications are under study. Among them are tethered momentum transfers between the Orbiter and various payloads, tethered platforms and constellations, power and thrust generation through electrodynamic tethers, and propellant storage and transfer by tethered fuel depots under fractional gravity (Figure 10). Efforts are underway to deter-mine tether applications to the Space Station. A study on the impact of tether operations to the Space Station was concluded and submitted to the Space Station Task Group.
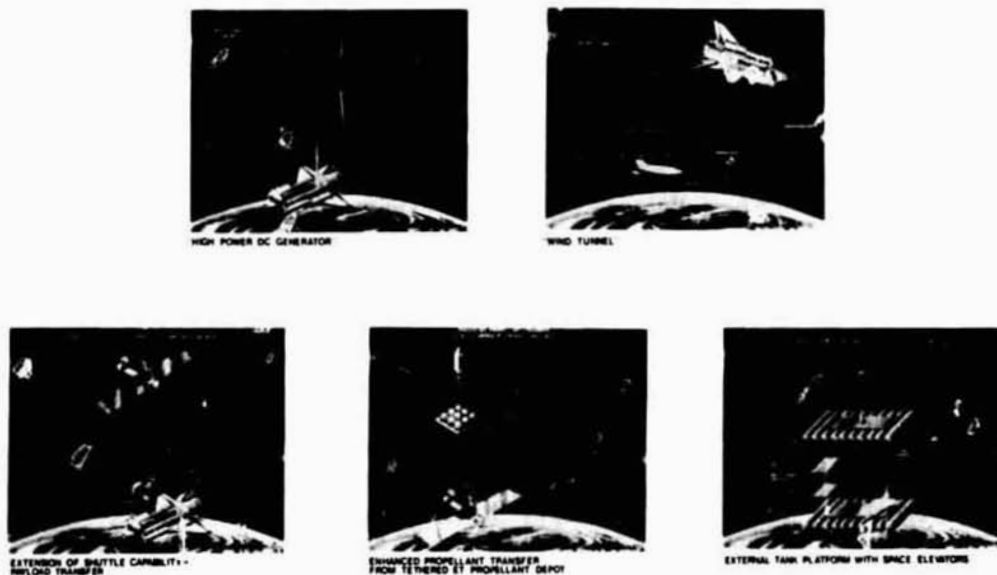
Figure 10. Tether Applications in Space.

The overall program planning for FY-85 and later years has been per-formed by a NASA Tether Applications in Space Task Group chaired by MSFC, and is continuing on an annual basis. Various promising concepts are under study by the Smithsonian Institution, Martin Marietta Aerospace Corporation, McDonnell Douglas Aerospace Corporation, and other organizations.

Major efforts are planned in tether applications to spacecraft deployment and unpowered reentry, to tethered constellations of spacecraft or payloads, and to electrodynamic power generation through tethers.

Although tether application investigations are a relatively new development, they indicate great promise in their potential to enhance mission economics in power generation, orbit change of spacecraft, and improved spacecraft serviceability by cluster formation. (G. von Tiesenhausen/PS01/205-453-2789)

Publications:

von Tiesenhausen, G., "Tethers in Space--Birth and Growth of a New Avenue to Space Utilization," NASA TM-82571, Marshall Space Flight Center, Alabama, 1984.

NASA Tether in Space Working Group (G. von Tiesenhausen, Chairman), "Tether Applications in Space, a 4-Year Program Plan, 1984-1987," Marshall Space Flight Center, Alabama, 1984.

GRAVITY PROBE-B (GP-B)

Stanford University and MSFC have for a number of years been developing experimental techniques aimed at detecting the gravitomagnetic field predicted by Einstein's General Theory of Relativity. This new test of the theory involves measuring the precession of an orbiting gyroscope as caused by the predicted gravitomagnetic field. Since this precession is only on the order of 0.05 arc second per year, the task of measuring it is indeed formidable. At the time this test was conceived, several areas of technology were required that were beyond the state-of-the-art. However, in June 1980, a review committee of specialists selected by NASA stated that the present technology was now ready for flight development, and the Gravitational Physics Committee of the Space Science Board identified it as the number one priority program in gravitational research. MSFC and Stanford University completed a comprehensive Phase B study on the GP-B observatory in November 1982. The design configuration and programmatic planning resulting from this study subsequently have been restructured to reduce the overall cost (see Figure 11). The National Academy of Sciences has given this restructured program a strong endorsement (December 1983) and has urged its near-term development for flight. In late 1983, several Nobel laureates wrote the NASA Administrator declaring the scientific importance of the GP-B mission and urging its support and implementation by NASA. In March 1984, a plan for the development of GP-B was presented to the NASA Administrator, and he agreed with the proposed development approach. Because GP-B requires that a number of high technology components be integrated into a functioning instrument/spacecraft system, the planned implementation approach includes an engineering development phase in which the integration and test of many of these technologies will be demonstrated on the ground and in a shuttle flight before initiating development of the actual science mission. The

present schedule and planning are for the engineering development phase to begin in FY-85 with a shuttle test flight in FY-89. The start of the science mission could begin as early as FY-88 and will be based on results of the overall program status and ground testing.

Advanced development efforts are continuing at Stanford and MSFC. A new suspension system for levitating the gyro rotor was tested and has apparently solved the problem of resonance pumping of energy into the rotor that resulted in considerable rotor damage. This advance, coupled with progress in rotor polishing and deposition of a thin niobium film of uniform thickness on the rotor, has resulted in the levitation and spin-up of a flight-quality rotor for the first time.

A three-axis, scanning Superconducting Quantum Interference Device (SQUID) magnetometer capable of mapping field regions of 10^{-8} gauss was developed and tested. In addition to obtaining a more detailed and accurate mapping of the on-axis magnetic field within the low field region, it also allows off-axis measurements to be accomplished, resulting in a complete topological map of the magnetic field. A facility consisting of a Wayne-George tilting/rotating table on which a slosh-proof liquid helium dewar can be mounted for testing a single gyro has been designed, fabricated, and partially assembled. This facility will allow very accurate drift tests of a single gyro to be accommodated.

An apparatus for measuring the electrical breakdown voltage of niobium-sputtered samples was designed, built, and tested. Samples produced by various sputtering techniques have been evaluated using this test device. Surfaces prepared by ion milling resulted in samples with the highest breakdown voltages, and burn-in of the surface also raised the breakdown voltage.

An analytical method of assessing the gyro torques due to surface topography, variations in coating thickness, and inhomogeneities was developed. This technique will allow more rapid turnaround on and insights into assessing the impact of tradeoffs among the various rotor parameters.
(A. Neighbors/PF16/205-453-5585)

Publications:

Cheng, J.-H., "Helium Thruster Propulsion System for Precise Attitude Control and Drag Compensation of Gravity Probe-B Satellite," Ph.D. Thesis, Stanford University, SUDAAR 538, December 1983.

Duhamel, T. G., "Contributions to Error Analysis in Relativity Gyro Experiment," Ph.D. Thesis, Stanford University, SUDAAR 540, April 1984.

Stanford University, "Request for Proposal for the Shuttle Test of Relativity Experiment," August 15, 1984.

MSFC GP-B Task Team, "Request for Proposal for the GP-B Engineering Development Shuttle Flight Experiment," Marshall Space Flight Center, Alabama, September 12, 1984.
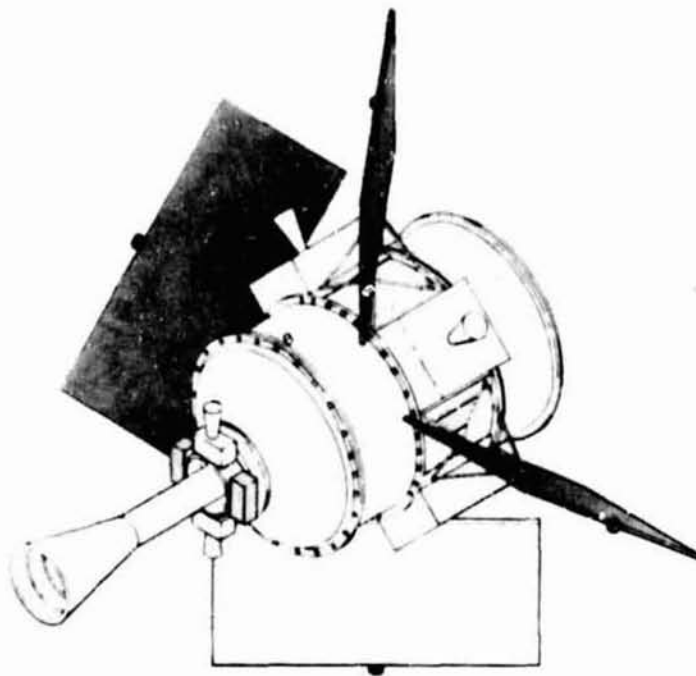
Figure 11.   Gravity Probe-B.

EXTENDING VLBI TO SPACE

Radio interferometry observations of celestial sources are routinely performed on Earth by using atomic frequency standards to synchronize radio telescopes that may be separated by as much as intercontinental distances. Angular resolution superior to that of Earth-based optical telescopes has been achieved. By placing one or more of the observing elements in Earth orbit and making observations in concert with those on the ground, significant advantages over purely ground-based systems can be obtained.

An initial step would be to utilize the capability of the space shuttle to demonstrate orbiting Very Long Baseline Interferometers (VLBI's) by deploying a large retrievable antenna attached to the shuttle. This mission could be part of the large Deployable Antenna Flight Experiment that has been under active study by MSFC and aerospace contractors during the past several years, providing an on-orbit test of an antenna system that has potential applications in communications and Earth observations. One possible antenna concept is shown in Figure 12. During the mission, about 3 days would be devoted to VLBI observations. An alternative system now under study at MSFC is a 15-meter antenna aboard the shuttle that could later be used on the Space Platform or perhaps on an Explorer-class mission. Although a larger aperture antenna is desirable, an important set of bright sources could be observed with a space antenna as small as 10 meters in diameter.

During 1981, a technical working group was established to assist in the science and mission design of a VLBI experiment. Scientific objectives and mission and system/subsystem requirements for performing a VLBI demonstration have been established.
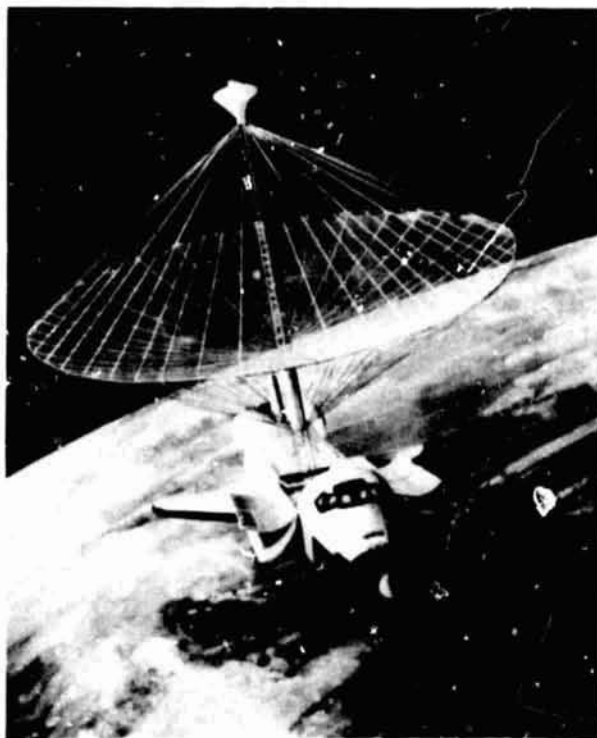
Figure 12. Very Long Baseline Interferometer (VLBI)
Possible Antenna Concept.

Future VLBI missions will be international in scope. The working group
has met several times with scientists from the Centre National D'Etudes
Spatiales (CNES) and European Space Agency (ESA) working groups in support
of a VLBI mission study which would use spacecraft developed by Europe and
the U.S. in highly elliptical orbits. One spacecraft concept which is now
being pursued in more depth is Quasat, based on a joint U.S./ESA proposal to
fly a 14- to 25-meter antenna in a 15,000 km apogee orbit. Study efforts at
MSFC are continuing to concentrate on a cooperative venture with Langley
Research Center to modify an antenna developed by the Harris Corporation.
This antenna could be used for a VLBI shuttle demonstration at a cost of
approximately $12-15 million. (M. Nein/PS02/205-453-3430)

ADVANCED X-RAY ASTROPHYSICS FACILITY (AXAF)

A critical element of the AXAF observatory is the High-Resolution
Mirror Assembly (HRMA), consisting of six concentric pairs of glass mirror
elements which are figured, polished, and precisely aligned to reflect and
focus high-energy x rays (up to 10 keV) at the focal plane of science in-
struments located 10 meters away. If the performance goals for the HRMA are
achieved, the AXAF observatory will offer an x-ray astronomy capability 100
times more sensitive than its predecessor, HEAO 2. AXAF, in conjunction
with large, ground-based radio telescopes and the optical Space Telescope
(ST) to be launched in 1986, will complete the triad of astrophysics capa-
bilities needed to support man's exploration of the universe through the

19

remainder of the 20th century. AXAF will have the capability to study all known categories of astronomical objects and to discover new ones. MSFC's ongoing Technology Mirror Assembly (TMA) program is structured to verify that the technology goals established for the HRMA are achievable in a time-frame compatible with initiating development go-ahead (Phase C/D) for AXAF in FY-87. Early in 1985, TMA test activities will be initiated at MSFC to assure that this technology is well in hand and well understood on a timely basis. Parallel Phase B observatory systems definition contracts were awarded in June 1984, and will be funded through June 1986. Forty-one responses have been received to an AXAF science announcement of opportunity. Science instruments for AXAF will be selected by a peer group in December 1984; 2-year definition efforts will be initiated in February-March 1985. These activities and the technology support efforts now in place will readily support the priority new start for AXAF in FY-87, leading to an operational AXAF observatory program starting in 1991. A 15-year program is planned based on provisions for on-orbit maintenance and refurbishment of both the observatory subsystems and the science instruments. An artist's rendition of the AXAF observatory is shown in Figure 13.
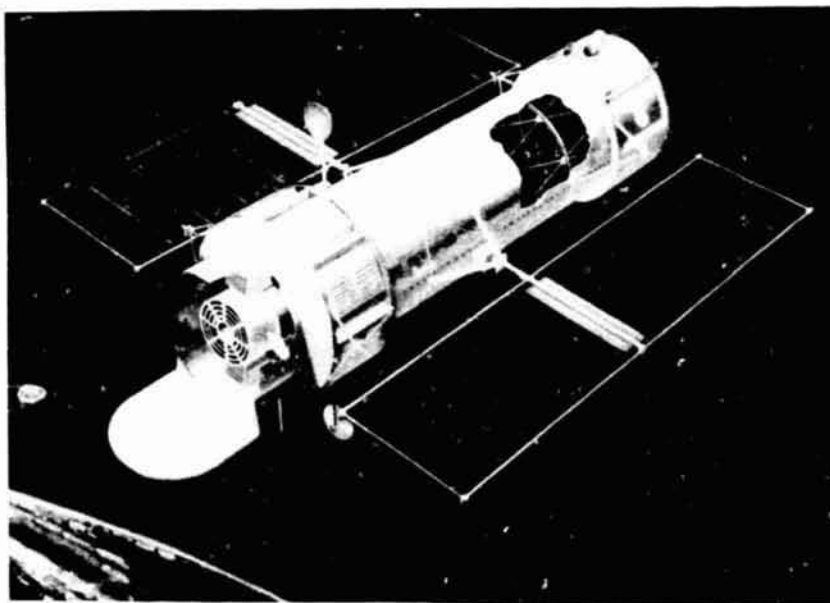
Figure 13. Advanced X-Ray Astrophysics Facility (AXAF).

Progress in mirror grinding and polishing in the TMA program proceeded toward completion in early 1985. Both the Perkin-Elmer (P-E) approach, which is based on an improved version of the HEAO 2 process, and the Itek vertical honing approach continue to show promise. The Itek process has never before been demonstrated but is considered very important because it is much faster than the P-E process. If it continues to be successful, it will represent a valuable option in the overall optics manufacturing process to be baselined later for AXAF. The mirror figure accuracy in the P-E process now exceeds 1 arc second, which is approximately four times better than the HEAO 2 overall mirror performance estimates. The goal for the TMA is 0.5 arc second (after assembly and alignment).

As part of the TMA effort, the MSFC x-ray test and calibration facility has been undergoing continued modification to support the evaluation of the completed and assembled TMA mirrors. Most modifications were completed during FY-84.

A key technology-related activity, started in late FY-84, is the motion detection system. This system will use a laser in conjunction with special detectors to sense small vibrations which will be present in the vacuum chamber and test fixture during mirror tests. The effect of these motions, which would otherwise degrade the test data, will be automatically removed from the data by software. The completion and successful operation of the motion detection system will be a significant accomplishment because it can be easily adapted to support the future AXAF flight optical system tests.

Also, a large Invar optical bench capable of supporting the TMA and the array of detectors needed to evaluate the optical system was designed during FY-84. Assembly will occur during early FY-85. The bench will also support a high precision turntable on which the TMA will be installed. This turntable will permit very accurate angular repositioning of the TMA over a range of about $\pm 0.5°$ to evaluate the performance of the mirror under off-axis conditions.

Plans were completed in FY-84 for a full-up test in November of the S056 mirror left over from the Apollo Telescope Mount program. S056, a small x-ray mirror, will simulate the TMA in a test of the overall test facility readiness, including the vacuum system, x-ray generator, instrumentation, and test procedures. Any problems encountered during this test can be corrected well in advance of the x-ray testing of the first TMA, scheduled for delivery in early April 1985. Facility readiness is crucial because of the short time available for accumulation of test data needed to support a major NASA review of the AXAF program in June 1985.
(D. C. Cramblit/C. Dailey/PF19/203-453-0788)

PINHOLE OCCULTER FACILITY (POF)

The POF is an observatory imaging the Sun and celestial objects in hard x rays and observing the solar corona in visible and ultraviolet wavelengths (Figure 14). It is initially to be flown as a shuttle-based payload, with eventual inclusion in semipermanent facilities such as the Space Station. The POF utilizes a 35-meter deployable boom of an existing design to position an occulting mask between the solar instruments and the solar disk. The coronal imaging instruments observe the solar corona around the edge of the disk, while multiple aperture imaging systems observe the hard x-ray activity of the Sun. The imaging systems, occulting mask, and deployable boom are pointed and stabilized by the Instrument Pointing System (IPS). Functioning in the celestial observing mode, the system can be used to form high-resolution images of celestial objects in much higher energies than previously possible.

An in-house Phase A feasibility study report was published in 1984 with the results given to NASA Headquarters in May 1984. In-house definition is underway of candidate aspect and alignment systems. Pointing and control studies are currently underway which will characterize control laws necessary for utilization of the IPS and associated systems. (J. Dabbs/PSO2/205-453-3430)

Publication:

MSFC, Program Development Office, "Pinhole Occulter Facility" (Phase A study, internal publication), Marshall Space Flight Center, Alabama, January 1984.

Figure 14. Pinhole Occulter Facility (POF) Initial Shuttle Deployment.

SPACE BASE COHERENT OPTICAL SYSTEM OF MODULAR IMAGING COLLECTORS (COSMIC)

Increased collecting area and higher overall precision to achieve higher resolution are the principal requirements for advanced telescopes of the future. Increasing the collecting area by simply scaling conventional telescope configurations seems to have reached its limits with the Space Telescope on one hand and the largest existing ground-based telescopes on the other. Of all new design concepts, the segmented mirror and phased-array telescopes have attracted the most attention.

To achieve high performance most economically, unconventional aperture shapes such as elongated or partially filled apertures are being investigated to comply with physical constraints imposed upon the overall system by the available shuttle payload space and weight limitations.

22

Despite the high degree of complexity, the phased-array telescope has some definite advantages which warrant further investigation. For instance, the linear arrangement of the telescope is particularly suitable for storage in the shuttle payload bay. Another major advantage is its potential to yield the highest possible resolution for any given collecting area. Even though maximum resolution is instantaneously obtained in only one dimension, a two-dimensional point spread function yielding high resolution may be synthesized by rotating the aperture. Because of these primary reasons, linear-phased arrays have been analyzed as potential next-generation ultraviolet/optical telescope systems.

Figure 15 shows the COSMIC concept and the evolutionary construction of a large array. The initial array contains four Afocal Interferometric Telescopes (AIT's) with a Beam Combining Telescope (BCT) at one end. The COSMIC spacecraft module pivots from its launch position at the end of the BCT to its deployed position below the BCT. The solar arrays deploy from stowed positions alongside the telescope module. The focal planes of the BCT and sunshades are extended above the telescope apertures.

In 1983, an in-house study of different concepts for COSMIC was completed to investigate various telescope configurations and launch options based on the assumption that a long baseline is more important than a light-gathering capability. The selected concept is to package two parallel arrays in the payload bay that can be deployed on-orbit into one long baseline configuration.

In June 1984, a technology study (funded by the Office of Aeronautics and Space Technology) was initiated with industry to assess the advanced technology requirements and to categorize generic and specific technology drivers to which solutions must be developed prior to developing realistic telescope designs. This study is also concentrating on the orbital assembly and maintenance requirements because of their determining influence on the design of the optical and structural systems. Another study is currently underway to develop novel optical concepts which would facilitate and simplify the manufacture of large numbers of optical mirror segments required for these advanced telescopes. Promising concepts such as spherical primary mirrors within two- and three-mirror systems are being evaluated based on point spread function analyses of the optical performances.

Figure 16 depicts another novel concept which is based on the assembly of several afocal telescopes forming a circular array. This offers some significant advantages because the resulting image is of uniform resolution without rotating the telescope, as is required in a linear array. Also, the stray light management is simplified over a single, large aperture system because of the compact short light shields which can be built as structural elements for the entire system. However, resolution is less since the baseline diameter increase for the amount of primary mirror area invested is less than in a linear array.

The simple comparison already indicates the difficult assessment of design approaches with due consideration of technology requirements and science objectives. (M. Nein/PS02/205-453-3430)

Publication.

Davis, B., G. Hunt, D. Korsch, and M. Nein, "Coherent Optical System of Modular Imaging Collectors (COSMIC): An Approach for a Large Aperture High Angular Resolution Telescope in Space," in SPIE Proceedings, Vol. 440, Synthetic Aperture Systems, 1984.
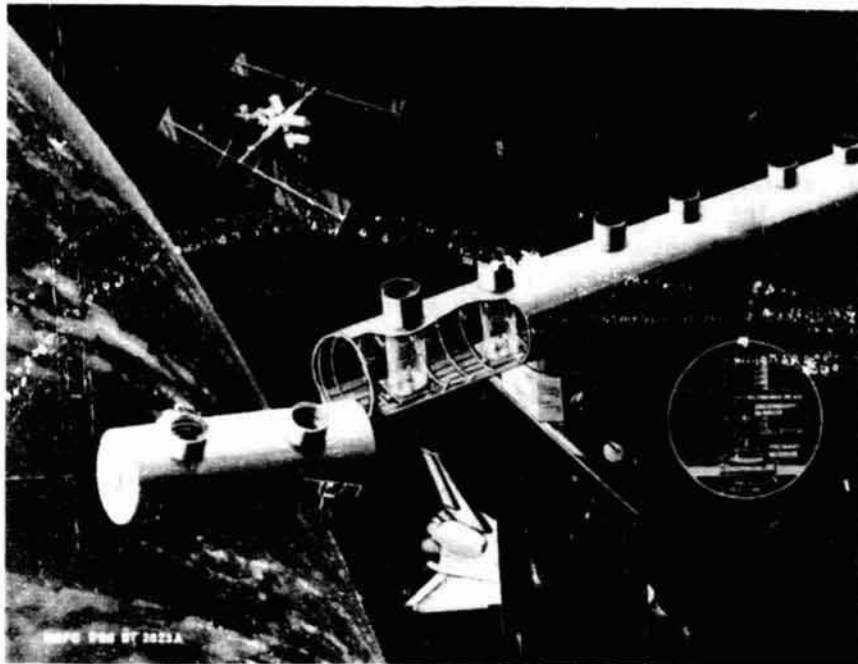
Figure 15. Coherent Optical System of Modular Imaging Collectors (COSMIC).
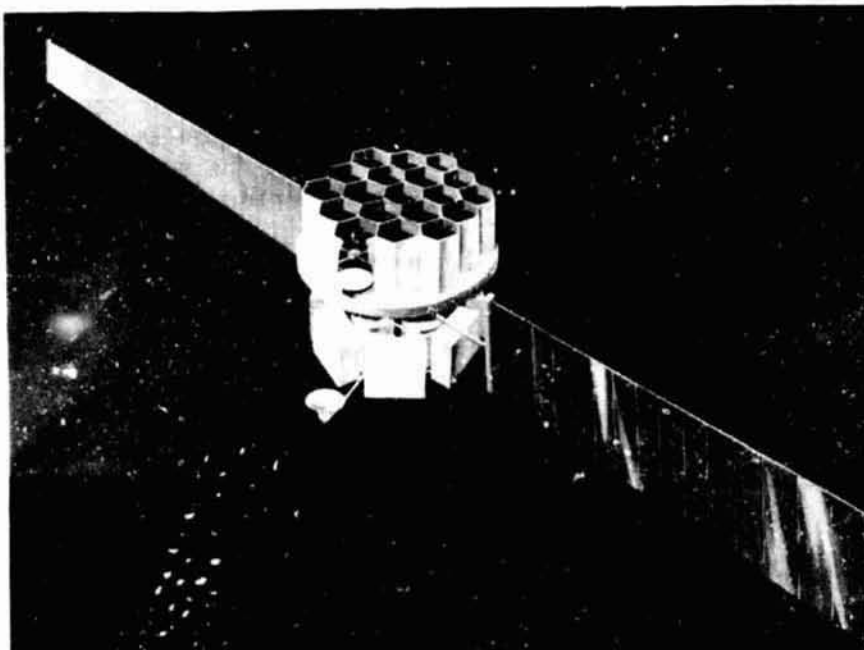
Figure 16. Modular Multimirror Telescope.

LONG-TERM CRYOGENIC STORAGE FACILITY

The recent approval of the NASA Space Station and the eventual space basing of a cryogenic Orbital Transfer Vehicle (OTV) will require orbital storage of large quantities (>100,000 pounds) of cryogenics. The capability to store large quantities of cryogenics in space for long periods of time will require thermally efficient systems to preclude excessive cost penalties resulting from Earth orbit resupply transportation costs. The loss of propellants stored in orbit must be minimized by use of advanced insulation design concepts, support systems, fluid acquisition/transfer systems, and refrigeration systems. A preliminary in-house study analyzed a lox/LH$_2$ orbital storage system. The study results concluded that a coupled tank design, utilizing vapor-cooled shields in conjunction with a refrigeration system and approximately 4 inches of multilayer insulation, appears to be a viable one. The use of liquefaction to control boil-off losses resulted in excessive power penalties. Fluid transfer losses less than 5 percent per transfer were calculated. Future studies are required to establish detailed design/performance data, technology requirements, and ground and flight testing. An overall test plan and a conceptual design of the test article, leading to a demonstration flight experiment (Figure 17), will be developed. (U. Hueter/PD22/205-453-4263)
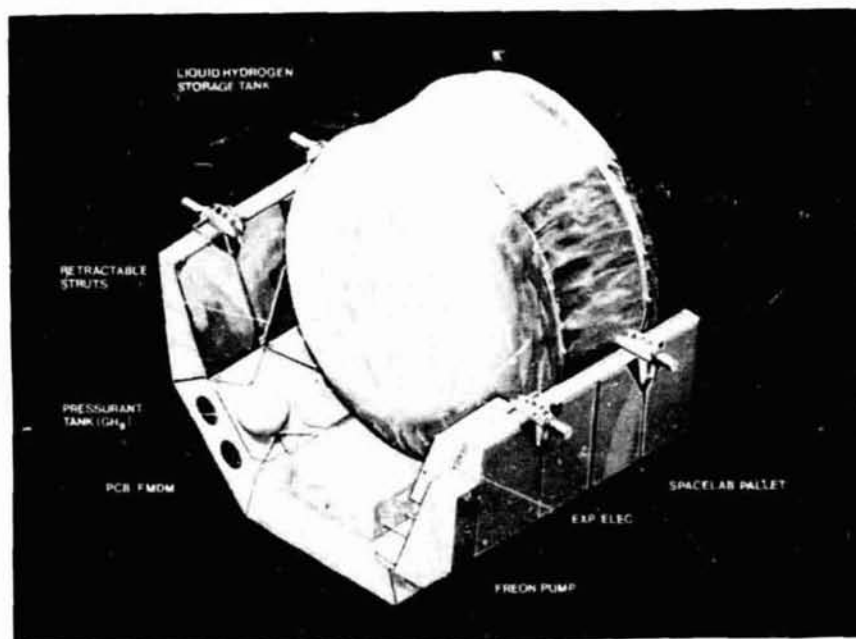
Figure 17. Long-Term Cryogenic Storage Facility Demonstration Experiment.

PROPOSED FLIGHT DEMONSTRATIONS

The Office of Space Flight issued the first annual call for flight demonstration proposals that will extend and exploit the capabilities of the space shuttle/Space Transportation System. MSFC prepared 13 proposals in response to this request, with 7 proposed for FY-85 funding new starts and 6 proposed for FY-86 funding new starts. While some of the proposed demonstrations were for programs described separately in this report, most were new and original submissions.

The proposed FY-85 new start demonstrations, arranged in MSFC's recommended priorities, are the: Structural Assembly Demonstration Experiment (SADE), Phased-Array Lens Flight Demonstration, Aerodynamics Demonstration Satellite (ADS), Tethered Satellite Engineering Demonstration Flight Experiment, Deployable Conductive Surface Sphere Technology Demonstrations for Tether Applications, Tether Applications Mother-Daughter Experiment, and Superfluid Helium Fluid Transfer. The proposed FY-86 new start demonstrations, arranged in MSFC's recommended priorities, are the: Major Repair of Structures in Orbital Flight Experiment, Long-Term Cryogenic Storage Facility, Spacecraft Servicing Demonstration, Recovery of Tumbling Satellite, Suspended Experiment Mount (SEM), and Remote Fluid Resupply Demonstration.

The proposed flight demonstrations are now under evaluation by a NASA Headquarters team. Following this evaluation process, certain experiments will be funded for potential flight demonstrations. (R. L. Middleton/PS04/ 205-453-2796)

Publication:

MSFC, Program Development Office, "Marshall Space Flight Center Proposed FY-85 Flight Demonstrations," Marshall Space Flight Center, Alabama, June 1984.

RESEARCH PROGRAMS

SPACE SCIENCES

Solar Physics

Ultraviolet Spectrometer and Polarimeter (UVSP)

The repair of the Solar Maximum Mission (SMM) satellite in April 1984 is making possible renewed observations of the Sun. Analyses of the new data are only just beginning. Some of the topics which are to be examined with the UVSP instrument on SMM are high time resolution observations of flares, statistics of UV bursts, high spatial resolution imaging, and polarization.

Studies in several areas of solar research are continuing using data obtained by the UVSP in 1980.

Physical conditions in a quiescent prominence were studied using spectral data covering a wide range of temperatures. The spectral lines included 1215 Å of H I, 1401 Å of Si IV, 1548 Å of C IV, 1640 Å of He I, and 1655 Å of C I. The conclusion was that the prominence consisted of flux tubes at various temperatures ranging from 5000 to 10^5 K. In the hotter regions of the plasma, the density reached values of about 3×10^{11} cm^{-3}. This work was done in collaboration with a colleague at the Goddard Space Flight Center.

The dynamics of prominences have also been studied. In the case of the surge of October 2, 1980, simultaneous observations in H-alpha and C IV show that the cold and hot material follow the same channel, and the event lasted about 10 minutes in both lines. There was good correlation between the H-alpha and C IV velocities, which were in the range 40 to 60 km s^{-1}. However, the strong upward accelerations did not appear at the same time and place in the two lines, which indicates that a model where a hot transition layer sheath surrounds a cool surge is not appropriate. Recurrent surges are often observed in active regions where flares occur. In the case of the event of September 1, 1980, two new active centers merged and squeezed an inverse polarity spot, causing recurrent ejection of matter at intervals of about 10 minutes. Both cold (H-alpha) and hot (C IV) material had the same projection, although the upward velocity structure could be seen further in C IV. This work was done in collaboration with colleagues at the Observatory of Paris, Meudon.

Possible magnetic field changes during solar flares are also being studied. In connection with a flare on July 13, 1980, there appear to have been some brief magnetic transients on the order of several thousand gauss observed in the transition region in C IV; however, the significance of the results may be open to doubt because of the difficulty of unraveling polarization changes, velocity changes, and intensity changes. This work is being done in collaboration with Dr. William Henze at Teledyne Brown Engineering, Huntsville, Alabama. (E. A. Tandberg-Hanssen/ES01/205-453-0027)

Publications:

Poland, A. I., and E. Tandberg-Hanssen, "Physical Conditions in a Quiescent Prominence Derived from UV Spectra Obtained with the UVSP Instrument on the SMM," Solar Phys., 84, 63-70 (1983).

Schmieder, B., J.-C. Vial, P. Mein, and E. Tandberg-Hanssen, "Dynamics of a Surge Observed in the C IV and H Alpha Lines," Astron. Astrophys., 127, 337-344 (1983).

Schmieder, B., J. M. Malherbe, P. Mein, and E. Tandberg-Hanssen, "Dynamics of Solar Filaments. III. Analysis of Steady Flows in Hα and C IV Lines," Astron. Astrophys., 136, 81-88 (1984).

Solar Magnetic Fields

Studies have continued of solar magnetic fields to determine and understand their basic empirical properties and their effects in the solar atmosphere. The approach is to analyze MSFC vector magnetograms together with complementary data from other observatories and from space-based instruments, especially the SMM instruments, and to interpret the observed effects with physical models.

Two developments in magnetostatic models of solar magnetic fields have been investigated to extrapolate observed photospheric fields into the transition region and corona in order to understand the morphology and energetics of these fields above the photosphere. From linear force-free field theory, a theorem has been derived stating that the photospheric transverse fields can be used to determine uniquely the extrapolated fields. Also, a computational procedure developed by Pridmore-Brown for extrapolating photospheric fields using nonlinear force-free field theory has been used for the first time with actual measurements from the MSFC vector magnetograph; some results are shown in Figure 18.

In a statistical study to correlate flare sites with observed stress in the photospheric magnetic field of an active region, it has been found that, in most cases, flares occur in areas of the magnetic neutral line where the transverse magnetic field is in a sheared orientation relative to the neutral line, and that the initial flare points are at the sites of maximum shear. The development and evolution of magnetic shear and its correlation with flare activity are shown in Figures 19 and 20. In conjunction with the Flare Buildup Study Workshops, a scenario was developed for flares in sheared fields such as those shown in Figure 21; the model is depicted schematically in Figure 22. Joint research between solar and magnetospheric scientists of the MSFC Space Science Laboratory yielded an array of evidence that the overall instability for magnetospheric substorms is essentially the same as that for two-ribbon flares such as shown in Figure 22.

Figure 21 also shows a clear example of flux disappearance in the active region between April 6 and 7. From analysis of the MSFC vector magnetograph data, together with associated structure and changes in the chromosphere and transition region observed from the ground and with the

28

UVSP on SMM, it was concluded that the magnetic flux was removed by submergence. These observations suggest that even during the growth phase of active regions, flux submergence is a strong process comparable in magnitude to flux emergence.

Observations of sheared, photospheric magnetic fields are interpreted as evidence of electric currents in the atmosphere above the photosphere. From measurements of sheared transverse magnetic fields obtained with the MSFC magnetograph, distributions have been calculated of the vertical component of the electric current density, J_z, in many active regions to study their correlations with flares and other manifestations of activity. In one example studied in detail, it was found that locations of maxima in J_z were approximately cospatial with the sites of flare onset; this result is illustrated in Figures 23 and 24. A study was initiated of the origination and evolution of these currents near flare sites. Early results seem to indicate that these patterns of J_z concentrations are fairly persistent throughout the periods of observations during which significant flare activity takes place; for example, Figure 25 shows that the general structure and location of the J_z pattern in a flare-productive active region were maintained over a 5-hour period.

For several years an observational and analysis program has been carried out to study the effects of Faraday rotation on measurements of vector magnetic fields and their implications for observations with space-based magnetographs. It has been found that substantial rotation of the plane of linear polarization occurs in a sunspot's umbra and outwards to about mid-penumbral areas. Recently, an investigation was completed of the magnitude of these magneto-optical effects in complex magnetic regions called deltas in which umbrae of opposite polarities occur within a common penumbra; these are generally areas of significant flaring activity. It was found that magneto-optical effects are not important in delta regions and should not affect the interpretation of sheared transverse fields in these areas. Figure 26 is an illustration of the analysis used in this study, and also shows results from the recently upgraded MSFC vector magnetograph.

In May 1984, a workshop on Measurements of Solar Vector Magnetic Fields was conducted in the Space Science Laboratory at MSFC. At this workshop, 12 international and 45 U.S. scientists met to discuss the various techniques available for vector fields measurements, to illuminate current methods for the interpretation of these measurements, and to develop dialogue between observers and theorists concerning the role of vector magnetic fields in our present understanding of solar processes. (M. J. Hagyard/R. L. Moore/ES52/205-453-0118)

Publications:

Wu, S. T., Y. Q. Hu, K. R. Krall, M. J. Hagyard, and J. B. Smith, Jr., "Modeling of Energy Buildup for a Flare-Productive Region," Solar Phys., 90, 117 (1984).

deLoach, A. C., M. J. Hagyard, D. M. Rabin, R. L. Moore, J. B. Smith, Jr., E. A. West, and E. Tandberg-Hanssen, "Photospheric Electric Current and Transition Region Brightness Distributions," Solar Phys., 91, 235 (1984).

Strong, K. T., A. O. Benz, B. R. Dennis, J. W. Leibacher, R. Mewe, A. Poland, J. Schrijver, G. Simnett, J. B. Smith, Jr., and J. Sylvester, "A Multiwavelength Study of a Double Impulsive Flare," Solar Phys., 91, 325 (1984).

Hagyard, M. J., J. B. Smith, Jr., D. Teuber, and E. A. West, "A Quantitative Study Relating Observed Shear in Photospheric Magnetic Fields to Repeated Flaring," Solar Phys., 91, 115 (1984).

Hagyard, M. J., E. A. West, and J. B. Smith, Jr., "Electric Currents in Active Regions," to appear in Proceedings of the International Workshop on Solar Physics and Interplanetary Travelling Phenomena, ed., Chen Biao, Kunming, People's Republic of China.

Hagyard, M. J., N. P. Cumings, and E. A. West, "The New MSFC Solar Vector Magnetograph," to appear in Proceedings of the International Workshop on Solar Physics and Interplanetary Travelling Phenomena, ed., Chen Biao, Kunming, People's Republic of China.

Hagyard, M. J., D. Teuber, E. A. West, E. Tandberg-Hanssen, and W. Henze, Jr., "The Vertical Gradient of Sunspot Magnetic Fields," to appear in Proceedings of the International Workshop on Solar Physics and Interplanetary Travelling Phenomena, ed., Chen Biao, Kunming, People's Republic of China.

Rabin, D., R. Moore, and M. J. Hagyard, "A Case for Submergence of Magnetic Flux in a Solar Active Region," The Astrophysics Journal, in press.

Hannakam, L., G. A. Gary, and D. L. Teuber, "Computation of Solar Magnetic Fields from Photopheric Observations," Solar Physics, in press.

Hagyard, M. J., R. L. Moore, and A. G. Emslie, "The Role of Magnetic Field Shear in Solar Flares," Advances in Space Research, in press.

Patty, S. R., and M. J. Hagyard, "Delta Configurations: Flare Activity and Magnetic Field Structure," Solar Physics, submitted.

Hagyard, M. J. "The Relation of Sheared Magnetic Fields to the Occurrence of Flares," Artificial Satellites, in press.

Hagyard, M. J., "Preflare Magnetic and Velocity Fields," to appear in Proceedings of the SMM Workshop on Solar Flares.

Ding, Y. J., Q. F. Hong, M. J. Hagyard, and A. C. deLoach, "Electric Current Flows in a Solar Active Region," to appear in Proceedings of the MSFC Workshop on Measurements of Solar Vector Magnetic Fields.

Wu, S. T., H. M. Chang, and M. J. Hagyard, "On the Numerical Computation of Nonlinear Force-Free Magnetic Fields," to appear in Proceedings of the MSFC Workshop on Measurements of Solar Vector Magnetic Fields.

West, E. A., "Analysis of the New Polarimeter for the Marshall Space Flight Center Vector Magnetograph," to appear in Proceedings of the MSFC Workshop on Measurements of Solar Vector Magnetic Fields.

Rabin, D., "Evidence for Submergence of Magnetic Flux in a Growing Active Region," to appear in Proceedings of the MSFC Workshop on Measurements of Solar Vector Magnetic Fields.

Rabin, D. M., and E. A. West, "Flexible Graphical Display of Vector Magnetograph Data," to appear in Proceedings of the MSFC Workshop on Measurements of Solar Vector Magnetic Fields.

Moore, R. L., G. J. Hurford, H. P. Jones, and S. R. Kane, "Magnetic Changes Observed in a Solar Flare," Astrophys. J., 276, 379 (1984).

Moore, R. L., J. L. Horwitz, and J. L. Green, "Implications of Solar Flare Dynamics for Reconnection in Magnetospheric Substorms," Planetary Space Science, in press.

Sturrock, P. A., P. Kaufmann, R. L. Moore, and D. F. Smith, "Energy Release in Solar Flares," Solar Physics, in press.

Tandberg-Hanssen, E., P. Kaufmann, E. J. Reichmann, D. L. Teuber, R. L. Moore, L. E. Orwig, and H. Zirin, "Observations of the Impulsive Phase of a Simple Flare," Solar Phys., 90, 41 (1984).

A. First iteration of current field

C. Eighth iteration of current field

B. Second iteration of current field

D. Magnetic field configuration
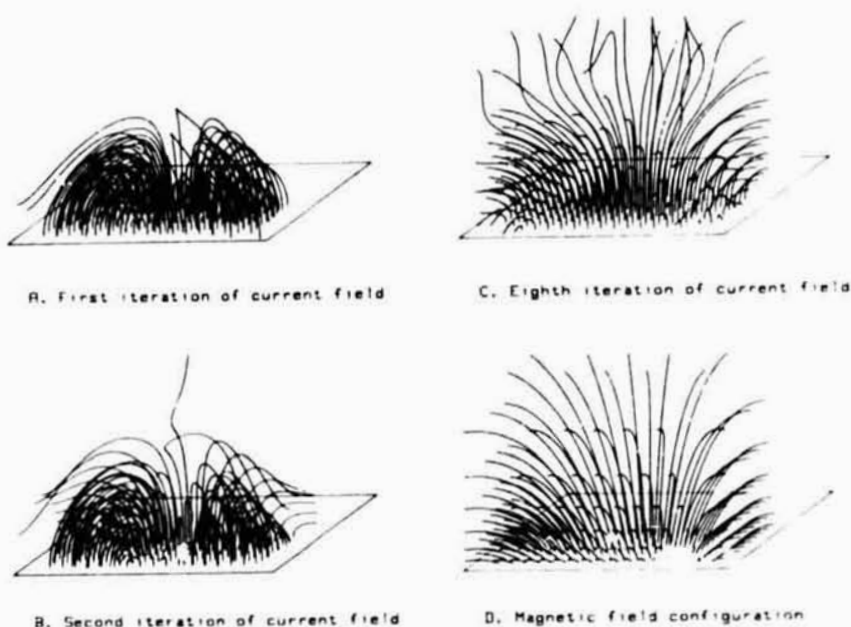
Figure 18. Computational Results of a Nonlinear Force-Free Field Model Showing the Convergence of Current Field (A,B,C) Towards the Magnetic Field Configuration (D). The variational procedure, developed by Pridmore-Brown, minimizes the Lorentz force in a volume. The current fields were generated from a set of basic functions whose coefficients are determined from minimizing the Lorentz force in the volume and requiring the magnetic azimuth directions to agree on the surface.
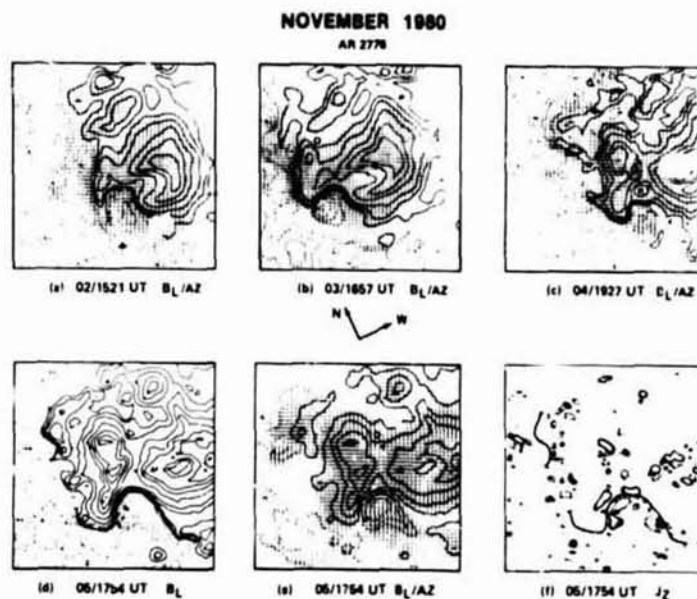
Figure 19. Magnetic Evolution of an Active Region (AR 2776) Over the Period November 2-5, 1980. In all line-of-sight magnetic field maps (B_L), solid (dashed) contours represent positive (negative) fields. In overlaid transverse field plots (AZ), the transverse field strength and direction are indicated by the length and orientation of the line segments. (a) Overlay of AZ and B_L for November 2. The area of interest and site of future flaring is the dividing line (neutral line) between the areas of positive and negative B_L polarity that lies just below the center of the panel. Analysis of the line segments reveals a generally unstressed field aligned more or less directly from the positive to the negative centers across the neutral line. (b), (c) Similar data for November 3 and 4; the field remains generally unsheared. (d), (e) Data for November 5; the field has become strongly stressed as seen in the orientation of the AZ line segments which are now lying along the neutral line instead of across it. (f) Contours of the vertical component of the electric current density (J_z) for November 5.
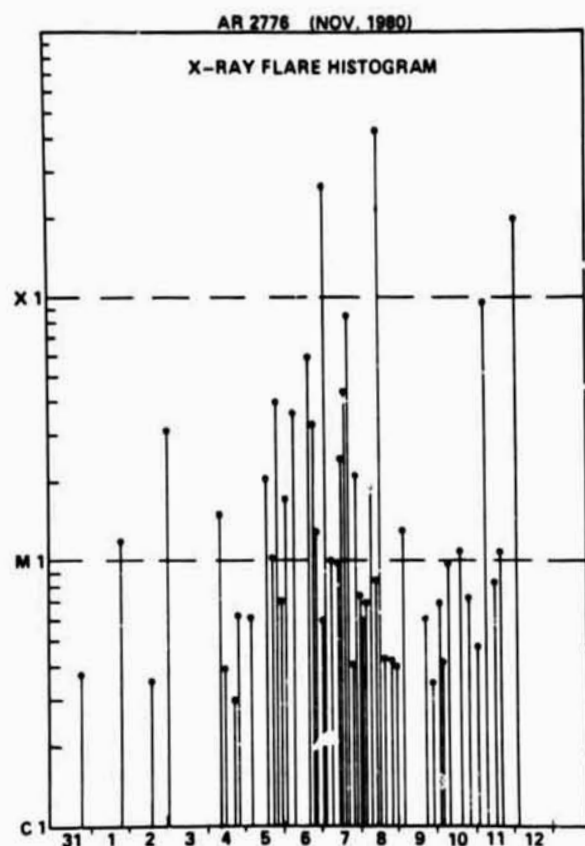
Figure 20. Histogram of X-Ray Flare Intensities for AR 2776 During the Period November 1-12, 1980. The peak soft x-ray intensity of flares observed in this active region are shown in a logarithmic scale with γ, M, and X denoting decimal powers of -3, -2, and -1 erg cm^{-2} s^{-1}. Note the increased flare frequency and magnitude starting on November 5 when the magnetic field developed a highly sheared configuration.

33
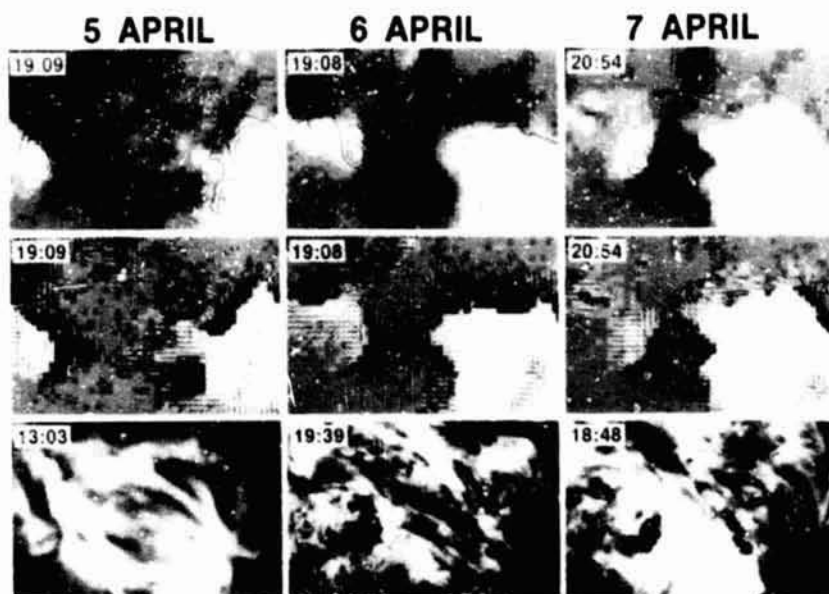
Figure 21. Sheared Magnetic Structure of AR 2372 in April 1980. The over-
all configuration of the magnetic field in the photosphere and
chromosphere is shown in these panels. Top row: grey scale
maps of the line-of-sight field with sunspot darkness contours
superposed. Middle row: maps of the direction (line segments)
and strength (grey tone) of the transverse field; in both rows
an area is light (dark) if the line-of-sight field is positive
(negative). The area of flaring is located along the neutral
line dividing the regions of positive and negative fields in
the left-of-center portions of all three panels in the middle
row. The stressed nature of the field is seen by the alignment
of the line segments along the neutral line instead of across
it. Note that the stress in the field in this area has dis-
appeared on April 7; flare activity was seen to decrease
also. Bottom row: center-line H-alpha filtergrams. The chro-
mospheric field inferred from the filamentary structures
reflects the sheared configuration of the photospheric field
seen in the panels of the middle row; this is particularly
evident in the middle panel.

PREFLARE **ONSET**

IMPULSIVE PHASE **LATE PHASE**
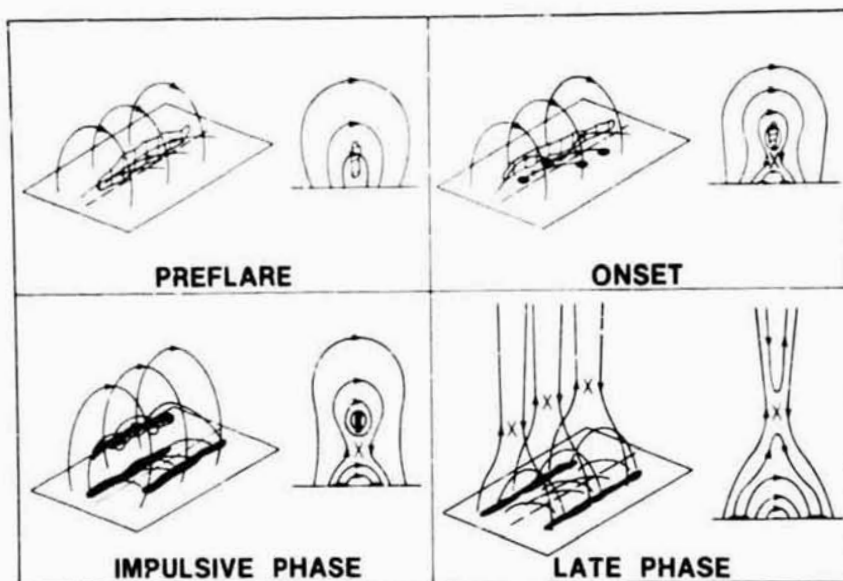
Figure 22. Overall Configuration of the Sheared Field and Its Eruption in a Flare (perspective and end views). The field is stressed until it reaches a critical configuration of shear, whereupon it begins to reconnect; this occurs in the closed, strongly sheared field below or low in the filament along the neutral line. The onset of reconnection releases the field in and around the filament from its ties to the photosphere and, in consequence, the field erupts upward. The overall field is thereby made globally unstable so as to drive further reconnection and eruption, etc.
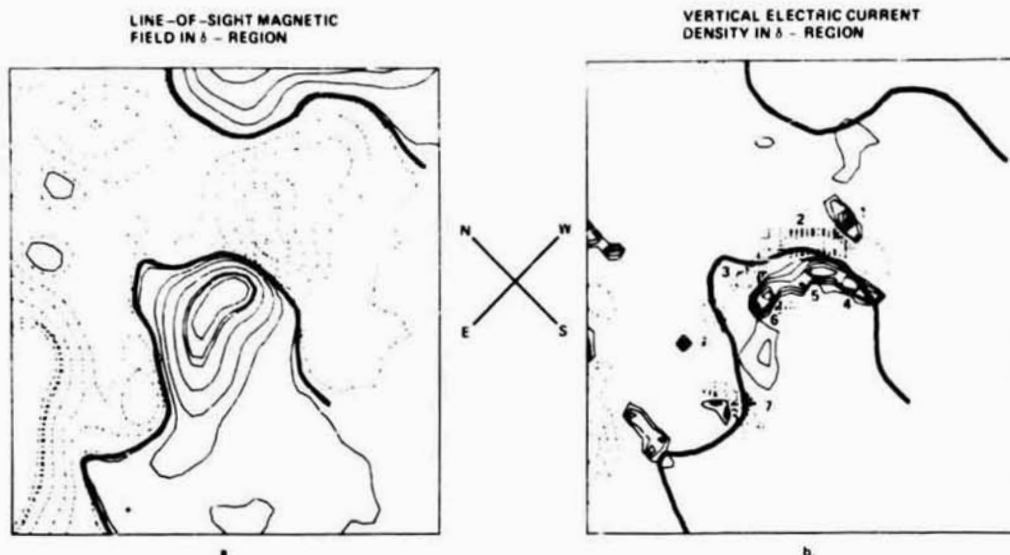
Figure 23. Concentrations of Electric Currents in AR 2372 on April 6, 1980. (a) The line-of-sight magnetic field in the area of the magnetic dipole that was internal to this region; the dipole was the site of most of the early flares in this region. Solid (dashed) curves denote positive (negative) contours of the field. (b) Calculated vertical electric current densities (J_z). The heavy solid curve delineates the magnetic neutral line in (a). Solid (dashed) contours represent positive (negative) values of J_z with positive indicating J_z flowing upward. Note the seven areas of concentrated maxima of J_z.

AR2372
APRIL 6, 1980
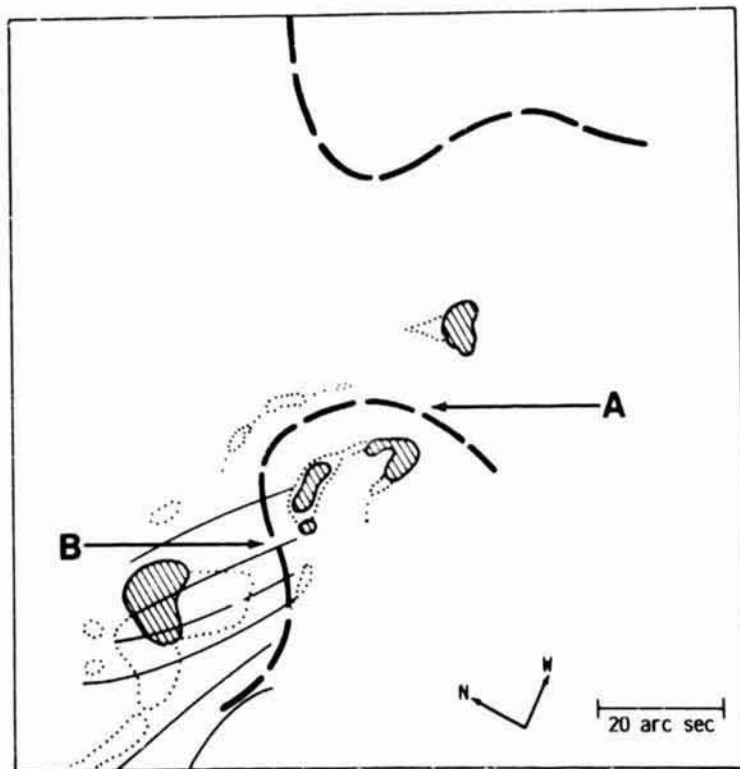
Figure 24. Locations of Flare Intensities in AR 2372. The field-of-view
of this figure is centered on the dipole area of the previous
figure, and the heavy dashed curves locate the two segments of
the neutral line corresponding to those shown in that figure.
The hatched regions show the areas of most intense off-band H-
alpha emission, while the dots outline areas of fainter emis-
sion. The loops sketched at B are inferred from the H-alpha
emission seen at line center and ± 0.4 Å. The area designated
by A marks the location of onset for a flare as seen in soft x-
ray observations from SMM. Clearly, the sites of flare onset
as inferred from the locations of these emissions were approxi-
mately cospatial with the areas of enhanced J_z as seen in the
previous figure.

37

EVOLUTION OF SHEAR AND ELECTRIC CURRENT DISTRIBUTIONS
5 APRIL 1980
AR 2372
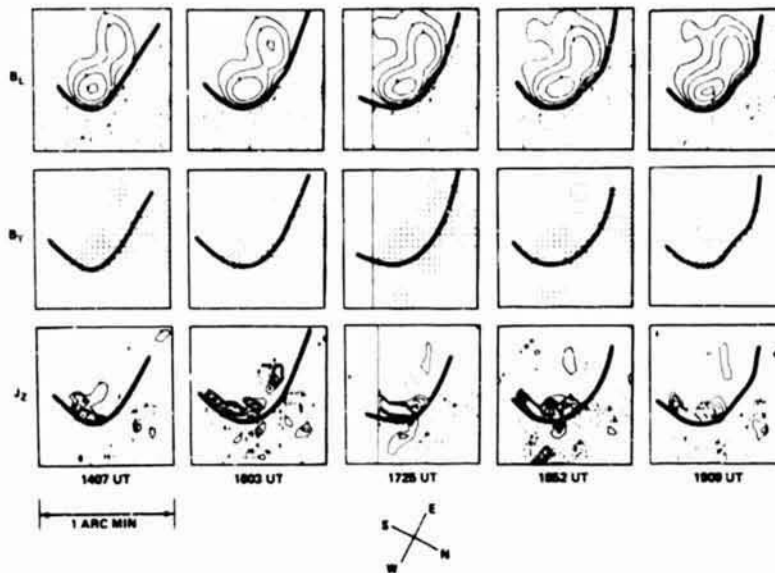
Figure 25. Evolution of Electric Currents in AR 2372 in April 1980. Top row: evolution of line-of-sight magnetic fields (B_L) over a 5-hour interval in the area of the dipole region where the majority of flares occurred. The heavy solid curve denotes the magnetic neutral line separating positive (solid curves) from negative fields. Middle row: the observed transverse field (B_T) with the neutral line superposed. The line segments represent in length and direction the strength and orientation of the transverse field. Bottom row: the derived vertical electric current density (J_z) again with the neutral line superposed. Contours denote positive (solid lines) and negative (dashed lines) values of J_z. Note the persistence of the positive area of J_z above the neutral line and the negative area below and to the right of that line.

38

MARSHALL SPACE FLIGHT CENTER MAGNETOGRAMS

APRIL 2, 1984   FOV: 1' X 1'   NOAA AR = 4455

LEADER

DELTA

FILTER   90 m Å   FILTER   0 m Å

MEASURED AZIMUTH ON LINE OF SIGHT MAGNETIC FIELD
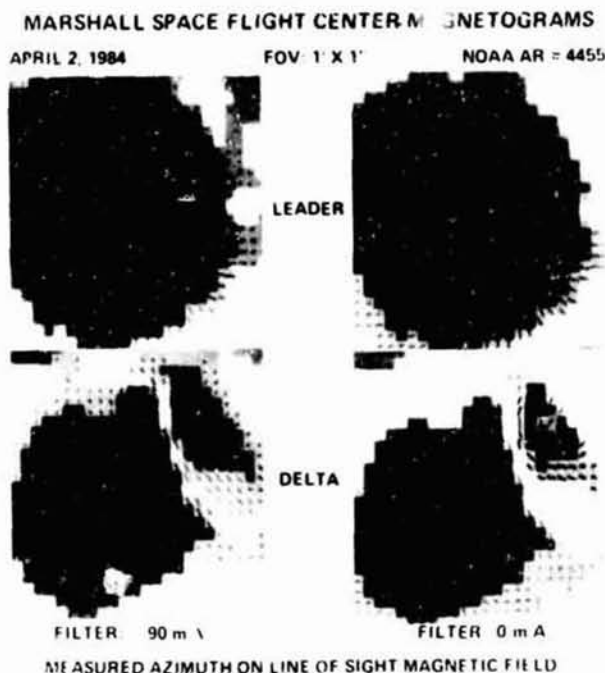
Figure 26. A Study of Magneto-Optical Effects in a Magnetic Delta Re-
gion. The line-of-sight component of the magnetic field is
shown in a grey scale format while the transverse field is
depicted by superposed line segments whose length and direction
give the magnitude and orientation of that field. (a), (b) The
magnetic field of a large sunspot, observed at -90 mÅ and at
line center, respectively. Notice the change in directions of
the line segments in the penumbral areas for the two different
spectral observations; this is indicative of Faraday rota-
tion. (c), (d) The magnetic field in the delta region at
-90 mÅ and line center. The sheared directions of the line
segments along the neutral line in the vicinity of the delta
configuration do not change appreciably at the two spectral
positions; this indicates that there is no Faraday rotation of
the linear polarization.

Coronal and Interplanetary Physics

Research on physical processes in the corona and interplanetary medium includes documenting the correlation between coronal mass ejections and disappearing filaments and between potential magnetic field models for the solar corona and solar wind speed. A magnetohydrodynamic model was used to understand the recent Pioneer 10 discovery of meridional transport in the outer solar system. A numerical model of time-dependent flow in the solar corona was applied to simulate shock effects, and development was begun on the computation of global coronal models at MSFC using data from the Stanford Solar Observatory. A completely new method of calculating the topology of the heliospheric current sheet is being applied to spacecraft data analysis.

The heliospheric current sheet, a thin layer separating regions of opposite magnetic polarity in the interplanetary medium, is formed high in the corona above streamers. In the highly idealized case of totally homogeneous solar wind flow, the form of the current sheet's intersection with a Sun-centered sphere is independent of the radius of the sphere. However, the real Sun produces solar wind which is inhomogeneous; it has a speed gradient along the current sheet at constant height in the corona. This inhomogeneity causes distortion in the current sheet of progressively greater amplitude with increasing distance from the Sun, and which occurs even for purely radial flow. A kinematic analysis of this effect has been made and shows how the originally smooth current sheet becomes ruffled (Figure 27). Even a small gradient produces significant and observable distortion so that, in order to know the shape of the current sheet, it is essential to consider the solar wind in which the sheet is embedded. At least three observational tests of the model predictions are identified.
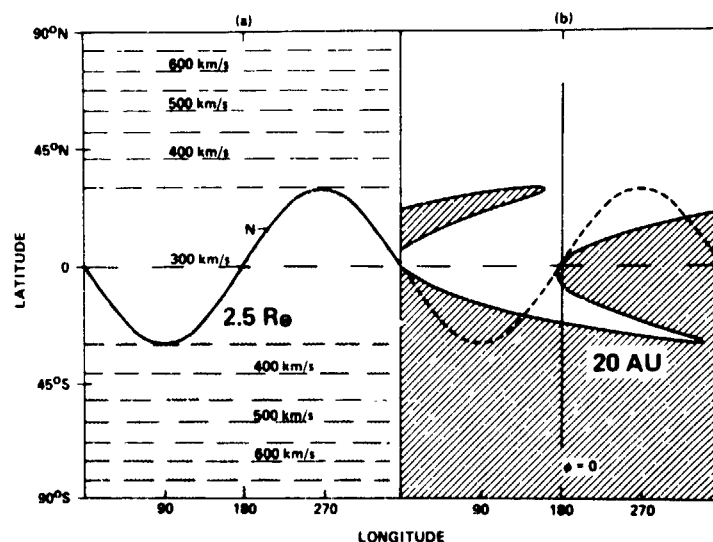
Figure 27. Current Sheet Cross Section at 2.5 Solar Radii and 20 AU.

A comparison was made between the properties at the source surface of a potential field model of the solar corona and solar wind properties observed with the International Sun-Earth Explorer (ISEE) 3 at 1 AU and extrapolated back to the Sun. This was done for three consecutive Carrington rotations in the summer of 1979. The already known properties of a velocity minimum at the interplanetary current sheet and a tendency for the average velocity to increase with longitudinal distance from the current sheet are recovered. A better correlation between source surface properties and velocity is demonstrated by using the field strength on the source surface rather than longitudinal distance from the current sheet (Figure 28). Applying a simple algorithm to distinguish between transient and corotating interplanetary variations substantially increases the correlation. However, given a reasonable estimate of the number of degrees of freedom for the sample, only the correlation between source surface field strength and flow speed after the transients have been eliminated is statistically significant at the 1-percent level.

CONTOURS OF CONSTANT RADIAL MAGNETIC FIELD STRENGTH
ON THE SOURCE SURFACE OF A POTENTIAL FIELD MODEL
THE SOURCE SURFACE RADIUS = 2.6 SOLAR RADII

Left Solar Wind Projected to One Solar Radius from One AU
Assuming Constant Velocity
Right Source Surface Magnetic Field Strength
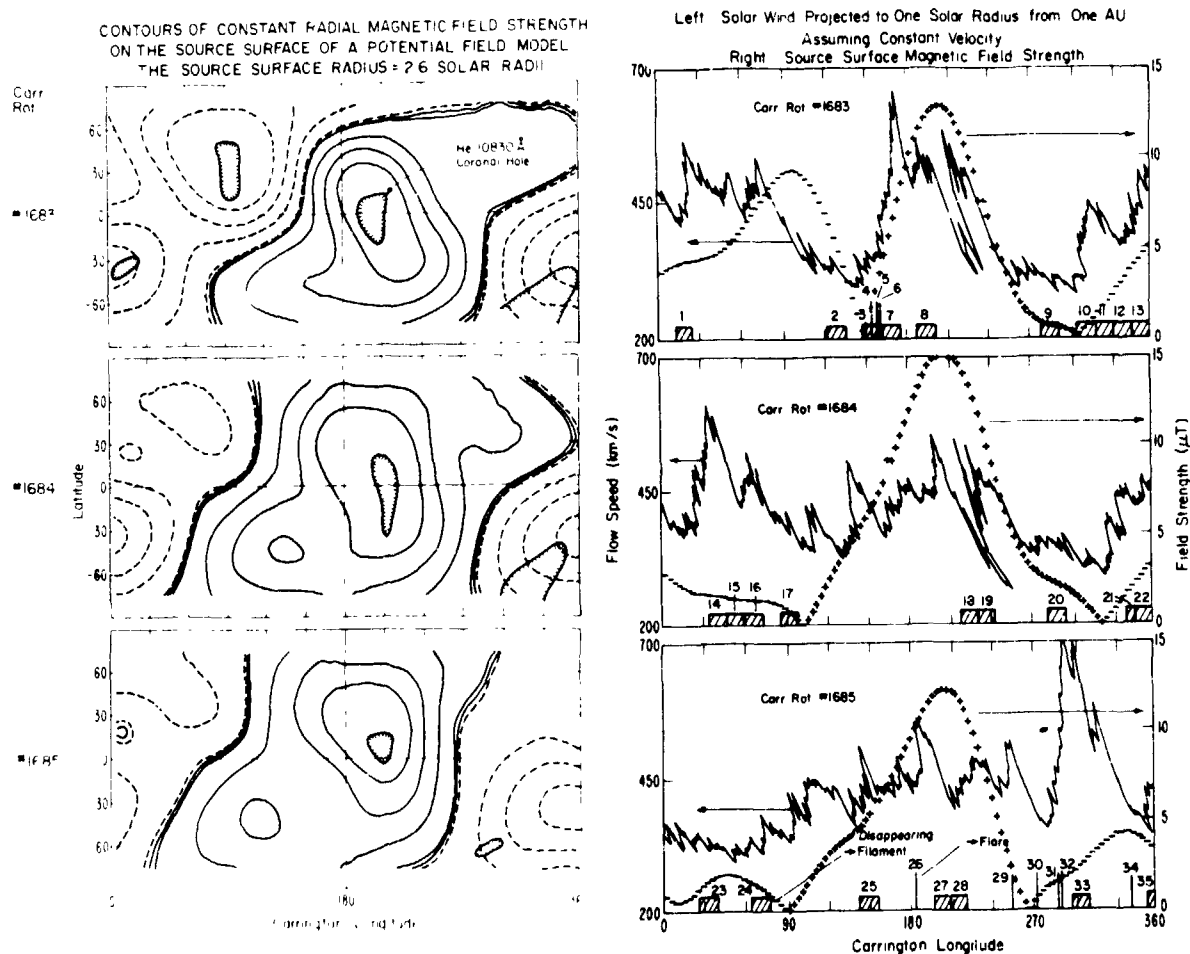
Figure 28. Relationships Between the Coronal Magnetic Field
and the Solar Wind.

41

The spiraling of the interplanetary magnetic field, which is largest at the equator and zero over the poles of the Sun, can drive a meridional transport of solar wind mass and magnetic fluxes. This effect has long been recognized. Recently, it has also been experimentally verified. These new observations were evaluated in the context of present theoretical models and show that the observed flux deficits at Pioneers 10 and 11 agree well with predictions. Important parameters in theory are the strength of the interplanetary magnetic field, the magnitude of the solar wind flow speed, and possible meridional gradients in the flow speed, temperature, density, and radial field strength. The original theory did not completely deal with the effects of large meridional gradients on the most observable feature--the azimuthal magnetic field strength. This last portion of the theoretical development has now been completed and awaits further data from the outer solar system. The analysis is also useful in stellar wind and mass loss modeling, and evaluation of the results for other stars is now in progress.

Large-scale magnetic field data from the Sun are used for determining the location of the neutral line at the photosphere and computation of potential field models of coronal structure. Further development has been conducted, under a contract with the Space Environment Laboratory of the National Oceanic and Atmospheric Administration (NOAA), to begin the steps necessary to make these results into a forecasting tool. A new program at MSFC has been instituted that will result in the computation of these coronal field models and application of the results to the interpretation of data from a variety of solar and interplanetary missions.

Numerical simulations of the phenomenon known as a thermal precursor have been carried out. This precursor is predicted to occur in the solar corona. Numerical simulations for adiabatic and polytropic flow understandably do not illustrate this effect. A new model developed at MSFC illustrates and accurately reproduces the effect, which only occurs in physical situations like that in the solar corona where the propagation speed of a thermal wave is much larger than the sound speed and Alfvén speed.

Research related to coronal mass ejections revealed a link between interplanetary magnetic clouds following shocks observed at Earth, on the one hand, and meter-wave, Type II, flare-related radio bursts, indicative of coronal shock waves and coronal mass ejections near central meridian, on the other. For clouds unrelated to shocks, correlative events are much more difficult to discern. Evidence has been found that many of the magnetic clouds can be associated with x-ray long decay events, and there is very convincing evidence associating at least one magnetic cloud with a disappearing filament. (S. T. Suess/ES52/205-453-2824)

Publications:

Suess, S. T., and E. Hildner, "Deformation of the Heliospheric Current Sheet," _Journal of Geophysical Research_, in preparation.

Suess, S. T., and E. Hildner, "Deformation of the Heliospheric Current Sheet," _Bull. AAS, 16_, 453 (1984).

Suess, S. T., J. M. Wilcox, J. T. Hoeksema, H. Henning, and M. Dryer, "Relationships Between a Potential Field-Source Surface Model of the Coronal Magnetic Field and Properties of the Solar Wind at 1 AU," J. Geophys. Res., 89, 3957 (1984).

Nerney, S. F., and S. T. Suess, "Modeling the Effects of Latitudinal Gradients in the Solar Wind in the Outer Corona," The Astrophysical Journal, in preparation.

Suess, S. T., B. T. Thomas, and S. F. Nerney, "Theoretical Interpretation of the Observed Interplanetary Magnetic Field Radial Variation in the Outer Solar System," Journal of Geophysical Research, in preparation.

Suess, S. T., B. T. Thomas, and S. F. Nerney, "Theoretical Interpretation of the Observed Interplanetary Magnetic Field Radial Variation in the Outer Solar System," EOS, 64, 822 (1983).

Wilson, R. M., and E. Hildner, "Evidence Linking Coronal Mass Ejections with Interplanetary 'Magnetic Clouds'," NASA Technical Memorandum TM-82564, Marshall Space Flight Center, Alabama, December 1983.

Wilson, R. M., and E. Hildner, "Are Interplanetary Clouds Manifestations of Coronal Transients at 1 AU?" Solar Phys., 91, 169-180 (1984).

Hildner, E., and R. M. Wilson, "Are Interplanetary Clouds Manifestations of Coronal Transients at 1 AU?" presented 164th Meeting of the American Astronomical Society, Baltimore, Maryland, June 10-13, 1984.

Statistical Solar Studies

A comparative study of sunspot cycles has revealed several cycle-related parameters that can be evaluated early in a cycle and then used to predict subsequent parameters (e.g., using early slope to predict the maximum sunspot number achieved a few years later). Evidence that the run of solar cycles is bimodal, each cycle occurring either as a short-period cycle (<128 months) or as a long-period cycle (>133 months), has been presented. Further, a period/growth dichotomy is apparent in the sunspot record (1755-1976), which predicts that the current cycle (No. 21) will be a long-period cycle, ending about February 1988 (±6 months). An empirical method for estimating sunspot number was also developed and published. (R. M. Wilson/ES52/205-453-2824)

Publications:

Wilson, R. M., "A Comparative Look at Sunspot Cycles," NASA Technical Paper TP-2325, Marshall Space Flight Center, Alabama, May 1984.

Wilson, R. M., "On Long-Term Periodicities in the Sunspot Record," NASA Technical Memorandum TM-86458, Marshall Space Flight Center, Alabama, July 1984.

Teuber, D. L., E. J. Reichmann, and R. M. Wilson, "Description of Sunspot Cycles by Orthogonal Functions," Astronomy & Astrophysics, in press.

Wilson, R. M., E. J. Reichmann, and D. L. Teuber, "An Empirical Method for Estimating Sunspot Number," presented Solar-Terrestrial Prediction Workshop, Meudon, France, June 18-22, 1984 (to appear in proceedings).

Wilson, R. M., E. J. Reichmann, and D. L. Teuber, "Estimating Sunspot Number," NASA Technical Memorandum, Marshall Space Flight Center, Alabama, in press.

Wilson, R. M., D. Rabin, and R. L. Moore, "Bimodality of the Solar Cycle," Science, submitted.

Transition Region

An empirical study by deLoach et al. of electric current and heating in an active region observed jointly by the MSFC vector magnetograph and the Solar Maximum Mission (SMM) Ultraviolet Spectrometer and Polarimeter (UVSP) led Rabin and Moore to develop a new model of the Sun's lower transition region. The solar transition region traditionally has been regarded as the thermal connection between the corona and the chromosphere; i.e., radiative losses from the transition region have been thought to be balanced by energy transferred down from the corona along magnetic field lines. However, sophisticated models based on this idea fail by orders of magnitude to produce enough emission from the lower transition region (T < 10^5 K). Because of this discrepancy, and because the lower transition region is structurally more like the upper chromosphere than the upper transition region, Rabin and Moore concluded that the lower transition region is not heated by energy transfer from the corona but by in situ heating, as are the chromosphere and corona. For this reason, and because of the suggestive results of deLoach et al., they explored a new model of the lower transition region based on ohmic heating by filamentary electric currents that flow along field lines in closed magnetic loops isolated from the corona (Figure 29).

To supply the observed radiative loss from the lower transition region, Rabin and Moore showed that the current filaments must be very thin (with a narrow dimension in the range 1 cm to 1 km), that the magnetic field must be greater than about 10 gauss (in agreement with the observed field strength in regions of enhanced heating), and that the ohmic heating is balanced locally by thermal conduction out the sides of the current filaments. In contrast to conventional models, this model produces a distribution of emission measure over temperature that is in good agreement with observations of the lower transition region (Figure 30).

In the new view of the transition region sketched in Figure 29, the magnetic field that fills the upper transition region and corona is rooted in a small fraction of the solar surface. The consequent constriction of this field inhibits the conduction of heat down from the corona, thereby strongly affecting the energy balance in the corona and upper transition region. Dowdy, Moore, and Wu clarified how the shape of the constriction acts together with the amount of constriction to inhibit the heat flow. This effect might allow the corona to be sustained by much less heating than previously thought.

3 X 10⁴ km ... ≲ 1 km
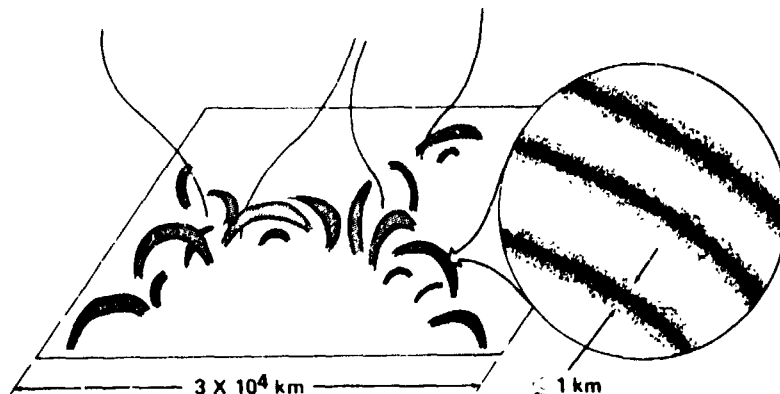
Figure 29. Sketch of the Magnetic Structure of the Transition Region Envisioned in the Model of Rabin and Moore. Most of the plasma in the lower transition region ($10^4 < T \lesssim 10^5$ K) is contained in small magnetic loops of length $<5 \times 10^3$ km distributed along the emission network; only a small fraction of the lower transition region is in the feet of field reaching into the corona. As depicted in the enlargement, the heating in the small loops is by field-aligned currents of much finer scale (<1 km in diameter), each surrounded by a sheath heated by cross-field thermal conduction.

Analysis of ultraviolet observations by Porter, Toomre, and Gebbie revealed frequent and rapid fluctuations in transition region line emission at selected bright points in an active region. The observations were obtained using a very high sampling rate mode of the UVSP onboard SMM. Intensity increases of 20 to 100 percent lasting for 20 to 60 seconds were common. The UV emission appears to be coming mostly from small unresolved elements within the spatial sampling window of 3 x 3 arc seconds. Some modulations in intensity were found to correlate with jitter in the satellite pointing, allowing estimates of the possible size and contrast of these bright elements.

These relatively weak brightenings occur more often than those of larger amplitude detected with the Orbiting Solar Observatory (OSO) 8; the energetic events classified as flares are even more rare. Further, the characteristics of the brightenings are consistent with an almost instantaneous heating event followed by radiative cooling. The results suggest that heating due to magnetic field reconnection within an active region is proceeding almost stochastically; events involving only a modest release of energy occur most frequently. (R. L. Moore/J. G. Porter/ES52/205-453-0118).

Publications:

Rabin, D., and R. Moore, "Heating the Sun's Lower Transition Region with Fine-Scale Currents," The Astrophysical Journal, in press.

deLoach, A. C., M. J. Hagyard, D. Rabin, R. L. Moore, J. B. Smith, Jr.,
E. A. West, and E. Tandberg-Hanssen, "Photospheric Electric Current
and Transition Region Brightness Within an Active Region," Solar
Phys., 91, 235-242 (1984).

Dowdy, J. F., Jr., R. L. Moore, and S. T. Wu, "Inhibition of Conduction
Heat Flow by Magnetic Constriction in the Corona and Transition
Region: Dependence on the Shape of the Constriction," Solar Physics,
in press.

Porter, J. G., J. Toomre, and K. B. Gebbie, The Astrophysical Journal, in
press.
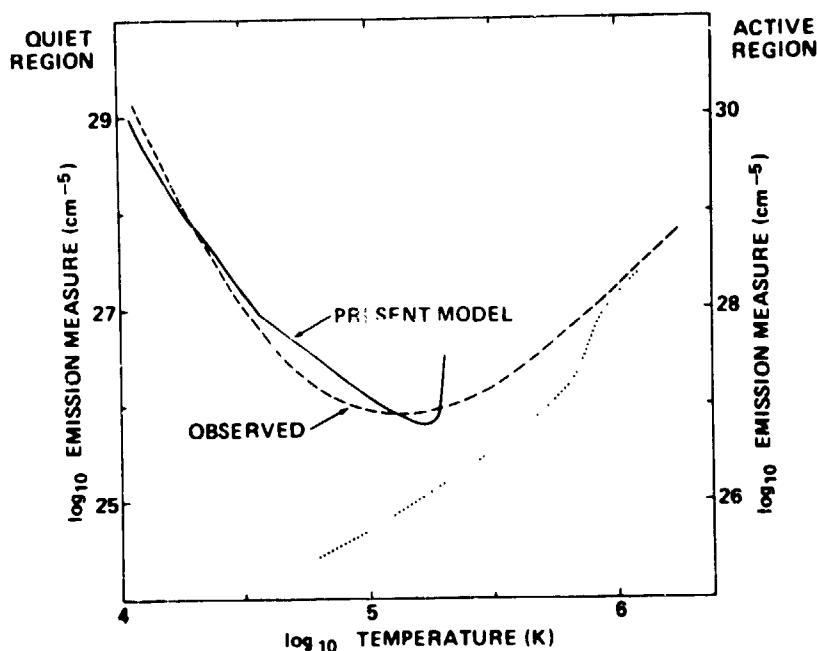
Figure 30. The Differential Emission Measure as a Function of Temperature
Through the Transition Region. The dashed curve is the ob-
served distribution. The solid curve is for the model of Rabin
and Moore: thin filaments heated by ohmic dissipation and
cooled by cross-field thermal conduction in combination with
radiation. The dotted curve is for a model of Athay; it illu-
strates that transition region models based on heating by ther-
mal conduction from the corona produce qualitatively correct
behavior in the upper transition region $(T > 10^5$ K) but fail
completely in the lower transition region $(T < 10^5$ K).

Magnetospheric Physics

Introduction

The relative importance of the Earth's ionosphere versus the solar
wind as the principal source of plasma in the terrestrial magnetosphere

46

continues to be the primary focus of research activities of the Magneto-spheric Physics Branch at MSFC. This research objective requires a complete understanding of the Earth's supply source, the ionosphere, which involves the effective measurement of the energy, composition, and dynamics of this plasma region combined with the measurement of the transport of these plasmas up into the magnetosphere. To aid in the understanding of the important physical processes that provide interchange of plasma between the ionosphere and magnetosphere, the Magnetospheric Physics Branch at MSFC is involved in the development, testing, and analysis of data from new instrumentation which measures the composition, transport, and energization of low-energy plasma in the near Earth environment. These R&T activities have laid the groundwork for the successful developmer of instrumentation for projects such as Spacecraft Charging at High Altitudes (SCATHA), Dynamics Explorer (DE), International Solar-Terrestrial Physics (ISTP), and Spacelab 1 and 2. These projects are major contributors to the knowledge of the origin of magnetospheric plasmas. The various R&T activities which have contributed to the development and testing of new instrumentation and to the analysis of the acquired data using the Space-plasma Computer Analysis Network (SCAN) are related to the overall discipline of solar-terrestrial physics in the following paragraphs. (C. R. Chappell/ES51/205-453-3036)

Retarding Ion Mass Spectrometer (RIMS)

Instrument development activities supported by R&T funds over the past several years made possible the successful design and development of the Retarding Ion Mass Spectrometer (RIMS) which was flown on the Dynamics Explorer (DE) 1 spacecraft. Since its launch in August 1981, it has functioned well and made possible an exploration of the near Earth thermal plasma in a manner never before possible. The instrument's ability to measure the low-energy (0 to 50 eV), three-dimensional distribution function for all major ion species has made possible the discovery of several new major components of magnetospheric plasma. These important new findings include (1) verification of the supersonic nature of the polar wind, (2) discovery of an ionospheric geomagnetic mass spectrometer in the polar cusp, (3) important new findings about low-energy plasma in the nightside plasmasheet, and (4) increased understanding of the refilling and energization of the plasmasphere.

One of the important theoretical questions concerning the light ion outflow from the Earth's ionosphere known as the polar wind is whether the ion outflow is subsonic or supersonic. Continued analysis of the DE 1/RIMS polar wind data has verified that the polar wind can indeed be super-sonic. The importance of the polar wind as a source of magnetospheric plasma remains an open question which is presently being pursued using the DE 1/RIMS data.

The polar wind is not the only source of low-energy ion outflow from the high-latitude ionosphere into the magnetosphere. Perhaps the most interesting discovery by RIMS this past year has been a statistical study of high-latitude outflows which has revealed an intense localized source of H^+, He^+, and O^+ ions in the region of the polar cusp. H^+, He^+, and O^+ with fluxes exceeding 10^9 cm^{-2} s^{-1} appear to be upwelling from the topside ionosphere in the region of the polar cusp. The ions appear to receive equal

amounts of energization regardless of their ion identity. As a result, H^+ ions have a larger field-aligned flow velocity than He^+ ions, which, in turn, have a larger field-aligned flow velocity than O^+ ions. As a result of the mass independent velocity filter due to $\vec{E} \times \vec{B}$ ion convection, the various ion species are spread across the polar cap by the action of the geomagnetic mass spectrometer. Such an example is shown in Figure 31, where a combination of ion trajectory modeling and DE 1 and 2 ion measurements have been used to trace the geomagnetic mass spectrometer from its localized source in the topside ionosphere (DE 2 data) to its extended outflow over the polar cap at high altitudes (3 R_E DE 1 data). This new source of O^+ ions appears to be connected to the earlier RIMS observations of low-energy O^+ over the polar cap, and its large source strength of $>10^{25}$ O^+ ions per second makes it an important, if not dominant, source of magnetospheric O^+. Indeed, one of the most intriguing attributes of this O^+ outflow is that its relatively small field-aligned velocity coupled with strong antisunward ion convection makes it an important potential source of O^+ to feed the auroral acceleration region and nightside plasmasheet.

The RIMS data taken during periods when the apogee of DE 1 was located near the equatorial plane afforded the opportunity to obtain field-aligned ion measurements for several hours near the plasmapause boundary and at the inner edge of the plasmasheet. The most intriguing aspect of this data has been the frequency of occurrence of equatorially trapped and heated ions and micropulsation-induced oscillations of the thermal plasma. Both of these processes indicate the importance of particle-wave interactions in the dynamics of the plasmasheet.

The RIMS Pc5 event on July 14, 1982, has been studied in detail using both wave and particle measurements onboard the DE 1 spacecraft. For the first time, particle measurements have been closely compared to direct measurement of the quasi-static electric field. A remarkable degree of similarity in the measurements is demonstrated in Figure 32. Such direct comparisons promise to give new insight into the source of energization of Pc5 oscillations. In addition, calculations of the resonant period from ion mass loading measurements indicate that both cold and hot heavy ions play a significant role in determining the propagation and standing resonance characteristics of low-frequency plasma waves in the plasmasheet.

The equatorial DE 1 apogee passes have also been used in conjunction with the Geosynchronous Earth Orbiting Satellite (GEOS) data to study the refilling of the outer plasmasphere. Here one finds an extremely complex picture that does not readily agree with the simple theory of an equatorial two-stream instability that leads to downward propagating shock fronts; i.e., a plasmasphere that fills from the top down. The DE/GEOS data set indicates an extremely dynamic situation with large hemispherical ion density and pitch angle asymmetries that seem to be present throughout the refilling process. This study has only begun to scratch the surface of this interesting subject, and much more research is needed before a coherent physical description of plasmasphere refilling can be introduced.

The study of the thermal structure of the plasmasphere is another major accomplishment of RIMS during FY-84. Initial results indicate a hot outer plasmasphere whose radial thermal gradient appears to be intimately tied to the level of geomagnetic activity; i.e., the higher the magnetic

activity, the colder the inner nightside plasmasphere, and the stronger the radial thermal gradient. These observations may suggest important propagation effects for wave-particle heating processes that are changed as a result of geomagnetic activity; i.e., the steepness of the plasmapause density gradient.
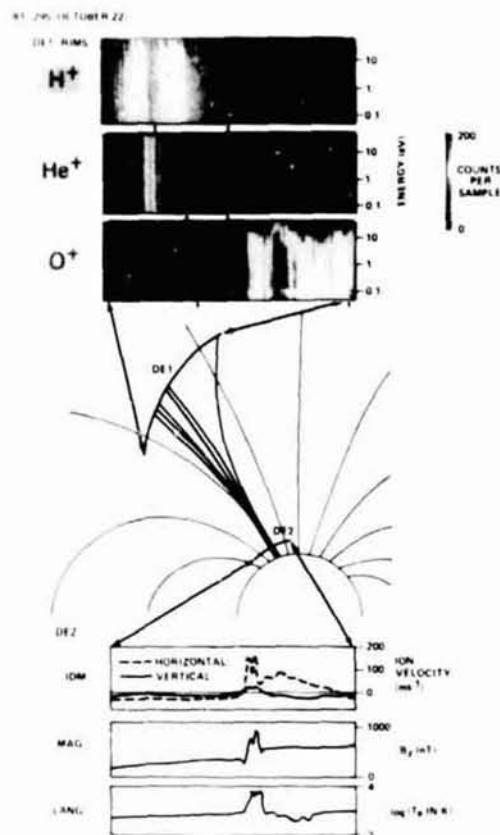
Figure 31. Energy Spectrograms from DE RIMS. Top three panels: sample modeled ion trajectories (O^+, He^+, and H^+). Lower portion: observations for three experiments on DE 2 for a close-field conjunction between the two satellites. The ions observed by RIMS are traced back to a narrow source region (common to all three ion species) at the dayside cusp for a model dawn-dusk convection electric field. Characteristic flow, temperature, and magnetic field signatures are observed by DE 2 at this source location. The RIMS spectrograms display mass and energy dispersions of ionospheric ions injected into the polar magnetosphere at the dayside cusp.

These are only a brief glimpse at a whole host of exciting discoveries of the near Earth low-energy plasma which have been made possible by the DE/RIMS project and the associated R&T research activities that are an intimate part of this research. (J. H. Waite/ES53/205-453-3918)
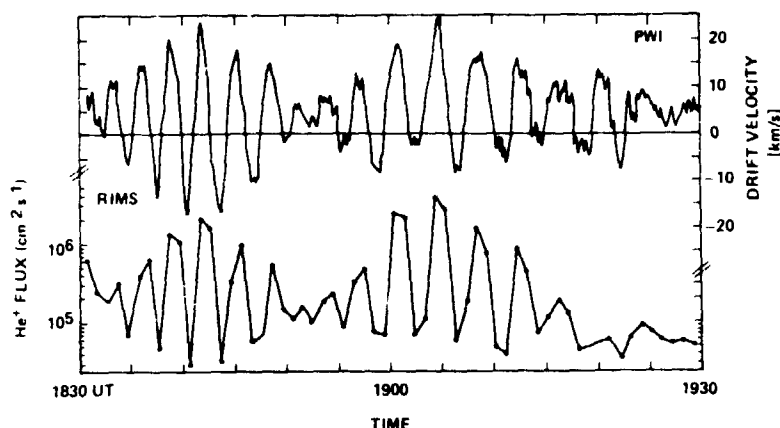
Figure 32. Close Correlation of Field-Derived Flow Velocity and Measured He$^+$ Flux along the DE 1 Spin Axis for the Pc5 Event of July 14, 1982. Upper panel: drift velocity component along the DE 1 spin axis. Drift velocity is derived from $\vec{E}$ x $\vec{B}$, where the electric and magnetic fields are measured by the static electric field (PWI) and magnetometer instruments, respectively. Bottom panel: flux of He$^+$ determined from measurements by the -Z head of the RIMS.

Publications:

Waite, J. H., Jr., J. L. Horwitz, and R. H. Comfort, "Diffusive Equilibrium Distributions of He$^+$ in the Plasmasphere," Planet. Space Sci., 32, 611 (1984).

Waite, J. H., Jr., T. Nagai, J.F.E. Johnson, C. R. Chappell, J. L. Burch, T. L. Killeen, P. B. Hays, C. R. Carigan, E. G. Shelley, and W. Peterson, "Escape of Suprathermal O$^+$ Ions in the Polar Cap," Journal of Geophysical Research, submitted.

Green, J. L., and J. L. Horwitz, "Magnetospheric Processes in the Plasmapause," EOS, 65, 110 (1984).

Horwitz, J., "Relationship of Dusk Sector Electric Field to Electron Dispersion at the Inner Edge of the Plasma Sheet," J. Geophys. Res., 89, 3011 (1984).

Horwitz, J., and C. R. Chappell, "Menu of DE-1 Low-Energy Plasma Phenomena for Finnish Collaboration," in Proceedings of Second United States-Finland Workshop on Magnetospheric and Ionospheric Phenomena in Auroral Regions, eds., T. J. Rosenberg and J. Oksmann (University of Maryland: College Park, Maryland), pp. 69-77 (1984).

Nagai, T., J. H. Waite, Jr., J. L. Green, C. R. Chappell, C. R. Olsen, and H. L. Comfort, "First Measuremens of Supersonic Polar Wind in the Polar Magnetosphere," Geophys. Res. Lett., 11, 669 (1984).

Chappell, C. R., "Cold Plasma Distribution Above a Few Thousand Kilometers at High Latitudes," in High-Latitude Space Plasma Physics, eds., Bengt Hultqvist and Tor Hagfors (Plenum Publishing Corporation: London), pp. 251-269 (1983).

Ionosphere/Plasmasphere Modeling and Coordinated Measurements

The results from the simultaneous observations of the high-latitude ionosphere and magnetosphere using Dynamics Explorers (DE) 1 and 2 and the Chatanika radar and from numerical simulations are reported in a research article which is currently under peer review. This work identified plasma boundaries at high latitudes and showed how the boundaries mapped from the ionosphere to the magnetosphere. Combining data from several instruments allowed the dynamics and energetics of these ions to be outlined. Numerical modeling results showed how plasma is exchanged between the ionosphere and the outer plasmasphere.

Data from the coordinated satellite and ground-based radar observations at low-latitudes have been reduced and initial comparisons made. The combination of these two data sets has provided profiles of temperature and density vs. altitude from 200 to 6000 km over a narrow range of L-values $(1.5 < L < 1.9)$. Further analysis is being done by the co-investigators to more fully understand some of the more interesting results such as the small gradients in ion temperature and the high ratio of electron temperature to ion temperature at high altitudes. Figure 33 is an example of one such comparison. Numerical modeling has continued with emphasis on understanding these interesting features in the thermal structure of the ionosphere and plasmasphere.

In an extension of the current plasmasphere modeling effort, a model of the density, temperature, and velocity of the minor ions O^{++} and N^+ has been added to the existing plasmasphere model. This work has been done in conjunction with scientists at the University of Michigan. Extensive testing of this new model and comparisons with previous models have been done. The contribution of thermal diffusion to the structure and composition of minor ions in the plasmasphere is being studied. Comparisons to observations of O^{++} and N^+ made by the DE/Retarding Ion Mass Spectrometer are being used in this study. (J. H. Waite/M. O. Chandler/ES53/205-453-3918)

Publication:

Green, J. L., J. H. Waite, Jr., M. O. Chandler, C. R. Chappell, J. R. Doupnik, P. G. Richards, R. Heelis, S. D. Shawhan, and L. H. Brace, "Observations of Ionospheric/Magnetospheric Coupling: DE and Chatanika Coincidences," Journal of Geophysical Research, submitted.

51
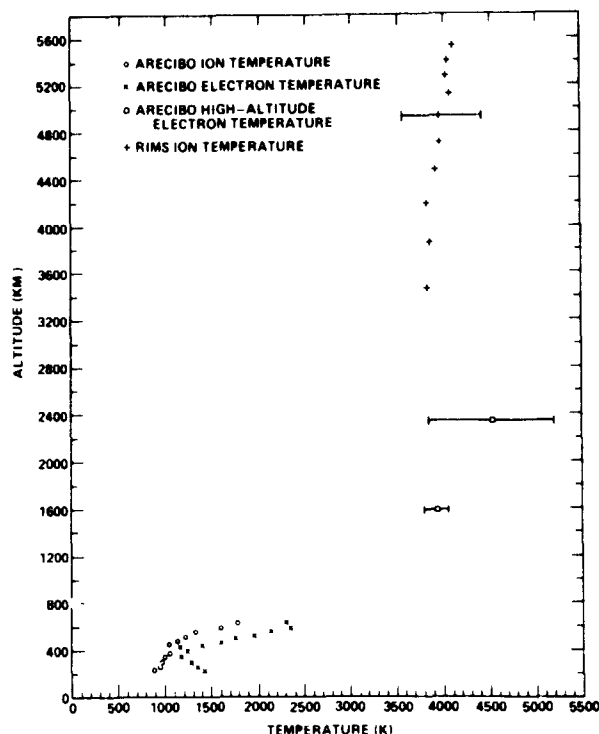
Figure 33. Electron and Ion Temperature Measurements from the Arecibo Radar and the RIMS taken on March 6, 1983 (data shown are 11 hours LT for the F-region, 11 to 13 hours LT for the high-altitude radar, and 11.6 hours LT for the RIMS).

Light Ion Mass Spectrometer (LIMS)

Analysis of data from the LIMS on the Spacecraft Charging at High Altitudes (SCATHA) satellite has continued. A characterization of the plasma in the plasmasphere and plasma trough regions in terms of density, temperature, mass composition, and flow velocity has been made and published. The data are presently being converted for storage and use on the VAX computer system at MSFC. Data tapes that are now aging will be copied for continued archiving. (D. L. Reasoner/P. D. Craven/ES53/205-453-3037)

Publication:

Reasoner, D. L., P. D. Craven, and C. R. Chappell, "Characteristics of Low Energy Plasma in the Plasmasphere and Plasma Trough," J. Geophys. Res., 88, 7913-7925 (1983).

Superthermal Ion Composition Spectrometer (STICS)

The Superthermal Ion Composition Spectrometer (STICS) was successfully flown on the Norwegian poleward leap sounding rocket. The primary objective of STICS in this program was the measurement of transversely accelerated ionospheric ions with energies in excess of 10 eV. Although the rocket passed over very active auroral forms, no evidence of such acceleration was observed in this flight, which had an apogee of 450 km altitude. It is known that such acceleration of ionospheric plasma is infrequent at such altitudes, there being only one observation of this phenomenon below 1400 km. One lesson learned from this program, and from the observations of the Retarding Ion Mass Spectrometer (RIMS) instrument on the Dynamics Explorer (DE) satellite, is that study of this phenomenon requires instrumentation capable of simultaneously observing both the thermal ionospheric plasma and its higher energy superthermal tail. Moreover, the optimal instrumentation will have differential energy response, so that the full distribution may be mapped out.

A more complete evaluation of STICS than had previously been possible was done in the Low-Energy Ion Facility at MSFC. Though the instrument behaved nominally at the energies for which it was designed, it became apparent that modifications will be necessary in order to achieve the desired response down to very low energies on the order of fractions of an electron volt. STICS will fly this winter on the University of New Hampshire's TOPAZ and ARCS 3 rocket payloads. The tight schedule and limited resources available do not permit a redesign prior to these flights; however, TOPAZ will fly to altitudes above 1000 km where it is much more likely to encounter transverse acceleration regions. ARCS 3 will contain an active experiment emitting ions in the tens of electron-volt energy range, so that STICS is needed to monitor the ion beam and any artificially induced ion acceleration processes. In addition to the analysis of results of these programs, FY-85 efforts will be directed toward the design of an instrument having the differential energy response of STICS and the low-energy range capability of RIMS. (T. E. Moore/ES53/205-453-0818)

Publications:

Kintner, P. M., J. LaBelle, M. C. Kelly, L. J. Cahill, Jr., T. E. Moore, and R. L. Arnoldy, "Interferometric Phase Velocity Measurements," Geophys. Res. Lett., 11 19 (1984).

Moore, T. E., "Superthermal Ionospheric Outflows," Reviews of Geophysics and Space Physics, in press.

Moore, T. E., A. P. Biddle, and J. H. Waite, Jr., "Auroral Zone Effects on Hydrogen Geocorona Structure and Variability," Planetary Space Science, submitted.

Moore, T. E., C. R. Chappell, M. Lockwood, and J. H. Waite, Jr., "Superthermal Ion Signatures of Auroral Acceleration Processes," Journal of Geophysical Research, in press.

Arnoldy, R. L., C. J. Pollock, L. J. Cahill, Jr., and T. E. Moore, "Low-Altitude Field-Aligned Electrons," Journal of Geophysical Research, in preparation.

Body-Plasma Electrodynamic Interaction Studies

The investigation of the electrodynamic interaction of a flowing, rarefied plasma with test bodies in the laboratory is an ongoing effort which continues to contribute to the understanding of this basic physical problem and its possible applications to solar system plasma physics and to spacecraft-space plasma electrodynamic interactions. Specifically, certain physical mechanisms can be studied (such as the dynamical behavior of binary or multispecies plasmas) which may have relevance to the plasma electrodynamic interaction with natural bodies in the solar system. From a technical point of view, the spacecraft-space plasma interaction creates a disturbed region in the ambient medium in which diagnostic instruments must operate to determine the ambient plasma characteristics. The laboratory results have proven to be useful in analyzing in situ data, particularly in a recent new look at data from the Ariel 1 and Explorer 31 satellites and in planning and interpreting experiments for Spacelab. In addition, enhanced investigation of the anomalous ionization of neutrals in the vicinity of positively charged surfaces in a background plasma has been made. This study may have broad applications to large structures in space and to the electrodynamic tethered satellite system missions. In addition, this ground-based effort points the way toward orbital experiments which make use of the same experimental techniques and instrumentation developed for the laboratory to simulate solar system body-plasma interactions such as the interaction caused by the moon Io moving within the Jovian magnetosphere. The dimensionless scaling parameters indicate that the ionosphere at 300 km provides similar conditions to the Jovian environment of Io. This makes possible a relatively inexpensive and timely method of investigating such solar system plasma phenomena which should permit a greater scientific return from subsequent planetary missions. Investigations have been made on the potential for orbital studies of a specific effect of interest to solar system plasma physics--the expansion of plasma into a vacuum or a more rarefied region.

The direction of the laboratory effort in FY-84 has been to continue the study of binary (two species) plasma flows in order to more accurately simulate the multiconstituent ionospheric plasma. This will permit investigation of the interaction between combinations of heavy and light ions in the presence of strong density and potential gradients. It is thought that this interaction may generate instabilities and oscillations in the wakes of ionospheric satellites and in the vicinity of natural density gradients produced in various solar system plasmas. This capability will also provide a more characteristic environment for flight instrument test and calibration.

A dual ion plasma accelerator which was breadboarded for this purpose has been studied, and the construction of an optimized design is nearing completion. This binary plasma source will allow the generation of two completely independent streams of ions which are then superimposed and neutralized to form a single binary plasma stream. This permits the

selection of different masses, drift energies, and densities for each species of the stream.

The Differential Ion Flux Probe (DIFP), which was previously developed to provide differential vector measurements of ion flow direction, density, and energy, has been successfully flown on the STS-3 mission as part of the Plasma Diagnostics Package experiment (Figure 34) and on two Project Centaur Multiple Auroral Probe sounding rocket missions. Initial results from the STS-3 mission have shown how the ionospheric environment is perturbed by the motion of the shuttle and have given new insights into plasma flow phenomena around large target bodies, including the creation of secondary ion streams at large angles of attack with respect to the ram current, as shown in the data insert of Figure 34. These ion streams are shown schematically in Figure 35. (N. H. Stone/ES53/205-453-0029)

Publications:

Stone, N. H., U. Samir, K. H. Wright, Jr., D. L. Reasoner, and S. D. Shawhan, "Multiple Ion Streams in the Near Vicinity of the Space Shuttle," Geophys. Res. Lett., 10, 1215 (1983).

Stone, N. H., B. J. Lewter, W. L. Chisolm, and K. H. Wright, "An Instrument for Differential Ion Flux Vector Measurements on Spacelab 2," Review of Scientific Instruments, in preparation.

Stone, N. H., K. H. Wright, Jr., and U. Samir, "The Extent of the Disturbed Plasma Environment of the Space Shuttle Orbiter: A Preliminary Assessment," Planetary Space Science, in preparation.

Murphy, G., N. DeAngelo, J. Pickett, S. D. Shawhan, U. Samir, N. H. Stone, and K. H. Wright, Jr., "Elevated Plasma Temperature in the Near Wake of the Shuttle Orbiter," Transactions American Geophysical Union, EOS, in press.

Samir, U., R. H. Comfort, N. H. Stone, and C. R. Chappell, "Thermal Ions in the Wake of the DE 1 Satellite," Transactions American Geophysical Union, EOS, in press.

Wright, K. H., Jr., N. H. Stone, and U. Samir, "A Comparison Between the Interactions of the Space Shuttle and Small, Unmanned Satellites with the Ionosphere," Transactions American Geophysical Union, EOS, in press.

Samir, U., N. H. Stone, and K. H. Wright, "The Excursion of Highly Rarefied Space Plasma into a Vacuum," presented General Assembly of the International Union of Radio Science, Florence, Italy, August 28-September 5, 1984.

Wright, K. H., Jr., N. H. Stone, and U. Samir, "A Study of Plasma Expansion Phenomena in Laboratory Generated Plasma Wakes: Preliminary Results," Journal of Plasma Physics, submitted.

STUDY OF BODY/PLASMA (ORBITER/IONOSPHERIC) ELECTRODYNAMIC INTERACTIONS
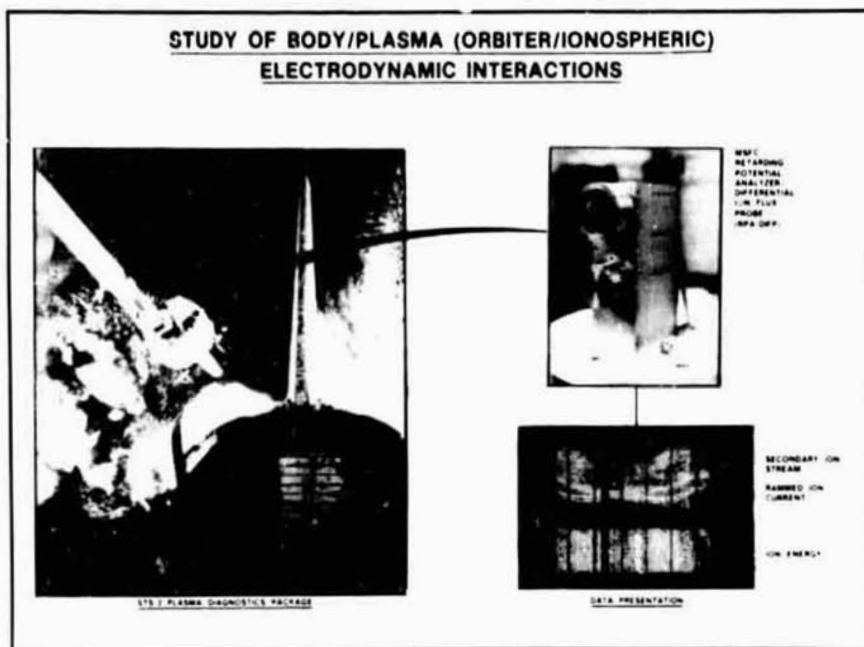
Figure 34. MSFC RPA/DIFP Instrument on the STS-3 PDP and Detection of Secondary Ion Streams in Addition to the Ram Ion Current.
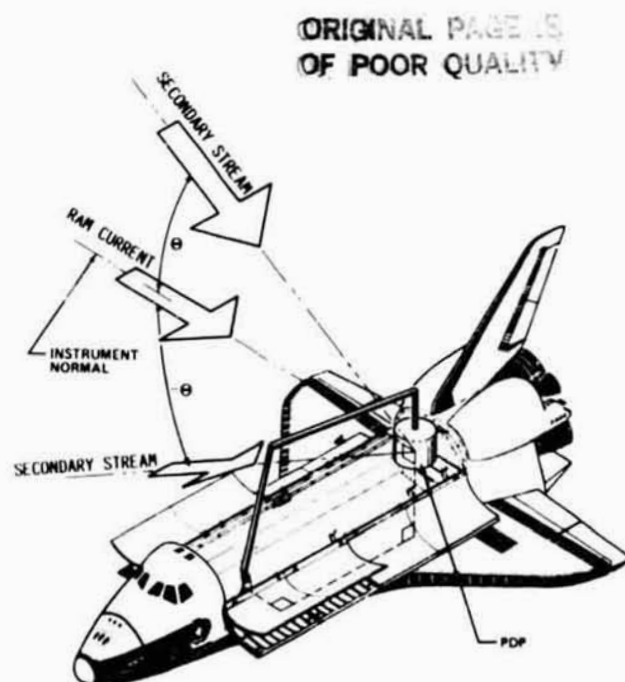
Figure 35. Position and Orientation of the PDP and the Ram and Secondary Ion Streams with Respect to the Space Shuttle Orbiter.

56

Particle Acceleration Mechanisms in the Auroral Zone

In December 1981, two Differential Ion Flux Probe (DIFP) instruments were provided for the Multiple Auroral Probe (MAP) 1 and 2 sounding rocket payloads. This campaign was designed to investigate charged particle acceleration mechanisms in the polar cleft region of the Earth's magnetosphere with the motion of the thermal ions being provided by the DIFP. The preliminary results show a strong azimuthal asymmetry (around the field lines) of the thermal ion motion with an upward drift within the cleft. As the rocket emerged from the cleft and passed into the polar cap region, the vertical component of the ion motion changed directions and became directed Earthward. In addition to geophysics effects, it appears that the data set will provide a significant insight into spacecraft charging effects in the polar region of the magnetosphere. Data from the Southwest Research Institute Charged Particle Spectrometer are now being analyzed to provide ion energy measurements when the range of the DIFP instrument was exceeded (this occurred much of the time within the cusp). This will allow ion pitch angle determinations for two active missions. These effects will be published next year in the Canadian Journal of Physics. (N. H. Stone/ES53/ 205-453-0029)

Retarding Potential Analyzer/Differential Ion Flux Probe (RPA/DIFP)

The RPA/DIFP was successfully flown on the University of Iowa Plasma Diagnostics Package on the STS-3 mission. The primary scientific objective of the instrument was to study the plasma environment around the shuttle Orbiter with particular emphasis upon perturbations to the plasma environment produced by the Orbiter wake and sheath effects and by electron beam emissions from the Fast Pulse Electron Gun experiment. The instrument performed perfectly in all respects, and approximately 64 hours of flight data were received. The data show that the Orbiter produces significant perturbations to the local plasma. Analysis of directional ion flow data has revealed the presence of multiple ion streams due to the interactions between the Orbiter and the ionospheric plasma.
(N. H. Stone/D. L. Reasoner/ES53/205-453-0029)

Spacecraft-Plasma Interactions

Environmental effects on spacecraft include the charging of spacecraft by the ambient plasma. Such charging can cause effects which range from the annoying, such as distortions in plasma measurements, to catastrophic, as in the loss of a satellite due to arcing and high-voltage (kilovolt) discharges. The study of such processes is based on analysis of the interaction between satellite and plasma, based, in turn, on studies of the environment.

During FY-84, analysis of thermal plasma data from the Retarding Ion Mass Spectrometer (RIMS) has been surveyed to determine the change in spacecraft potential which occurs when the satellite is eclipsed. When the plasma density is over 100 cm^{-3}, i.e., in the plasmasphere, potential shifts of less than a volt are observed. The bulk of the plasma population can be observed, and there are no hidden populations for this experiment.

An apparent cold population noted previously has been shown to be an instrumental artifact.

Application of the aperture bias charging model developed last year has been made in the analysis of the supersonic polar wind and in the interpretation of a cold plasma background discovered high above the polar cap.

Data from the European Geosynchronous Earth Orbiting Satellite (GEOS) 2 were compared with data from the Spacecraft Charging at High Altitudes (SCATHA) satellite to determine if the particle and wave experiments on GEOS could observe the hidden ion population observed by the SCATHA electrostatic analyzers in eclipse. It was found that the active boom bias technique used on GEOS 2 was generally successful in making the hidden ion population visible even when GEOS 2 was in sunlight.

Electric field observations on high-altitude satellites are heavily contaminated by a 1 mV/m sunward electric field caused by Sun-induced photo emission. Measurements taken in eclipse allow observation of electric fields at substantially lower levels (down to 0.1 mV/m on the SCATHA satellite). Analysis of such data taken near the plasmapause at local midnight allows sensitive tests of the continuity of the electric field across that boundary. Generally, there is little or no variation, only a monotonic variation with penetration into the plasmasheet. Figure 36 shows one example. (R. C. Olsen/ES53/205-453-0505)

Publications:

Olsen, R. C., P.M.E. Decreau, J.F.E. Johnson, G. L. Wrenn, K. Knott, and A. Pedersen, "Comparison of Thermal Plasma Observations on SCATHA and GEOS," in Proceedings of the 17th ESLAB Symposium on "Spacecraft-Plasma Interactions and Their Influence on Field and Particle Measurements," ESA SP-198, eds., A. Pedersen, D. Guyenne, and J. Hunt (ESTEC: Noordwijk), pp. 57-61 (1983).

Nagai, T., J. H. Waite, Jr., J. L. Green, C. R. Chappell, R. C. Olsen, and R. H. Comfort, "First Measurements of Supersonic Polar Wind in the Magnetosphere," Geophys. Res. Lett., 11, 669-672 (1984).

Olsen, R. C., D. L. Gallagher, C. R. Chappell, J. L. Green, and S. D. Shawhan, "The Hidden Ion Population - Revisited," EOS, 65, 256 (1984).

Gallagher, D. L., J. D. Menietti, A. M. Persoon, J. H. Waite, Jr., and C. R. Chappell, "Evidence of High Densities and Ion Outflows in the Polar Cap During the Recovery Phase," EOS, 65, 256 (1984).

Ledley, B. G., R. C. Olsen, and T. L. Aggson, "Observation of dc Electric Fields Near the Plasmapause," EOS, 65, 256 (1984).
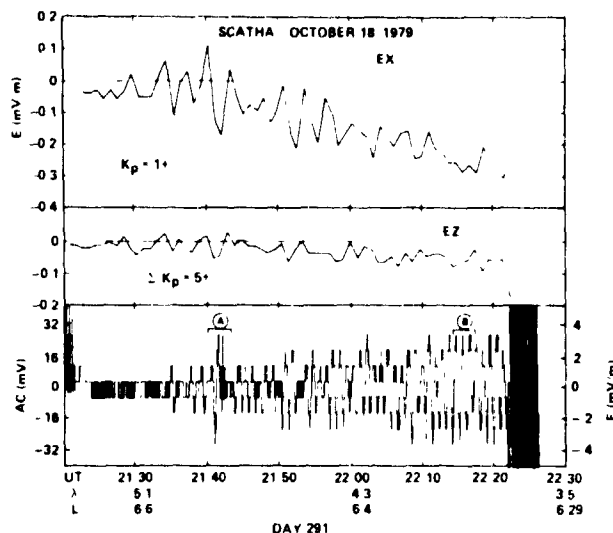
Figure 36. Electric Field Data from the SCATHA Satellite. The satellite moves from the plasmasphere, at the beginning of the plot, through the plasmapause, at 21:40, on into the plasmasheet. Top panel: electric field component in the Sunward direction. Bottom panel: raw data showing field fluctuating briefly at the plasmapause. As the satellite moves into the plasmasheet, there is a monotonic increase in the field in the tailward direction.

MSFC/SPAN System

The Space Physics Analysis Network or SPAN (formally called SCAN) has expanded greatly this year from 9 to 22 remote computer nodes. The SPAN system has continued to be used as a test bed between space science investigators with the intent of exploring and employing modern computer and communication technology as a tool for doing space science research. This can be accomplished since SPAN is not a project-dependent system that requires a static hardware and software configuration for the duration of a mission.

As shown in Figure 37, the location of the nodes in the network are: the Southwest Research Institute (Texas), University of Texas at Dallas, Los Alamos National Laboratory, Stanford University, Utah State University, the University of Iowa, the University of Michigan (Space Physics Research Laboratory), Goddard Space Flight Center, the University of Alabama-Huntsville, TRW, Lockheed, University of California-San Diego, University of California-Los Angeles, and the Space Science Laboratory at Marshall Space Flight Center (MSFC). The number of computers linked into the network at each of the above listed nodes is shown in Figure 37 in parentheses. The central node of the SPAN system is at MSFC.

There are several capabilities and features that the SPAN network is developing which make it unique within the space science community. SPAN can support many users simultaneously at each remote node through computer to remote computer communication software. Users at their institutions can

participate in a number of network functions involving other remote computer facilities. Data files and graphics files can be transferred between network nodes. Program execution can be initiated from any of the network nodes (distributive processing). All of the nodes have the capability for message routing enabling the remote nodes to communicate with each other as if a direct phone line existed between them even though they may not be adjacent nodes.
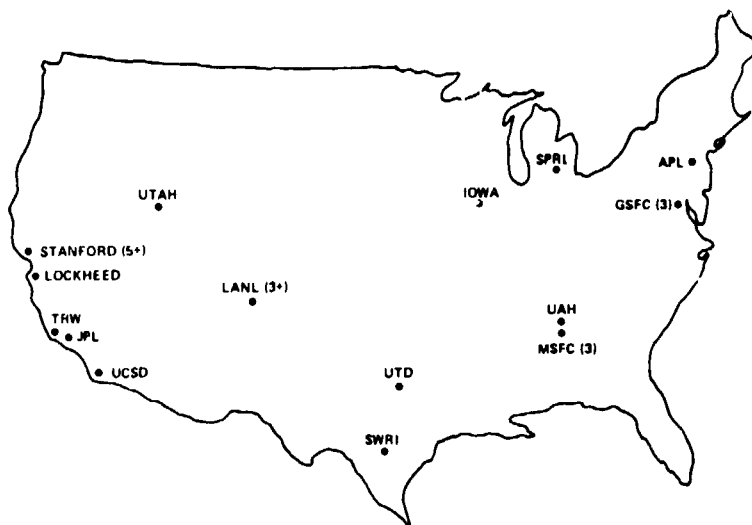
Figure 37. Current SPAN System Nodes. The number of computers linked into a local area network is shown in parentheses.

Another important feature of this network is that remote users have easy access to each other through an electronic mail facility. Data and message communication over the SPAN network is done routinely with relative ease and is not labor intensive. Coordinated workshop periods enable physicists to attack a science problem by interactive analysis utilizing both local and remote computing facilities and data bases.

The trading of software has been extensive in the space science community over SPAN with strong indications that it will continue in the following years. The network has also been extensively used for the transmission and reception of scientific manuscripts. All the above capabilities of SPAN have helped scientists to significantly reduce the time it takes to perform correlative work with authors located across the country. SPAN has been used to complete the analysis of more than 30 scientific papers.

Because of SPAN's distributive nature, computational and technological systems are available for remote investigator use. A new technological system nearing completion is being developed at MSFC under the Data System Technology Program (DSTP). The DSTP utilizes large optical disk storage and the latest in fiber optics technology to create a system capable of capturing up to 10^{13} bits of data at rates up to 50 Mb/s. This large archive keeps all its data online and accessible through a developed data base management system. The DSTP has been used by many space scientists at the remote network nodes.

60

Because of SPAN's capabilities, the use of this network for Spacelab-related activities occurred naturally this year. Spacelab 1 investigators used SPAN for devising instrument operation plans, message or mail transmission, data analysis, data storage, data retrieval, data exchange, and software development tasks. Also, investigators connected to SPAN have been utilizing the network for development of investigations to be flown on Spacelab 2 and 3 and have demonstrated the effectiveness of the network in reducing the time required to transfer mission specific information, to respond to queries from the project office, and to develop instrument requirements. As more Spacelab Principal Investigators and Co-Investigators are connected into the network, the Spacelab-related activities will greatly increase.

Another space facility that is now available through the SPAN system is the MSFC Mission Integration and Planning Systems (MIPS). Investigator inputs into the MIPS through SPAN include: experiment functional objectives, physical size and pointing information, and other similar payload information required for mission implementation. In return, MIPS electronically provides a large amount of vital mission schedule information.

The SPAN system currently connects the largest number of U.S. Spacelab investigators into a common computer network. It is anticipated that this network will continue to provide a means for accomplishing scientific research in the easiest and most cost effective manner. The network, with advice from the Data System Users' Group (consisting of SPAN and prospective SPAN science users), brings into NASA and the scientific community needed technological expertise, thus increasing the capabilities and productivity of today's scientists. (J. L. Green/ES53/205-453-0028)

Publications:

Baker, D. N., R. D. Zwickl, and J. L. Green, "NASA Data Systems Users," EOS, 65, 46 (1984).

deLoach, A. C., M. J. Hagyard, D. Rabin, R. L. Moore, J. B. Smith, Jr., E. A. West, and E. Tandberg-Hanssen, "Photospheric Electric Currents and Transition Region Brightness Within an Active Region," Solar Phys., 91, 235-242 (1984).

Green, J. L., "The Io Decametric Emission Cone," Radio Science, 19, 556 (1984).

Green, J. L., "Spacelab Data Analysis Using the SCAN System," to appear in Proceedings, National Symposium and Workshop on Optical Platforms, Huntsville, Alabama, June 11-14, 1984.

Green, J. L., J. H. Waite, Jr., M. Chandler, C. R. Chappell, J. R. Doupnik, P. G. Richards, R. Heelis, S. D. Shawhan, and L. H. Brace, "Observations of Ionospheric/Magnetospheric Coupling: DE and Chatanika Coincidences," Journal of Geophysical Research, submitted.

Green, J. L., and J. L. Horwitz, "Magnetospheric Processes in the Plasmapause," EOS, 65, 110 (1984).

Green, J. L., D. N. Baker, and R. D. Zwickl, "SPAN Pilot Project Report," Transactions American Geophysical Union (EOS), in press.

Lockwood, M., J. H. Waite, Jr., T. E. Moore, J.F.E. Johnson, and C. R. Chappell, "A New Source of Suprathermal O^+ Ions Near the Dayside Polar Cap Boundary," Journal of Geophysical Research, submitted.

Isbell, J., A. J. Dessler, and J. H. Waite, "Magnetospheric Energization by Interaction Between Planetary Spin and the Solar Wind," Journal of Geophysical Research, in press.

Menietti, J. D., J. L. Green, N. F. Six, and S. Gulkis, "Three-Dimensional Ray Tracing of the Jovian Magnetosphere in the Low-Frequency Range," J. Geophys. Res., 89, 1489 (1984).

Menietti, J. D., J. L. Green, N. F. Six, and S. Gulkis, "Three-Dimensional Ray Tracing of High Curvature Decametric Arcs," Journal of Geophysical Research, accepted.

Nagai, T., J. H. Waite, J. L. Green, C. R. Chappell, C. R. Olsen, and H. Comfort, "First Measurements of Supersonic Polar Wind in the Polar Magnetosphere," Geophys. Res. Lett., 11, 669 (1984).

Olsen, R. C., S. D. Shawhan, D. L. Gallagher, J. L. Green, and C. R. Chappell, "Observations of Plasma Heating at the Earth's Magnetic Equator," Journal of Geophysical Research, submitted.

Olsen, R. C., D. L. Gallagher, C. R. Chappell, J. L. Green, and S. D. Shawhan "A Potential Control Method for Thermal Plasma Measurements on the DE-1 Spacecraft," in Proceedings of the 17th ESLAB Symposium on "Spacecraft/Plasma Interactions and Their Influence on Field and Particle Measurements," ESA SP-198, eds., A. Pedersen, D. Guyenne, and J. Hunt (ESTEC: Jordwijk) pp. 178-184 (1983).

Rasmussen, C. E., P. M. Banks, and K. J. Harker, "The Excitation of Plasma Waves by a Current Source Moving in a Magnetized Plasma: The MHD Approximation," Journal of Geophysical Research, submitted.

Waite, J. H., Jr., J. L. Horwitz, and R .H. Comfort, "Diffusive Equilibrium Distributions of He^+ in the Plasmasphere," Planet. Space Sci., 32, 611 (1984).

Waite, J. H., Jr., T. Nagai, J.F.E. Johnson, C. R. Chappell, J. L. Burch, T. L. Killeen, P. B. Hays, C. R. Carigan, E. G. Shelley, and W. Peterson, "Escape of Suprathermal O^+ Ions in the Polar Cap," Journal of Geophysical Research, submitted.

Waite, J. H., Jr., D. L. Gallagher, J.F.E. Johnson, R. C. Olsen, R. H. Comfort, C. R. Chappell, W. K. Peterson, D. Weimer, S. D. Shawhan, and E. G. Shelley, "Observations of a ~5 Wave Event on 1982 Day 195 by Particle and Wave Instruments on the DE 1 Spacecraft," Journal of Geophysical Research, submitted.

Waite, J. H., Jr., and C. R. Clauer, "Yosemite Conference," EOS, 65, 384-386 (1984).

Schoeberl, M. R., and D. F. Strobel, "Nonzonal Gravity Wave Breaking in the Winter Mesosphere," to appear in Proceedings, U.S.-Japan Symposium on the Middle Atmosphere, Terrapub, 1983.

Schoeberl, M. R., And R. S. Lindzen, "A Numerical Simulation of Barotropic Instability. Part 1: Wave-Mean Flow Interaction," Stratospheric General Circulation, in press.

Stone, N. H., U. Samir, K. H. Wright, Jr., D. L. Reasoner, and S. D. Shawhan, "Multiple Ion Streams in the Near Vicinity of the Space Shuttle," Geophys. Res. Lett., 10, 1215 (1983).

Astronomy

X-Ray Astronomy

The research program in x-ray astronomy is divided into three areas: analysis and interpretation of data from the Time Interval Processor of the Monitor Proportional Counter that flew onboard the HEAO-2 Observatory, the laboratory development of x-ray detectors that exploit fluorescence of the detector gas, and support to the Advanced X-Ray Astrophysics Facility (AXAF) program.

A large number of interesting HEAO observations were analyzed and interpreted during FY-84 which led to the majority of refereed literature publications this year. These publications include a comparison of the two black hole candidates, Cygnus X-1 and LMC X-3, and part of a series of papers relevant to the study of x-ray polarization. Work on the development of the x-ray detectors continues and was incorporated in a proposal for an AXAF experiment. The AXAF technology program tests of x-ray scattering from flat samples of glass were completed and published. Preparations are being made for tests of the technology mirrors which will be completed in 1985. This research is sponsored by the Office of Space Science and Applications. (M. C. Weisskopf/ES62/205-453-5133)

Publications:

Weisskopf, M. C., S. M. Kahn, W. A. Darbro, R. F. Elsner, J. E. Grindlay, S. Naranan, P. G. Sutherland, and A. C. Williams, "X-Ray Observations of LMC X-3 with the Monitor Proportional Counter Aboard the HEAO 2 Einstein Observatory: A Comparison with Cygnus X-1," Astrophys. J. (Lett.), 274, L65-L69 (1983).

Williams, A. C., R. F. Elsner, M. C. Weisskopf, and W. Darbro, "Photon Escape Probabilities in a Semi-Infinite Plane-Parallel Medium," Astrophys. J., 276, 691-705 (1984).

Grindlay, J. E., D. Band, F. Seward, D. Leahy, M. C. Weisskopf, and F. E. Marshall, "The Central X-Ray Source in SS 433," Astrophys. J., 277, 286-295 (1984).

Elsner, R. F., and F. K. Lamb, "Accretion by Magnetic Neutron Stars. II. Plasma Entry into the Magnetosphere via Diffusion, Polar Cusps, and Magnetic Field Reconnection," Astrophys. J., 278, 326-344 (1984).

Weisskopf, M. C., R. F. Elsner, W. Darbro, S. Naranan, V. J. Weisskopf, A. Williams, N. E. White, J. E. Grindlay, and P. G. Sutherland, "X-Ray Observations of X Persei," Astrophys. J., 278, 711-715 (1984).

Williams, A. C., and J. C. Reily. "Experimental Results for the Scattering of X-Rays from Smooth Surfaces," Opt. Engrg., 23, 177-186 (1984).

Williams, A. C., "Polarization of Comptonized Photons," Astrophys. J., 279, 401-412 (1984).

Apparao, K.M.V., "Cyclotron Emission from Stellar Mass Black Holes," Astronomy & Astrophysics, in press.

Apparao, K.M.V., "Self Absorption of High Energy Gamma-Rays in Cyg X-3," The Astrophysical Journal (Letters), in press.

Apparao, K.M.V., "X-Ray Emission from Be Star Binaries," The Astrophysical Journal, submitted (short version to appear in Proceedings X-Ray Astronomy '84, edited by Y. Tanaka, D. Reidel Publishing Company).

Apparao, K.M.V., H. Antia, and S. M. Chitre, "Origin of the Be Star Phenomenon," Astronomy & Astrophysics, submitted.

Williams, A. C., W. Darbro, M. C. Weisskopf, and R. F. Elsner, "Hydrogenlike Atoms on the Surface of Neutron Stars--Intense Magnetic Field Effects," The Astrophysical Journal, in press.

Naranan, S., R. F. Elsner, W. Darbro, P. E. Hardee, B. D. Ramsey, D. A. Leahy, M. C. Weisskopf, A. C. Williams, P. G. Sutherland, and J. E. Grindlay, "On Fast X-Ray Rotators with Long-Term Periodicities," The Astrophysical Journal, submitted.

Weisskopf, M. C., P. G. Sutherland, R. F. Elsner, and B. D. Ramsey, "On the Viability of Exploiting L-Shell Fluorescence for X-Ray Polarimetry," Nuclear Instruments and Methods in Physics Research (NIM-A), submitted.

Gamma-Ray Astronomy

Data analysis was completed from two balloon flights of large area scintillation detector arrays in 1980 and 1982. Results of gamma-ray burst observations show a deficiency of weak gamma-ray bursts. This would indicate a galactic origin for the bursts and the possible existence of a minimum burst luminosity threshold at approximately 10^{37} erg. A more definitive measurement will require longer duration balloon flights. Modifications to the present balloon-borne experiment have begun to allow flight durations of up to 2 weeks. An initial test of a long-duration balloon flight system from Australia is planned for January 1985.
(G. J. Fishman/ES62/205-453-0117)

Publications:

Meegan, C. A., G. J. Fishman, and R. B. Wilson, "The Frequency of Weak Gamma-Ray Bursts," The Astrophysical Journal, submitted.

Meegan, C. A., G. J. Fishman, and R. B. Wilson, "Measurement of the Rate of Weak Gamma-Ray Bursts," in AIP Conference Proceedings, 115, pp. 422-427 (1984).

Fishman, G. J., C. A. Meegan, T. A. Parnell, R. B. Wilson, and W. Paciesas, "BATSE/GRO Observational Capabilities," in AIP Conference Proceedings, 115, pp. 651-662 (1984).

Cosmic Ray and Particle Physics

The fourth in a series of balloon-borne cosmic ray experiments designed to study high-energy cosmic rays and the interactions produced by them was flown from Palestine, Texas, on September 23, 1983, and attained an exposure of 57 hours above 120,000 feet. This was the longest ever flown from Palestine, Texas.

The series of investigations is being performed by a collaboration which includes members of several U.S. and Japanese universities. The experiments are called Japanese-American Cooperative Emulsion Experiments (JACEE). The principal objectives are the study of the composition and energy spectra of the cosmic rays between 10^{12} and 10^{15} eV, and the study of interactions between heavy nuclei at high energies. The nucleus-nucleus interaction studies extend from 20 GeV/atomic mass unit to around 10^{14} eV. The lower end of the range is a factor of 10 larger than that available at heavy ion particle accelerators. The data analysis from past flights has achieved major results concerning composition of cosmic rays and interaction studies.

An analysis of the small sample of heavy nuclei measured above 10^{14} eV on the first two JACEE flights has revealed that the cosmic ray composition in that energy range is not radically different from that previou'' measured by other experiments around 10^{12} eV. This is a different res ᶠrom that predicted by some cosmic ray air shower experiments, and ᵤ ᵉ is different from an extrapolation of the lower energy spectra, which would predict a much larger component of heavy nuclei (Mn, Cr, Fe, Ni) above 10^{14} eV. The spectra of the heavy nuclei apparently steepens above the energy region covered by previous balloon-borne experiments.

Data gathered during the 1982 hybrid counter-emulsion chamber experiment (JACEE 3) have produced a set of 650 nuclear interactions between cosmic ray projectiles (nuclei of Ne, Mg, Si, etc., to Fe) which strike targets (C, Pb, Ag, Br) in the emulsion chamber. This sample has an average energy 15 times that available at acceleration. The data have been excellent and, in many respects, unexpected when compared with a simple superposition model of heavy nucleus collisions. Simple superposition means that the results might be predicted by superimposing the number of produced pi mesons and angular distributions (from accelerator data) from an equivalent number of wounded protons and neutrons. The average number

of produced particles is higher than simple superposition models would predict. Collisions between Fe projectiles and carbon targets show some events with many more participant protons and neutrons interacting or wounded than predicted by geometrical arguments. This may be taken as evidence for a collective behavior in the interactions rather than an independent nucleon picture. About one-fourth of the interactions from this flight have been analyzed. (T. A. Parnell/ES62/205-453-5130)

Publications:

Burnett, T. H., et al., "Proton Helium Energy Spectra Above 1 TeV for Primary Cosmic Rays," Phys. Rev. Lett., 51, 1010 (1983).

Burnett, T. H., et al., "Extremely High Multiplicities in High Energy Nucleus-Nucleus Collisions," Phys. Rev. Lett., 50, 2062 (1983).

Hayashi, T., et al., "Chemical Composition of Primary Cosmic Rays Above 10^{14} eV with Emmision Chambers," to appear in International Symposium on Cosmic Rays and Particle Physics, Tokyo.

Miyamura, O., et al., "Characteristics of JACEE Heavy Ion Events at Energies Above 1 TeV/Nucleon," to appear in Proceedings of the QUARK MATTER '84 Conference, Springer-Verlag.

The Marshall Mid-Infrared Array Camera

MSFC has developed a camera detector system for astronomical observations in the wavelength range 5-30 μm. Although this highly sensitive system is applicable to a broad range of programs, its primary purpose is to obtain infrared maps of star-forming regions in the Milky Way and other galaxies and to investigate sources discovered by the Infrared Astronomical Satellite (IRAS). In collaboration with several university groups, it will also be used to study comets, particularly Halley and Giacobini-Zinner in 1985/86. An external view of the camera is shown in Figure 38. During astronomical observations, the telescope focal plane is re-imaged onto the camera's array of 20 square field mirrors arranged in 4 columns and 5 rows. The mirrors are close-packed with essentially no dead space between. Each field mirror will provide a pixel size of 5 arc seconds when used at the NASA 3-meter Infrared Telescope Facility telescope on Mauna Kea, Hawaii, with a corresponding total array size of 20 x 25 arc seconds. The radiation incident on each field mirror is focused onto a square bolometer detector chip 0.3 mm in size. To achieve high sensitivity, the bolometers and camera optics are cooled to below 1.6 K using liquid helium. The first field test of the array (without the MSFC data system) occurred in June 1984 at the 2.4-meter Wyoming Infrared Observatory (WIRO) telescope using the WIRO data system. The array performed very well, and maps of two galaxies and a gamma-ray burster region were obtained. Full characterization of the camera, including the MSFC data system, is scheduled for November 1984 at WIRO. (C. M. Telesco/ES63/205/453-5136)
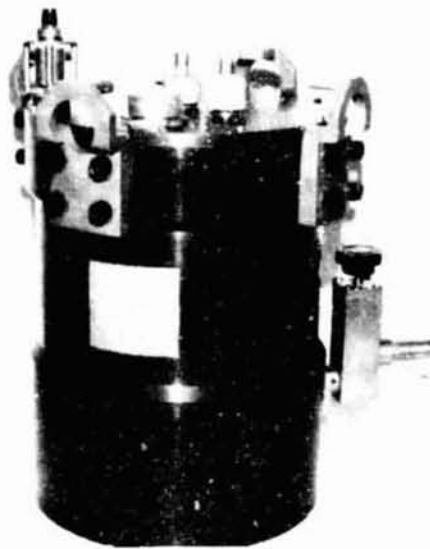
Figure 38. External View of the MSFC Mid-Infrared Array Camera (called Big
MAC for Marshall Array Camera). The height and diameter of the
cylindrical cryogenic dewar are 12.5 and 10 inches, respective-
ly. During operation, the four flanges near the dewar top are
used to suspend the camera from an interface box, which in turn
is bolted to the telescope Cassegrain focus. The infrared beam
from the telescope passes vertically through the pressure
window (located on far side of dewar top) and is then incident
on the camera optics and detectors. Filters are changed using
the knob at upper left. The two tubes near top center access
the liquid helium and liquid nitrogen chambers for cooling the
detectors.

Infrared Astronomy

Development continued on flight hardware for the Infrared Telescope
(IRT) experiment scheduled for the Spacelab 2 mission in 1985. The IRT is
a joint endeavor of the Smithsonian Astrophysical Observatory (SAO), the
University of Arizona (UA), and MSFC. SAO is providing the Principal In-
vestigator (G. Fazio), project management, and post-flight data analysis;
UA is responsible for the infrared optics; and MSFC provides the cryogenic
system, mechanical equipment, and all integration and test functions. The
University of Alabama-Huntsville has collaborated with MSFC in the develop-
ment of the cryogenic apparatus.

The infrared optics are carried in a helium gas-cooled, articulated
cryostat which will scan about a single axis. Coupled with Orbiter motion,
this will generate an extensive map of low-surface brightness and diffuse
astronomical objects and will produce data on the Orbiter/Spacelab induced
environment and its effect on cryogenic infrared astronomy. Superfluid
helium is stored in a 250-liter dewar which provides the cooling gas to the
cryostat.

Following extensive cryogenic and mechanical qualification testing of the cryostat and the dewar subsystems, the IRT was assembled and qualified as a system. Testing at MSFC included mechanical and electrical functional tests, cryogenic performance tests with superfluid helium, an acoustic test, and a thermal vacuum test. The experiment was also fit checked with an engineering model Spacelab pallet, as shown in Figure 39. The IRT was delivered to KSC in April 1984 and installed into the Spacelab 2 payload. In preparation for the Level IV Mission Sequence Test (MST) in July, the system underwent high vacuum and liquid helium servicing operations, as they will be performed during Level I. Most test objectives were successfully completed prior to and during MST. However, it has been necessary to repeat some infrared detector tests and simulation of the superfluid helium conversion and topoff servicing which will be performed on the launch pad. This effort is sponsored by the Office of Space Science and Applications. (E. W. Urban/ES63/205-453-5132)
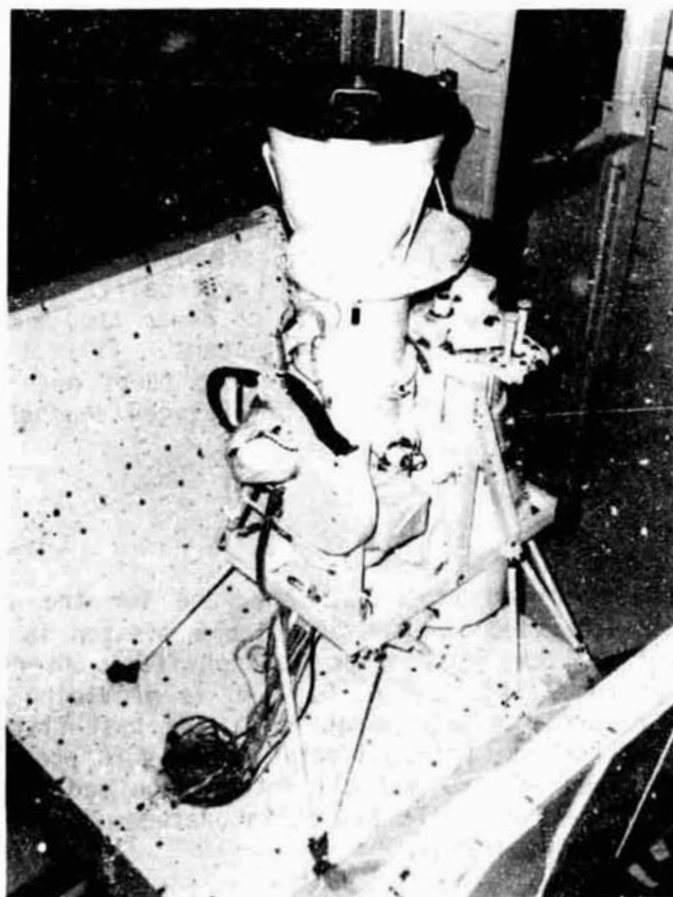
Figure 39. Infrared Telescope Mounted in Spacelab Pallet.

MATERIALS PROCESSING IN SPACE

Vapor Crystal Growth

Professor Wiedemeier (Rensselaer Polytechnic Institute) recently completed the analysis of his vapor crystal growth experiment on STS-7. GeSe crystals were grown by physical vapor transport in closed ampoules with an Xe buffer gas at 4 and 8 atmospheres. The source end of the ampoules was maintained at 600 °C, and the growth region was maintained at 500 °C using the MSFC-developed general-purpose rocket furnace. The original purpose of the experiment was to resolve the anomalous transport rates observed in the growth of GeSe by chemical vapor transport using halogen-carrier gases on Skylab and Apollo Soyuz.

The transport rates observed on STS-7 were within 20 percent of those predicted by simple one-dimensional diffusion theory and approximately a factor of 2 lower than the ground control tests in a vertical stabilizing configuration (hot over cold). This is consistent with the recent theoretical results from Rosenberger (University of Utah) who has shown that convection is impossible to avoid with such a system in a gravity field. The difference between the observed low-gravity transport rate and the one-dimensional diffusion model is probably due to wall effects which Rosenberger has shown are important in such a process. The results are in contrast to the fourfold increase in transport observed by Wiedemeier in his earlier flights using a chemical transport agent. This tends to confirm his conjecture that the anomalous results were due to thermochemical effects of the homogeneous gas phase reactions. A two-dimensional transport code is being developed at MSFC utilizing the theory developed by Rosenberger to check the details of these results. This code will also be used to model the vapor crystal growth experiment being developed by 3M Corporation.

Wiedemeier's experiment not only accomplished its original objective, but produced a surprising and unexpected result. The ground control experiments conducted by MSFC produced a thin crust of polycrystalline material on the wall of the growth region with individual crystallites no larger than ∿1 mm. This was acceptable since the objective of the experiment was to measure transport rates--not grow good crystals. The flight samples, however, produced loose web-like structures of large thin crystals that grew in the interior of the growth ampoule instead of on the wall, suggesting that the crystals nucleated homogeneously in the gas phase. Some of these crystals were as large as 4 x 10 mm and were 10-100 microns thick. The most striking feature is the surface morphology shown in Figure 40. The ground control crystallites show numerous and irregular growth terraces with a swirl-like pattern, suggesting significant convective flow. Also, the Earth-grown crystals show a high density of surface pits, the origin of which has not been identified. In contrast, the space samples are extremely smooth with more regular and widely spaced growth terraces and show no evidence of surface pitting. These samples were grown under identical conditions except for the gravity field. It is clear that the more uniform growth conditions in the absence of gravity-driven convection have a profound effect on surface morphology. (R. J. Naumann/ES71/205-453-0940)

a   b
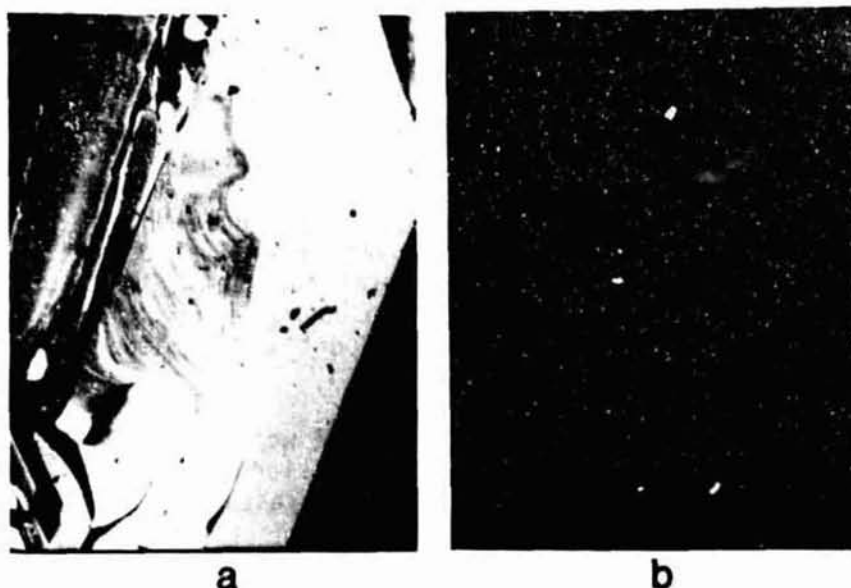
Figure 40.   Optical Photomicrographs of GeSe Crystal Surfaces Using Nomarski
Differential Interference Illumination and Magnification of
100X. The ground control sample (a) was grown under identical
conditions except for gravity as the flight sample (b). Compare
the smooth surfaces and widely spaced growth terraces on the
flight sample with the irregular growth terraces and surface
pitting on the ground control sample.

Crystal Growth and Characterization

Substantial progress has been made in the development of theoretical
models for the temperature distribution and compositional redistribution
during the directional solidification of solid solution alloy systems. Such
models are needed for requirement definition and for the interpretation of
experimental data from spaceborne crystal growth experiments. In particu-
lar, accurate numerical codes have been generated for the analysis of the
thermal and compositional fields during the Bridgman-type growth of
$Hg_{1-x}Cd_xTe$ ($0 \leq x \leq 1$) semiconducting alloys. The calculations in-
clude previously measured temperature and composition dependences for the
melt and solid thermal diffusivities. The calculations allow for both
radiative and conductive heat exchange between the furnace walls and the
alloy samples. Based on the calculations and a conceptual analysis of the
heat flow patterns during Bridgman-type crystal growth, a novel method has
been described for interface shape control during Bridgman-type crystal
growth of HgCdTe alloys. The method requires a proper combination of
furnace geometry, upper- and lower-zone temperatures, and growth rate to
realize the desired growth interface shape. It has been demonstrated ex-
perimentally that the proposed method works well for all alloy compositions
of technological interest.

An experimental apparatus has been designed and developed to make high temperature electrical conductivity measurements of materials by a contactless technique and has been used to acquire data on HgTe from room temperature to temperatures above the melting point. The results for the melt show a marked increase in conductivity with temperature and thus support the existence of the recently discovered semiconductor-to-metal transition in the liquid state for HgCdTe alloys. The apparatus is sensitive enough to detect changes in conductivity due to thermal annealing which affects the concentration of point defects in the material.

The design and development of an engineering prototype of an Advanced Automated Directional Solidification Furnace (AADSF) system for the processing and crystal growth of electronic materials (e.g., HgCdTe) has been nearly completed. The AADSF shown in Figure 41 was designed to provide a broad range of materials processing conditions. It is a multizone furnace capable of establishing very steep thermal gradients as well as long isothermally heated regions. The highly modular design allows it to be assembled in many different forms to meet a wide array of anticipated materials processing needs. (S. L. Lehoczky/ES72/205-453-3090)
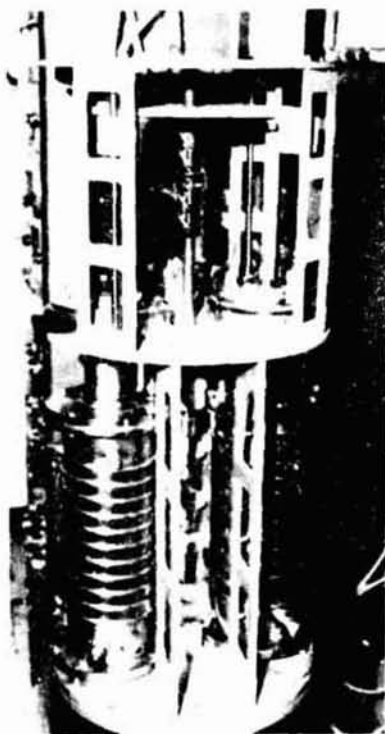
Figure 41. Prototype of AADSF System.

Publications:

Lehoczky, S. L., F. R. Szofran, D. Chandra, and J.-C. Wang, "Growth Rate Dependence of the Axial Compositional Variations in Bridgman-Grown $Hg_{1-x}Cd_xTe$ Crystals," presented Fall Meeting of the American Physical Society, San Francisco, California, November 20-23, 1983; Bull. APS, 28, 1313 (1983).

Szofran, F. R., and S. L. Lehoczky, "High Temperature Electrical Properties of HgTe," presented Fall Meeting of the American Physical Society, San Franciso, California, November 20-23, 1983; Bull. APS, 28, 1313 (1983).

Jasinski, T., and R. J. Naumann, "One-Dimensional Modeling of Vertical Bridgman-Type Crystal Growth," J. Crys. Growth, 66, 469 (1984).

Holland, L. R., "Sealed Silica Pressure Ampoules for Crystal Growth," J. Crys. Growth, 66, 501-513 (1984).

Szofran, F. R., and S. L. Lehoczky, "A Method for Interface Shape Control During Bridgman-Type Crystal Growth of HgCdTe Alloys," presented Sixth American Conference on Crystal Growth/Sixth International Conference on Vapor Growth and Epitaxy, Atlantic City, New Jersey, July 15-21, 1984 (proceedings to appear in Journal of Crystal Growth).

Szofran, F. R., D. Chandra, J.-C. Wang, and S. L. Lehoczky, "Effect of Growth Parameters on Compositional Variations in Directionally Solidified HgCdTe Alloys," presented Sixth American Conference on Crystal Growth/Sixth International Conference on Vapor Growth and Epitaxy, Atlantic City, New Jersey, July 15-21, 1984 (proceedings to appear in Journal of Crystal Growth).

Holland, L. R., "VLS Growth to Purify Elements of Groups II and VI," presented Sixth American Conference on Crystal Growth/Sixth International Conference on Vapor Growth and Epitaxy, Atlantic City, New Jersey, July 15-21, 1984 (proceedings to appear in Journal of Crystal Growth).

Lehoczky, S. L., and F. R. Szofran, "Further Comments on Segregation During Bridgman Growth of $Hg_{1-x}Cd_xTe$," Journal of Crystal Growth, in press.

Chandra, D., "An Analysis of Anomalous Volume Expansion in $Hg_{1-x}Cd_xTe$ Melts Employing the Inhomogeneous Structure Model," Journal of Applied Physics, in preparation.

Szofran, F. R., "Contactless Electrical Measurements of High Vapor Pressure Materials at High Temperatures," Review of Scientific Instruments, in preparation.

Szofran, F. R., and P. N. Espy, "Automated ac and dc Measurement System for the Determination of the Temperature Dependence of the Galvanomagnetic Properties of Semiconductors," Review of Scientific Instruments, in preparation.

Szofran, F. R., L. R. Holland, R. E. Taylor, D. Chandra, and S. L. Lehoczky, "Experimental Evidence for Semiconductor to Metallic Transition in HgCdTe Liquids," Physical Review Letters, in preparation.

Dakhoul, Y. M., and R. C. Farmer, "Simulation of Solidification in a Bridgman Cell," NASA Contractor Report, Marshall Space Flight Center, Alabama, in press.

Lehoczky, S. L., and F. R. Szofran, "Growing Crystals for Infrared Detectors," NASA Tech Briefs, 8(1), 136 (1983).

Lehoczky, S. L., and F. R. Szofran, "Solidification and Crystal Growth of Solid Solution Semiconducting Alloys," presented Second Symposium on Space Industrialization, Huntsville, Alabama, February 13-15, 1984 (to appear in NASA Conference Proceedings, Marshall Space Flight Center, Alabama).

Model Immiscible Systems

There exist a large number of metallic systems that do not form alloys from the melt because they exhibit a region of liquid-phase immiscibility. As a melt is cooled into this region, the density differences between the two liquid phases result in rapid phase separation. Early experiments in low gravity found that phase separation still occurred even in the absence of buoyancy, indicating the existence of other phase separating mechanisms that had been previously masked by the gravitation effects.

Research with transparent model systems with similar properties has revealed a number of interesting surface and capillarity effects that play a role in phase separation. These effects are being isolated and studied individually.

Fundamental to such a study are accurate phase diagrams of the proposed model systems. A light-scattering technique for determining cloud points has been developed by James Smith (University of Alabama-Huntsville). Significant corrections (as much as 11.4 percent in monotectic composition) have been made to the succinonitrile-water system which is somewhat of a standard. These improvements will have an impact in the interpretation of previous experiments. Phase diagrams of combinations of succinonitrile and other materials such as benzene, cyclohexanol, anhydrous ethanol, azeotropic ethanol-water, and mixtures of D_2O and H_2O (which allow adjustments to provide neutral buoyancy) have been improved or determined for the first time.

One of the mechanisms responsible for such phase separations is critical wetting and spreading on the contained surface. Theory predicts that one of the two immiscible phases will become perfectly wetting above a particular critical wetting temperature. In Earth's gravity, the interface between the two phases is flattened because of the density differences, thus giving the appearance of a 90° contact angle rather than the expected 0° contact angle. Techniques to measure the liquid-solid interfacial energies are being developed by K. Chang (Alabama A&M University) which will allow the prediction of the critical wetting temperature as well as the modeling of the nucleation and growth of the liquid phases. Removal of gravity should allow the interface to relax so that its true shape may be observed. Attempts to observe this directly in the drop tower and the KC-135 aircraft have produced some interesting results; the interface tends to become flatter instead of more hemispherical as the temperature approaches the critical consolute point. It is suspected that this is caused by the fact that the interfacial energy becomes vanishingly small at the consolute point. At these low interfacial energies, the driving force is probably not sufficient

to form the equilibrium interface shape in the time available. A space shuttle experiment is needed to resolve this effect.

Key to the control of unwanted phase separation from critical wetting is selection of a container that is wet by the host phase rather than the minority phase. A technique for reversing the hydrophillic nature of pyrex has been developed in this study.

Another unexpected effect has been observed in the solidification of succinonitrile-H_2O monotectic. A peculiar worm-like structure is observed at the solidification interface (see Figure 42). The stalks meander about, and occasionally the heads may pop off and rapidly move away. The exact nature of this structure has not yet been determined, but it is believed to occur because the critical wetting temperature is below the monotectic temperature, thus preventing a stable trijunction between the two liquid phases and the monotectic solid. (D. O. Frazier/ES74/205-453-3090)

Figure 42. Succinonitrile-Benzene Solid-Liquid Interface. Worm-stalk phase widths are typically less than 10 μm for most systems and growth conditions.

Publications:

Smith, J. E., Jr., D. O. Frazier, and W. F. Kaukler, "A Redetermination of the Succinonitrile-Water Phase Diagram," Scripta Met., 18, 677-682 (1984).

Frazier, D. O., B. R. Facemire, W. F. Kaukler, W. K. Witherow, and U. Fanning, "Separation Processes During Binary Monotectic Alloy Production," NASA Technical Memorandum TM-82579, Marshall Space Flight Center, Alabama, 1984.

Kaukler, W. F., D. O. Frazier, and B. R. Facemire, "Determination of the Succinonitrile-Benzene and Succinonitrile-Cyclohexznol Phase Diagrams by Thermal and UV Spectroscopic Analysis," NASA Technical Memorandum TM-82581, Marshall Space Flight Center, Alabama, 1984.

74

Witherow, W. K., and B. R. Facemire, "Optical Studies of a Binary Misci-
    b'lity Gap System," _Journal of Colloid and Interface Science_, in
    press.

Kaukler, W. F., and D. O. Frazier, "Observations of a Monotectic Solidifi-
    cation Interface Morphology," _Journal of Crystal Growth_, in press.

Frazier, D. O., J. E. Smith, Jr., and W. F. Kaukler, "A Method to Reverse
    Surface Wetting Properties of Pyrex," NASA Tech Briefs, Marshall Space
    Flight Center, Alabama, in press.

Electrophoresis

A more detailed study of the role of the sample constituents and prop-
erties in Continuous Flow Electrophoresis (CFE) was begun this year.
Flight experiments on STS-6 and -7 showed the importance of different elec-
trical properties. The electrical conductivity of the sample and the
buffer solution must be carefully matched to fully utilize the high sample
concentration possible in low gravity. Otherwise. electric field distor-
tions near the buffer cause an increased bandspread and reduced resolution
(the advantage of low-gravity operations). It has been shown that dramat-
ic increases in throughput can be realized in CFE performed in low gravity
by increasing the flow channel width and the concentration of the sample
stream. This is highly significant for McDonnell Douglas Aerospace Cor-
poration which is developing a space CFE device for commercial use since
this is the major advantage of low-gravity operation that has been identi-
fied. From a scientific point of view., the sample runs for NASA, as part
of the Joint Endeavor Agreement, revealed some interesting insight on the
effect of conductivity mismatch between the sample stream and the buffer.
The high sample concentration attainable only in low gravity allows con-
siderably more mismatch between the electrical conductivity than is usually
experienced on Earth. This causes a distortion in the electrical field in
the vicinity of the buffer which causes the sample to migrate toward the
walls.

These results have been confirmed by a series of laboratory experi-
ments done with hemoglobin (the sample material of STS-6) and polystyrene
latex (used on STS-7). Conducting two-dimensional analogs of CFE, hemo-
globin samples of different electrical conductivity have been inserted into
cellulose acetate gel strips. The spread of the sample during electro-
phoresis has been measured and correlated with a mathematical model.
Figure 43 shows the distortion of the electrical field in the vicinity of a
sample of hemoglobin. The hemoglobin was placed on a cellulose acetate
plate with an electrical field at 150 volts applied as shown. These re-
sults simulate electrical field distortion in a CFE chamber; this, in turn,
causes the sample to move toward the chamber walls, thus causing sample
bandspreading and, hence, degradation in chamber resolution. Since this
phenomenon is not gravity dependent, it is important to investigate ways to
attenuate its effect so that optimum performance can be obtained from
space-based electrophoresis devices.
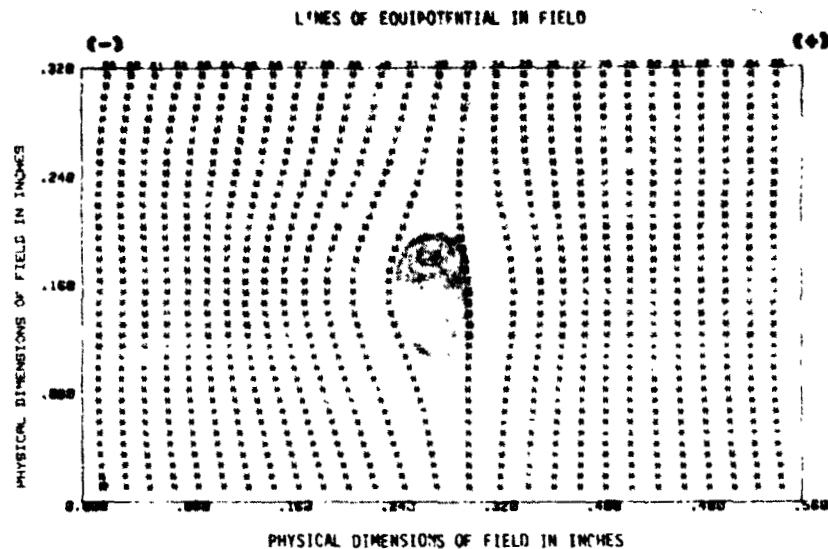
Figure 43. Distortion of Electric Field Around a Sample of Hemoglobin Applied : Cellulose Acetate.

Polystyrene latex samples of different concentration and conductivity have shown comparable results in the Beckman Continuous Particle Electrophoresis System. Conducting experiments both in space and in the laboratory have yielded significant scientific results that will impact future separation technology.

Electroosmosis has been a subject of intense research since the Apollo 16 electrophoresis experiment. Although electroosmosis can be utilized to advantage during CFE, it indirectly caused most of the bandspreading during the Continuous Flow Electrophoresis System experiments. Electroosmosis also influences isoelectric focusing, and a flight experiment to measure and control it by a combination of barriers and coatings was done on STS-11. The experiment showed that electroosmosis is a much more complex phenomenon in the presence of an amphoteric buffer used in isoelectric focusing than it is in electrophoretic buffers. Also, the flows in isoelectric focusing chambers show unexpected size scale effects, unlike flows in electrophoretic chambers, which are invariant with size. Such flows are being modeled, and a follow-up experiment to test these models is ready for the next flight opportunity.

Mathematical modeling and analysis for both electrophoresis and isoelectric focusing is provided by Princeton University (D. A. Saville) and Roberts Associates (G. O. Roberts). The Isoelectric Focusing Experiment was developed by the University of Arizona (M Bier). This research is sponsored by the Microgravity Sciences and Applications Division of the Office of Space Science and Applications. (R. S. Snyder/ES73/205-453-3537)

Publications:

Naumann, R. J., and P. H. Rhodes, "Thermal Considerations in Continuous
    Flow Electrophoresis," Sep. Sci. and Tech., 19, 51-75 (1984).

Omenyi, S. N., and R. S. Snyder, "Vertical Ascending Electrophoresis of
    Cells with a Minimal Stabilizing Medium," Prep. Biochem., 13, 437-459
    (1983).

Omenyi, S. N., and R. S. Snyder, "Settling of Fixed Erythrocyte Suspension
    Droplets," Biorheology, 20, 109-118 (1983).

Snyder, R. S., P. H. Rhodes, B. J. Herren, T. Y. Miller, G.V.F. Seaman, P.
    Todd, M. E. Kunze, and B. E. Sarnoff, "Analysis of Free Zone Electro-
    phoresis of Fixed Erythrocytes Performed in Microgravity," Electro-
    pnoresis, submitted.

Snyder, R. S., P. H. Rhodes, T. Y. Miller, F. J. Micale, R. Mann, and
    G.V.F. Seaman, "Polystyrene Latex Separations in a Continuous Flow
    Electrophoresis System on the Space Shuttle," Electrophoresis, in
    preparation.

Growth of Precision Latex Microspheres in Low Gravity

The purpose of the Monodisperse Latex Reactor (MLR) is to produce
larger, more uniform particle-size monodisperse polystyrene latexes in
microgravity than can be manufactured on Earth.

A latex is a suspension of very tiny (micrometer-size), plastic
spheres in water, stabilized by emulsifiers. The objective of this ex-
periment is to grow billions of these microspheres to larger sizes than can
be grown on Earth, while keeping them perfectly spherical and monodis-
perse. The word monodisperse means all exactly the same size, and it is
defined in this experiment as maintaining a standard deviation of diameter
of less than 2 percent for all microspheres in the batch. Thus far, latex
batches have been returned to Earth from several of the MLR flights with
standard deviations better than 1.4 percent. A typical latex recipe, such
as that carried aboard the most recent shuttle flight (STS-11), produces
1.7 billion microspheres of 30 μm diameter, or 45 billion microspheres
of 10 μm diameter; the difference in numbers is due to each latex recipe
being held constant at about 25 percent total solid content by weight. The
microspheres comprising these latexes can only be grown in quantity on
Earth to about 5 μm diameter while remaining monodisperse due to buoyancy
and sedimentation effects. They cannot be stirred sufficiently to maintain
the suspension during polymerization because they would undergo shear-
induced coagulation. However, in microgravity the absence of buoyancy
effects has thus far allowed growth of these spheres to 30 μm diameter.
The MLR has now flown five times on the space shuttle (STS-3, -4, -6, -7,
and -11), and three more flights are presently scheduled to be completed by
mid-1985.

This experiment has now produced the first commercial space product;
i.e., the first commercial material ever manufactured in space to be

marketed on Earth. The 10 μm latex manufactured during the STS-6 mission was officially accepted by the U.S. National Bureau of Standards (NBS) on July 17, 1984. NBS plans to market this latex to researchers worldwide as the United States national 10 μm Standard Reference Material. NASA transferred 15 g of this 10 μm latex to NBS where it was diluted and packaged by NBS into 700 vials of 4 mL each. Each of these vials was priced by NBS at $400, thus giving the batch of 15 g a total market value of $280,000. This computes to about $18,700 per gram of solid polymer, or $530,000 per oz. If the chemistry and all four reactors operate properly, about 2 to 3 million dollars' worth of latex can be produced on each space shuttle flight. NBS has also officially requested that NASA produce 30 g of 30 μm latex and 80 g of 100 um latex which they also plan to market. The goal is to accomplish this by the end of the next three flights. Figure 44 graphically illustrates the difference in quality between the latex made in space (a) which was transferred to NBS and the ground control latex (b) which was made from the same seed latex from the same bottle and was polymerized on Earth under identical conditions except for micro-gravity.
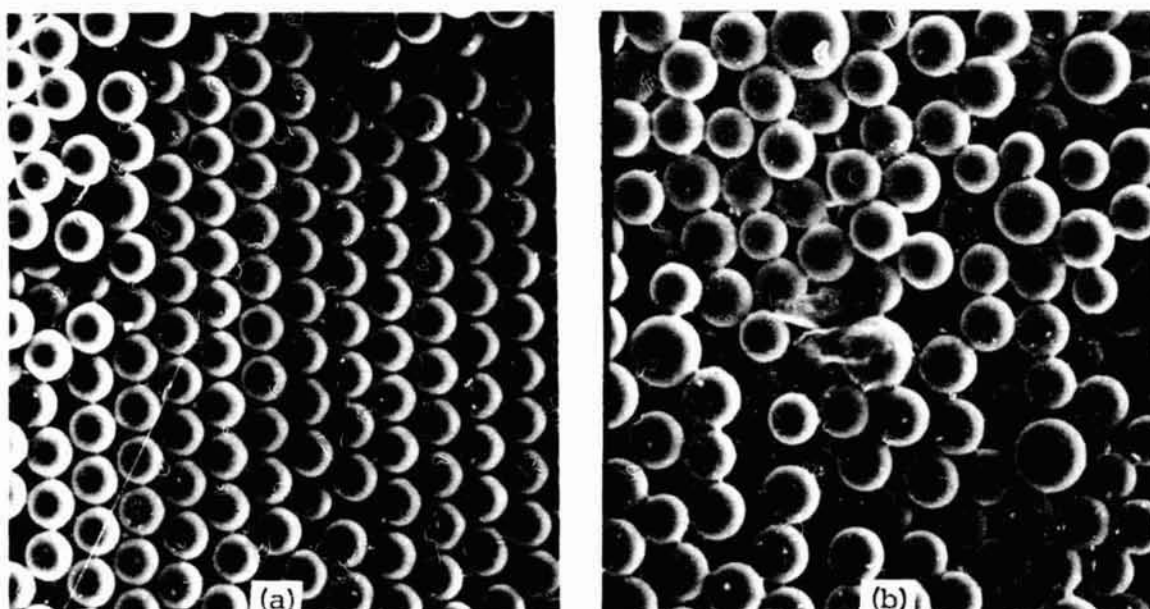
Figure 44. 10 μ Latexes. (a) NBS flight latex (800X; standard deviation: 1.15 percent). (b) Ground control latex (800X; standard deviation: ~6 percent).

Once it is demonstrated that these large-size monodisperse latexes can be routinely produced in quantity and quality, they can be marketed for many types of scientific applications. Biomedical research applications include such things as drug carriers and tracers in the body, human and animal blood flow studies, membrane and pore sizing in the body, and medical diagnostic tests. Other applications include use as calibration standards for optical and electron microscopes, Coulter counters, light-scattering equipment, and many other types of laboratory equipment.

This project was directed by Dr. John W. Vanderhoff, Principal Investigator (Lehigh University, Bethlehem, Pennsylvania), along with Co-Investigators, Drs. Fortunato J. Micale and Mohammed S. El-Aasser (also of Lehigh University), and Dale M. Kornfeld (MSFC). This effort was sponsored by the Microgravity Sciences and Applications Division of the Office of Space Science and Applications, with the hardware development being managed by MSFC. (D. M. Kornfeld/ES73/205-453-0185)

Publications:

Vanderhoff, J. W., M. S. El-Aasser, F. J. Micale, E. D. Sudol, C. M. Tseng, A. Silwanowicz, and D. M. Kornfeld, "Preparation of Large-Particle-Size Monodisperse Latexes in Space: The STS-6 and STS-7 Mission Results," presented AICHE 1984 Summer National Meeting, Philadelphia, Pennsylvania, August 19-22, 1984.

Vanderhoff, J. W., M. S. El-Aasser, F. J. Micale, E. D. Sudol, C. M. Tseng, A. Silwanowicz, and D. M. Kornfeld, "Preparation of Large-Particle-Size Monodisperse Latexes in Space: The STS-3, STS-4, STS-6, and STS-7 Mission Results," to appear in Proceedings of the Second Symposium on Space Industrialization, Huntsville, Alabama, February 13-15, 1984.

Vanderhoff, J. W., M. S. El-Aasser, F. J. Micale, E. D. Sudol, C. M. Tseng, A. Silwanowicz, and D. M. Kornfeld, "Preparation of Large-Particle-Size Monodisperse Latexes in Space: Polymerization Kinetics and Process Development," Journal of Dispersion Science and Technology, in press.

ATMOSPHERIC SCIENCES

Introduction

Research efforts are directed toward increased understanding of atmospheric processes through the application of space technology. This involves the diagnostic and modeling studies in which space-based (shuttle and free-flyer satellites) sensor data are required inputs. In the pursuit of this objective, extensive use is made of large computer systems that are required to accommodate current theoretical and analytical models representative of the behavior of the atmosphere. Field experiments are also required to provide ground truth data for comparison with the airborne and space-based sensor systems that are being developed to provide the more accurate and higher resolution data required as inputs to the models. Laboratory support is also required in the development, refinement, and calibration of these measurement systems. The complete system for studying atmospheric processes consists of theoretical modeling, laboratory and field experiments, and shuttle/satellite sensor data.

Global Scale Atmospheric Processes

Applications of remotely sensed atmospheric variables in the lowest 20 km are being made to diagnostic and predictive studies of atmospheric flows. Two main areas of investigation have been pursued. The first of these is a study of long wave and planetary wave structures and how they are maintained by boundary forcing. Global observations of solar and infrared radiation taken from polar orbiting satellites have been used to show that there exist prominent 20-25 day periodicities in the strength of westerly tropospheric winds and that these periodicities are dynamically linked to fluctuations in cloud cover and net solar infrared heating.

Condensation and how it alters baroclinic waves has been investigated in some detail. Observational determination of how condensation alters wave energetics has been completed at Purdue University and Penn State University in association with MSFC scientists. Satellite-observed cloud populations have proven integral to these studies. Theoretical models of the moisture process and cloud formation have been developed and can now be compared to satellite-observed cloud cover. A technique for inferring rainfall from geostationary satellite infrared imagery has also been developed.

Results from all of these investigations have defined requirements for remotely sensing atmospheric moisture on a global basis. A Shuttle Atmospheric Science Experiment (SASE) has been suggested as a means of making the required measurements.

Science recommendations and strawman payloads have been established. (J. W. Kaufman/ED42/205-453-3104)

Publications:

Tang, C-M., and G. H. Fichtl, "Non-Quasi-Geostrophic Effects in Baroclinic Waves with Latent Heat Release," J. Atmos. Sci., 41, 1498-1512 (1984).

PRECEDING PAGE BLANK NOT FILMED

PAGE 80 INTENTIONALLY BLANK

Robertson, F. R., G. S. Wilson, H. J. Christian, Jr., S. J. Goodman, G. H. Fichtl, and W. W. Vaughan, "Atmospheric Science Experiments Applicable to Space Shuttle Spacelab Missions," Bull. AMS, 65, 692-700 (1984).

Geophysical Fluid Flow Cell (GFFC)

The GFFC experiment, designed to simulate geophysical atmospheric dynamics using a scaled model atmosphere with a radial gravity-like body force, will fly on Spacelab 3. The GFFC will be used to conduct more basic experiments in fundamemtal fluid mechanics and heat transfer. Computer simulations have been developed to understand the fluid flows expected to occur in the GFFC. Conversion of a numerical simulation code to NASA's Cyber 205 computer has also been initiated to expedite data interpretation. Ground experiments have been performed with the GFFC to evaluate the instrument's performance and capability. Results were coupled with numerical simulations and Earth-based laboratory experiments to develop the flight scenarios which were programmed into the instrument. Experiments were prioritized for the mission, and a contingency strategy was developed. The data reduction system for analyzing the GFFC data film has been improved to reduce analysis time. The flight hardware was calibrated, readied for flight, and delivered to KSC. It has been integrated into Spacelab and successfully completed the Level III/II Mission Sequence Test. (F. W. Leslie/ED42/205-453-2047).

Numerical Studies of Geophysical Fluid Dynamics

Theoretical studies of baroclinic instability applicable to the atmospheres of Earth, and (possibly) Jupiter and Saturn, were conducted. A journal article was published on the fully nonlinear equilibrated symmetric (two-dimensional) instabilities, and another was accepted on the detailed energetics of the linear symmetric instabilities. More recent results of three-dimensional linear stability analysis indicated that the purely symmetric disturbances may not be as important in the atmosphere as nearly symmetric disturbances of mesoscale size. Plans include: (1) developing a fully nonlinear three-dimensional Navier-Stokes model to study the competition between various modes of instability, (2) designing laboratory experiments, and (3) performing analysis of satellite and mesoscale modeling data. Numerical models of the stratified spin-up experiments to be conducted in the Geophysical Fluid Flow Cell (GFFC) apparatus on Spacelab 3 are being developed, and a cylindrical version of the code has been validated by comparing the results with previous ones in the literature. Work is underway to validate the spherical code. (T. L. Miller/ED42/205-453-5508)

Publications:

Miller, T. L., "The Structures and Energetics of Fully Nonlinear Symmetric Baroclinic Waves," J. Fluid Mech., 142, 343-362 (1984).

Miller, T. L., "On the Energetics and Non-Hydrostatic Aspects of Symmetric Baroclinic Instability," Journal of Atmospheric Science, accepted.

Monte Carlo Turbulence Simulation Work

Two separate Monte Carlo turbulence simulation programs were developed, tested, and documented during FY-84. The spatial model of wind shear and turbulence combines measured three-dimensional atmospheric wind shear data with simulated three-dimensional turbulence. The result is the most realistic wind simulant available today. At the other end of the spectrum, a Von Kármán Approximant (VKA), one-dimensional model was developed. Atmospheric turbulence outside of the planetary boundary layer obeys the irrational Von Kármán spectrum, but a high computational price is paid for irrational simulations. An excellent rational approximation to the Von Kármán spectrum was found and explicit turbulence difference equations generated. The VKA method provides the solution to the problems of accuracy and stability encountered in earlier studies. The best feature of irrational simulations, i.e., realism, is combined with the computational simplicity of the rational simulation. (W. Campbell/ED42/205-453-1886)

Remote Wind Measurements

During the past year the Fluid Dynamics Branch has developed and conducted experiments with an airborne-based (CV-990) Doppler Lidar System (DLS) to remotely measure wind flows associated with small-scale (mesoscale) atmospheric phenomena. These experiments involved scientists from various universities and research institutions. Studies have been conducted relative to developing design and operational requirements for a satellite DLS wind profiler. The studies focused on availability of sufficient aerosol to backscatter laser radiation to make a Doppler shift wind measurement, scanning concepts, and hardware technology issues. It has been recognized that a satellite DLS will provide fundamental new measurements to advance the art of computational fluid dynamics of large-scale atmospheric flows. (D. Fitzjarrald/ED42/205-453-3104)

Analysis of MSFC Ground-Based Doppler Lidar Data

The MSFC 10.6-micron-pulsed Doppler Lidar System (DLS) and another Doppler lidar were used in the Joint Airport Weather Studies (JAWS) project field experiment. Subsequent data analysis successfully demonstrated that observations from more than one Doppler lidar can be combined to derive the three-dimensional Cartesian wind field. Findings were consistent with surface anemometers. A collocated comparison with a 5-cm Doppler radar for the case of clear air returns at low elevations showed the lidar velocity measurements to be free of bias from ground clutter contamination. These and other findings were presented at radar and lidar conferences and in a journal article. Activities during FY-84 also included participation in the fall 1984 airborne Doppler lidar flight series. At MSFC, detailed measurements of horizontal winds and vertical profiles of tropospheric backscatter and extinction were acquired during over 60 days of operation. Analysis of the data is continuing, and several journal articles are forthcoming. The data, collected under a variety of atmospheric conditions, are being used to define future flight experiments and design of a satellite-borne Doppler lidar wind measurement system. (Jeffry Rothermel/ ED42/205-453-2283)

Warm Fog Dispersal Research

A patent application was filed on a new technique for improving the visibility in warm fogs. If the proposed technique proves successful, it should be of substantial benefit in clearing fog along aircraft and shuttle runways. The concept utilizes large-volume (approximately 100,000 gal/min) recyclable water sprays. As fog passes through a curtain of water spray created by high-volume water jets, spray drops coalesce with fog drops and precipitate to the ground, thereby dissipating the fog in the area of and somewhat downwind of the water sprays. The efficiency of the fog drop removal process and the resultant visibility improvement in the cleared area critically depend upon the size spectra of the spray drops. Present research emphasis is on identification of water nozzles and operating conditions which will produce and project optimum drop spectra (0.3 to 1.0 mm diameter) to heights in excess of 25 meters. (V. Keller/ED43/205-453-0941)

Publication:

"Warm Fog Dissipation Using Large Volume Water Sprays," NASA Patent Case No. MFS-25962 (1983).

Natural Environment Design Criteria

The Atmospheric Sciences Division of the Systems Dynamics Laboratory has the responsibility for developing and defining the natural environment criteria for the Space Station program elements and other flight projects. This requires the maintenance of a source for current models and data bases on key natural environments such as atmospheric thermodynamic and kinematic parameters, atmospheric composition, meteoroids, radiation, physical constants, etc. This also includes maintaining an understanding of the various flight projects design and operational requirements, especially those concerning interaction with the natural environment. In a new approach to automate these criteria, development has started on a software package designed for use with the Space Station program element preliminary design and definition studies. This should permit more rapid retrievals and enable users to incorporate updated criteria into the various design studies. The initial data base being used was reported in a NASA Technical Memorandum. (W. Vaughan/ED41/205-453-3100)

Publication:

Vaughan, W. W., "Natural Environment Design Criteria for the Space Station Definition and Preliminary Design (First Revision)," NASA Technical Memorandum TM-86460, Marshall Space Flight Center, Alabama, September 1984.

Wind Shear

Horizontal wind profile measurements recorded at the NASA 150-meter Ground Winds Tower Facility at Kennedy Space Center, Florida, were analyzed to evaluate wind shears known to be hazardous to the ascent and descent of the space shuttle and conventional aircraft. Graphical and mathematical

descriptions of speed and direction shears with altitude and along the flight path were presented as functions of intensity categories and significant values. (M. B. Alexander/ED42/205-453-2087)

Publication:

Alexander, M. B., and D. W. Camp, "Analysis of Low-Altitude Wind Speed and Direction Shears," Journal of Aircraft, submitted.

Atmospheric Turbulence

Experiments were conducted in a small wind tunnel in which atmospheric flow around arrays of one, two, three, and four model buildings was analyzed. Wake profiles of velocity and turbulence were measured to indicate the effect of obstacles on the wind environment encountered by aircraft during landing or take-off operations. (M. B. Alexander/ED42/205-453-2087)

Publication:

Logan, Earl, Jr., Shu Ho Lin, and M. B. Alexander, "Wakes from Arrays of Buildings," Journal of Atmospheric and Oceanic Technology, submitted.

Turbulence Modeling

Two-dimensional geostrophic turbulence driven by a random force was investigated. A group-kinetic theory of turbulence was developed, and the kinetic equation of the scaled singlet distribution was derived to investigate the spectrum of turbulence. The hydrodynamical equations of turbulence were transformed into a master equation for the velocity distribution function. Group scaling was introduced for the closure. (M. B. Alexander/ED42/205-453-2087)

Publication:

Tchen, C. M., "Theory and Modeling of Atmospheric Turbulence," NASA Contractor Report CR-3817, August 1984.

PROPULSION TECHNOLOGY

Carbon Deposition from Oxygen-Hydrocarbon Propellant

Rocket engine combustion products resulting from combustion of liquid oxygen and hydrocarbon fuel contain various amounts of carbon depending upon the hydrocarbon fuel used and the combustion conditions such as mixture ratio and chamber pressure. Past engine experience has shown that at low mixture ratios large amounts of carbon tend to be produced which deposit on turbine nozzles, reducing flow area and thus decreasing engine performance. This deposition process is of concern for advanced high pressure hydrocarbon engines because of potential degradation of engine performance over long engine use periods and potentially increased maintenance costs due to clogged main injectors in staged combustion engines.

Work recently sponsored by the Marshall Space Flight Center and conducted by the Aerojet Tech Systems Company has acquired data on carbon deposition characteristics for the liquid oxygen/RP-1 propellant combination. At preburner/gas generator ratios, test data revealed a marked change in exhaust gas carbon content as mixture ratio was varied. This is illustrated in Figure 45 where the exhaust gas condition can be seen at various mixture ratios. The highest carbon content occurs at a mixture ratio of about 0.55. Carbon deposition rates on a turbine simulator device during these tests were typically 0.005 inch per 100 seconds of run time. Carbon deposition at main chamber mixture ratios was not detected. This effort was sponsored by the Office of Aeronautics and Space Technology. (F. Braam/EP22/205-453-4827)
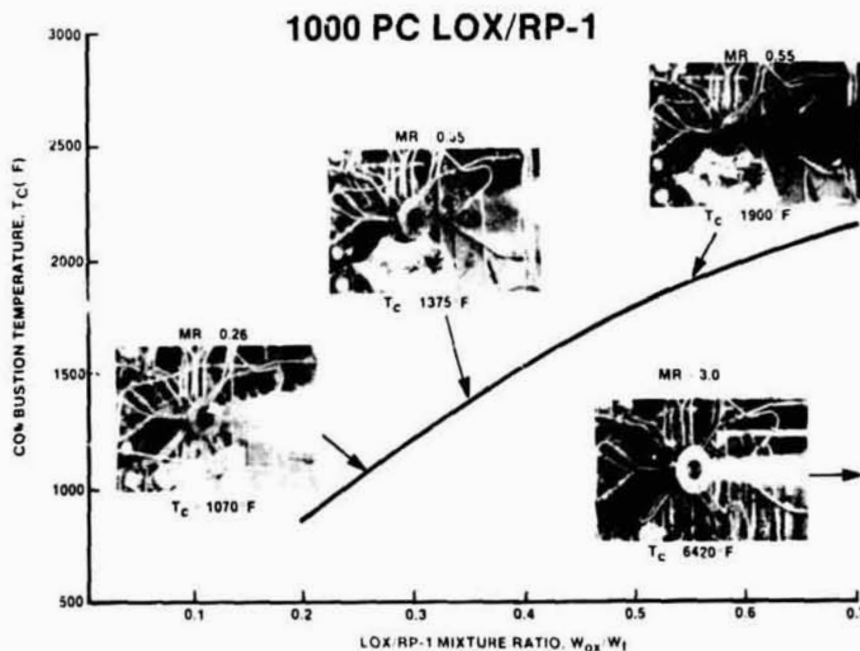

Figure 45. Lox/RP-1 Exhaust Gas Characteristics for Various Mixture Ratios.

High Pressure Lox/Natural Gas Staged Combustion Technology

During the past several years, interest has increased in the potential use of hydrocarbon fuels in combination with liquid oxygen for launch vehicle booster engines. Several fuels have been considered, including RP-1 and methane. Although neither of these generates a specific impulse as high as hydrogen, the greater densities and reduced tankage weights associated with the hydrocarbon fuels offer the potential of payload increases. To support this interest, a program was conducted to investigate ignition, combustion, and heat transfer characteristics of liquid oxygen and high methane content natural gas applicable to high pressure staged combustion rocket engines. A pressure-fed combustion system rated at a 40,000 pound thrust at 3000 psia chamber pressure was used for all testing.

Preburner performance data were obtained during nine preburner tests. Mainstage gas temperature uniformity and combustion performance at chamber pressures to 3100 psi either met or approximated program goals. Combustion gas temperature data measured by a six-thermocouple rake is shown in Figure 46. There was no combustion instability during any preburner tests. Flush-mounted, fast-response pressure instrumentation indicated that combustion pressure oscillation amplitudes were well within the program goals. Although these results cannot be extrapolated to full-size preburner combustion chambers, they provide a level of confidence that instability in larger chambers would be manageable by either using baffles or acoustic cavities.
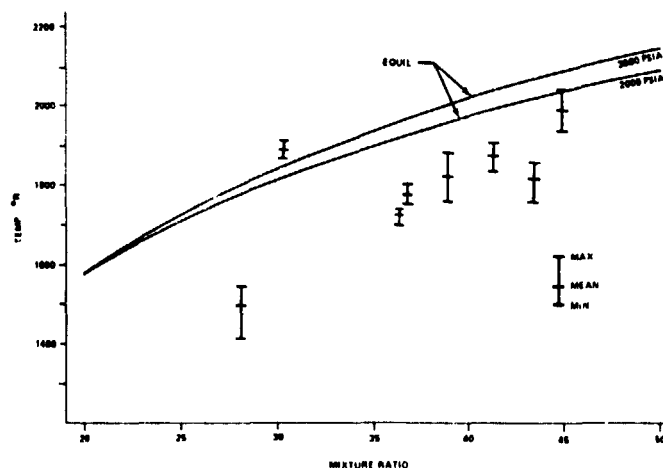
Figure 46. Comparison of Test Data to Theoretical Combustion Temperature.

Carbon accumulation as a result of preburner combustion does not appear to be a potential problem for oxygen-methane engines. The amount accumulated in either the preburner chamber or the fuel inlets to the main injector was insignificant at the end of the test series.

The only preburner problem encountered during the program was difficulty with propellant ignition using normal turbine drive-gas mixture ratios. A temporary solution of shifting the overall preburner mixture ratio to more oxidizer rich during the start transient allowed the program to continue, but it is unacceptable for an engine system because of turbine blade

88

exposure to the resulting high temperature spike. Additional work will be required to develop an injector design which will provide zones of higher mixture ratio near the injector face to promote ignition yet still provide the subsequent mixing required for a uniform temperature profile.

The calorimeter chamber was tested nine times at pressures ranging from 1382 to 2135 psia with propellant mass mixture ratios from 2.38 to 3.52. Characteristic velocity efficiencies exceeded 97 percent during all calorimeter tests. Combustion chamber heating rates were as predicted at the lower mixture ratios but exceeded the prediction in the nozzle throat by approximately 17 percent at the higher mixture ratios. Biasing the outer ring of injector elements to a mixture ratio of approximately 2.5 proved to be effective in reducing heating rate. Details are shown in Figure 47. This is an acceptable approach only for large engines in which the number of outer ring injector elements is a small percentage of the total. For a 600,000-pound thrust engine, the predicted performance loss using a biased mixture ratio is 2.0 to 3.8 sec specific impulse. Test hardware deterioration during the calorimeter testing was limited to relatively minor erosion of several main injector fuel sleeves. Erosion occurred only during the lower pressure tests, and this is believed to have been caused by injector element operation at mixture ratios greater than stoichiometric, not counting the face coolant flow.
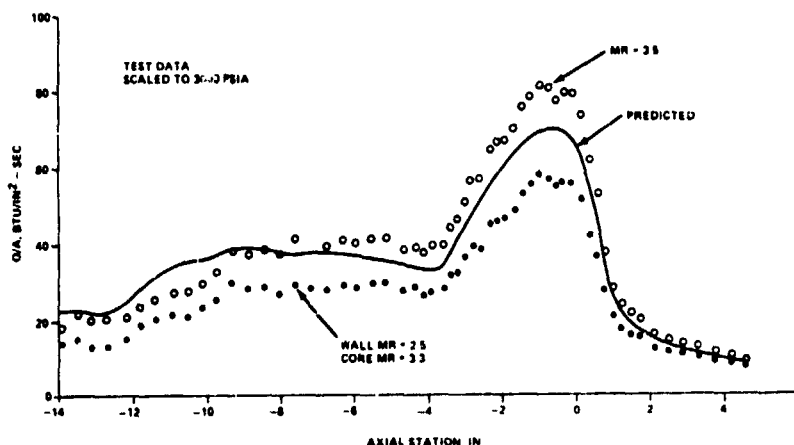
Figure 47. Heat Flux Profiles, 3000 psi Oxygen-Natural Gas Combustion.

The regenerative chamber was tested four times. The results were characterized by a sharp reduction in combustion efficiency and an increase in nozzle throat heating rate as propellant mass flow rates were increased. It is suspected that the increased liquid oxygen flow rate results in reduced oxygen vaporization which, in turn, disrupts the nozzle boundary layer and increases the heating rate. The primary contributor to reduced vaporization rate as compared to the oxygen-hydrogen system is believed to be the lower fuel injection velocity associated with the higher molecular weight fuel. An injector redesign will be required to improve both vaporization and mixing. This effort was sponsored by the Office of Aeronautics and Space Technology. (C. R. Bailey/EP23/205-453-1049)

Publication:

Bailey, C. R., "CPIA Publication 390," JANNAF Propulsion Meeting, February 1984.

Ignition Flow Visualization System Concept

Special instrumentation techniques were required to provide hot test empirical data to support development of a comprehensive combustion analytical code. Specifically, a better flow visualization technique was developed to compare with the analytical code predictions of pre-ignition injection flow field mixture ratios and resulting ignition processes.

Most of the data collected is in the form of high-speed laser Schlieren cinematography and ultraviolet cinematography of the actual ignition and combustion process inside a combustion chamber system. A laser Schlieren system (9000 frames/sec) was used to observe a combustion model of the Space Shuttle Main Engine (SSME) oxidizer preburner coaxial injector element. The combustion assembly used for the ignition test series is shown in Figures 48 and 49.

The chamber has two unique fused-silica window assemblies through which the combustion process can be viewed optically.

The high-speed cinematography diagnostic system is shown in Figure 50. The primary diagnostic system consisted of two separate subsystems: a high-speed ultraviolet cinematography system and a high-speed laser Schlieren cinematography system. The high-speed ultraviolet cinematography system was used to view the OH species concentrations in the combusting flow. The ability to view only the OH concentrations is very useful in studying the oxygen/hydrogen combustion process. The OH radical is very short-lived and kinetic (at the test conditions), and exists mainly as a part of the overall chain of reactions in the combustion process. Therefore, the OH concentrations are a direct indicator of the locations where the actual combustion reactions are taking place. The high-speed laser Schlieren cinematography system proved to be a very useful diagnostic tool for the oxygen/hydrogen combustion system. Run at very high framing rates (9000 frames/sec), the system was able to record flow patterns, spark-heated gas puffs, spark ignition, propagation of the ignition process, flame outs, and steady-state combustion/flow patterns.

The review of the high-speed laser Schlieren and ultraviolet films has yielded some new insights into the mechanisms of gas/gas coaxial element ignition.

There appears to be a feature within the coaxial element flow stream that is acting as a flame holder near the injector face. This feature is able to flamehold even though the mean jet velocities are several times the theoretical flame propagation speed for a well-mixed gas of similar mixture ratio. Since the combustion process is unable to propagate upstream in the high-velocity jet flow, another ignition mechanism is required to ignite the flame holding feature near the injector face. The observed mechanism appears to have two basic requirements. First, the gas/gas flow stream must

be disturbed, either slowed down, reversed, or blown sideways away from the element. Second, this disturbing action must take place while there is combustion (an ignition source) present in the recirculating gases surrounding the jet flow near the injector face. When the high-velocity jet is disturbed, the flame holding feature becomes exposed and can be ignited by the combustion in the surrounding gases.

Two forms of the required disturbance were observed. First, the rapid flame propagation within the high mixture ratio recirculation gases present in the oxidizer lead tests provided the required disturbance. The rapid pressure increase from combustion in the recirculation gases actually reversed the element flow stream in some of the tests. Second, ignition of a high mixture ratio flow stream (approximately 2 inches from the injector face) was violent enough to disturb the element flow stream and allow ignition of the flame holder near the face. The phenomenon was observed on fuel lead tests that had sufficiently high mixture ratios in the recirculation zones to allow flame propagation within the slow moving recirculation gases that in turn ignited the element stream approximately 2 inches from the face. The ignition of this zone propagated rapidly and provided a pressure surge and the required disturbance of the element stream near the face. However, the flame did not propagate up the element stream. Only after the element stream was disturbed was the flame holding region able to be ignited.

The Schlieren system utilized a 0.5-watt argon ion laser, standard Schlieren/laser optics, and a Hycam camera with 400 ASA film. Figures 51 and 52 show the actual diagnostic setup. The use of a laser light source for the Schlieren work is advantageous for two reasons. First, the intensity of the laser makes it possible to record Schlieren data at high framing rates on standard film. Second, it is a simple task to filter out the lumination created by the combustion process and view only the narrow band wavelengths of the laser Schlieren system flow field data. An additional benefit is that a laser system is easier to work with optically.

Figure 53 is a collection of prints made from the high-speed laser Schlieren film from Test No. 10.1, which was a typical fuel lead test with a high mixture ratio (1.1 oxygen/hydrogen). The sequence of photos (only 15 frames out of a 400-foot roll) is presented to give a representation of the type of information available from the laser Schlieren films. Every fifth frame of the actual sequence was printed. The sequence goes from left to right. The actual framing rate was near 9000 frames/sec. Unfortunately, the reproduction of the film does not portray the quality and the information available from these films.

The high-speed laser Schlieren and ultraviolet diagnostics have proven to be extremely useful tools in the study of the low-mixture ratio ignition and combustion of hydrogen and oxygen in a rocket combustion system. With the high-speed laser Schlieren cinematography system flow patterns, the actual spark ignition process, combustion propagation, and flame outs can be visualized with great detail. The high-speed ultraviolet cinematography has allowed visualization of high OH concentrations and zones of the actual combustion process. These very graphic visualization techniques complement each other.

91

Because of the successful application of these techniques and the large amount of insight gained, additional refined studies into low-mixture ratio oxygen/hydrogen ignition and combustion are being pursued to further understand the mechanisms involved. This effort was sponsored by the Office of Aeronautics and Space Technology. (D. Pryor/EP25/205-453-3793)

Publication:

Fisher, S. C., "Laser Schlieren and Ultraviolet Diagnostics of Rocket Combustion," presented Advanced High Pressure Oxygen/Hydrogen Conference, Huntsville, Alabama, June 1984.
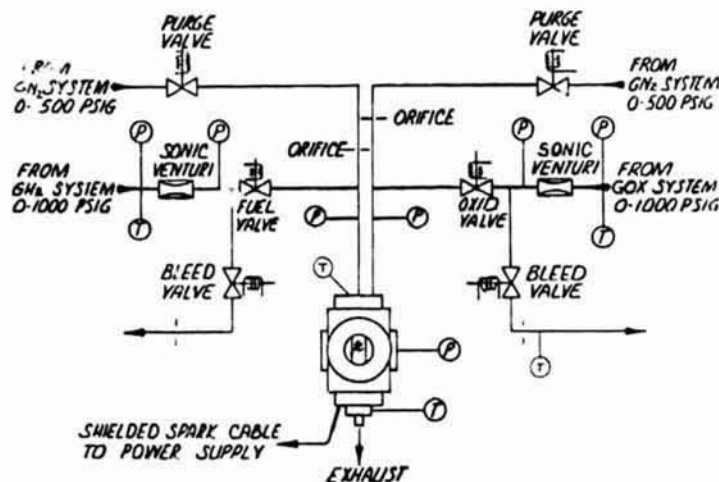
Figure 48. Combustion Assembly Schematic Used for Ignition Test Series.
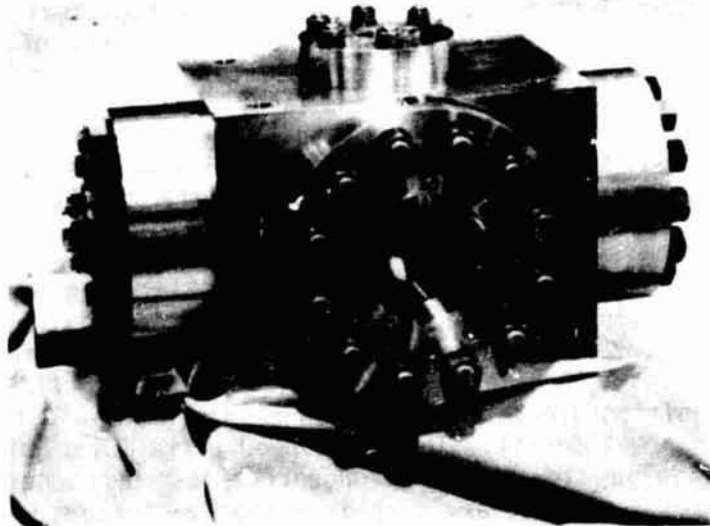
Figure 49. Combustion Assembly Used for Ignition Test Series.

A) 4x5 WITNESS CAMERA
B) IMAGING LENS
C) IMAGING LENS
D) VARIABLE BEAM SPLITTER
E) HYCAM CAMERA
F) SCHLIEREN FILTER
G) SCHLIEREN OBSTRUCTION

H) FLAT TURNING MIRROR
I) FLAT TURNING MIRROR
J) 60 IN FL SPHERICAL MIRROR
K) TV MONITOR
L) FASTAX CAMERA QUARTZ
   LENS AND SAPPHIRE PRISM
M) FASTAX FILTER

N) COMBUSTION CHAMBER
   FUSED – SILICA WINDOWS
O) 60 IN FL SPHERICAL MIRROR
P) FLAT TURNING MIRROR
Q) 10 x MICROSCOPE OBJECTIVE AND
   25 MICRON PINHOLE ASSY
R) ARGON ION LASER

Figure 50.   High-Speed Cinematography Diagnostic System.

Figure 51.   Diagnostic Setup of Schlieren/Laser Optics.

93
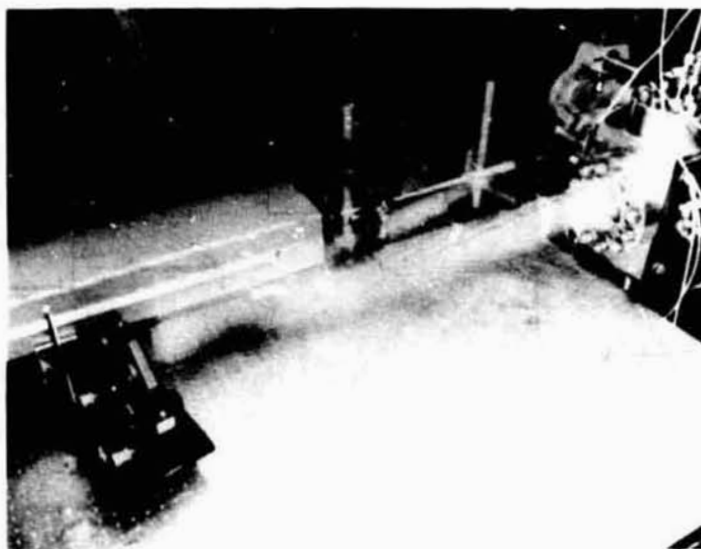
Figure 52. Diagnostic Setup of Schlieren/Laser Optics.
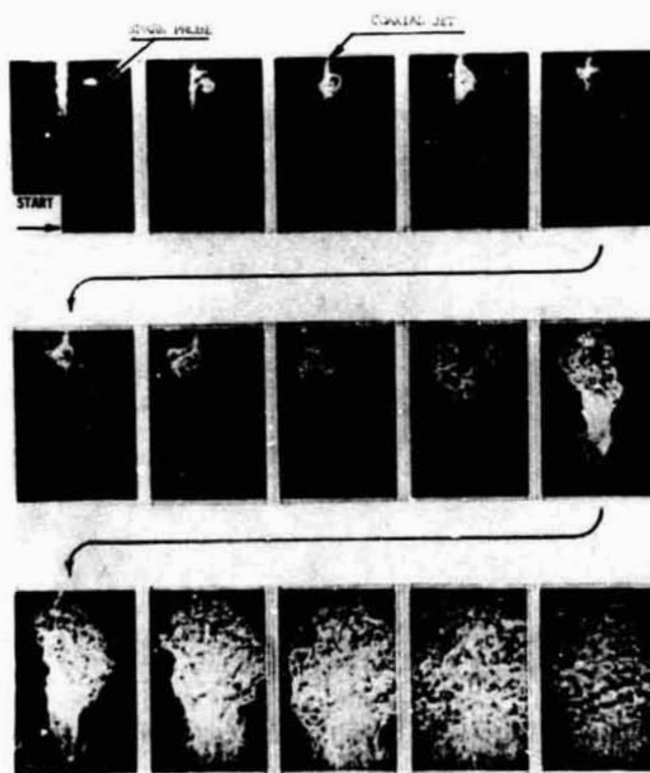
Figure 53. Collection of Prints from High-Speed Schlieren Film.

Space Shuttle Alternate Nozzle Ablatives Program

The objective of this effort is to develop and demonstrate alternate shuttle Solid Rocket Motor (SRM) nozzle ablatives. Concern has been expressed about the volume requirement of the present ablative precursor being insufficient to ensure continued profitability and retention of the supply source. Two other precursors have been investigated in this effort. Pitch is an attractive alternate precursor for carbon fibers because it is readily available, is low in cost, has a high carbon content, and requires a relatively low amount of energy for conversion into a pyrolized product. Likewise, polyacrylonitrile (PAN) is attractive because it has a stable market, is low in cost, has a high carbon content, and has multiple producers.

Four 10-inch-throat-diameter tests were conducted to investigate pitch- and PAN-based ablatives at selected nozzle locations. Figure 54 depicts a typical subscale test nozzle configuration. All four SRM subscale nozzle assembly tests were conducted successfully. In these four tests, eighteen alternate carbon-phenolic, tape-wrapped ablatives were tested in a selected nozzle location; e.g., throat, nose, or exit cone. F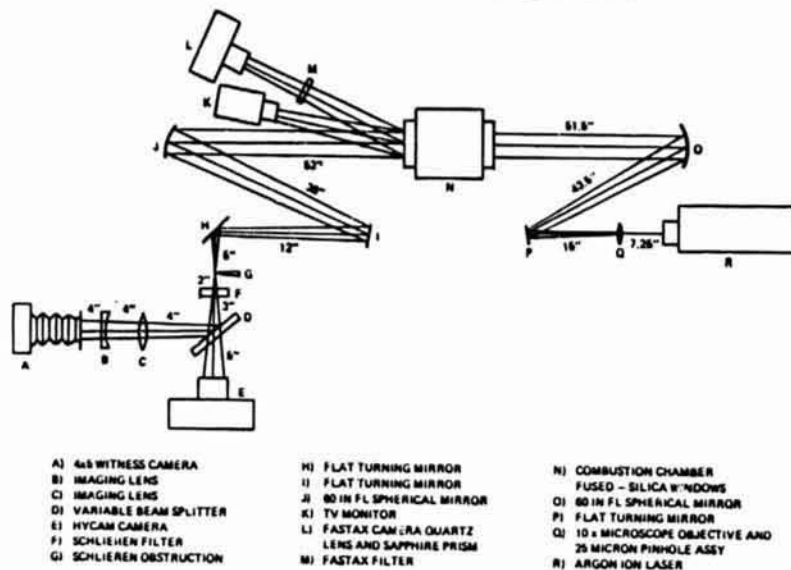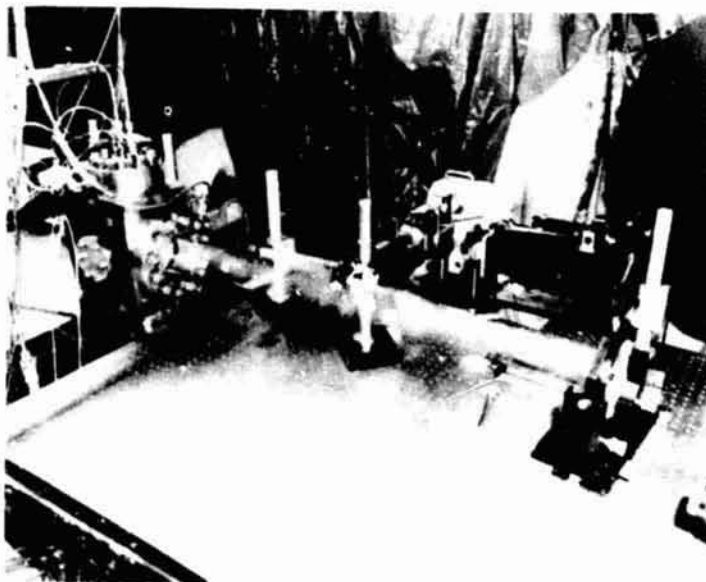ifteen contained reinforcement fabric made of carbon yarn that utilized a PAN precursor, and three contained reinforcement fabric made of carbon yarn that utilized a pitch precursor. Three of the PAN carbon-phenolic materials were made using no filler in the phenolic resin, and another four used carbon microballoons as the filler in the phenolic resin to achieve a low density (1.21 to 1.30 g/cm^3) in the as-cured state. The remainder of the PAN carbon-phenolic materials used carbon powder as the filler in the phenolic resin at various percentages by weight loading (5 to 18 percent), and had densities in the as-cured state that ranged from 1.50 to 1.56 g/cm^3. The three pitch-based, carbon-phenolic materials all contained carbon powder as a filler in the phenolic resin (ranging from 10 to 18 percent by weight), and had as-cured densities ranging from 1.63 to 1.66 g/cm^3. Three alternate composite materials were tested as the backface insulator of the nozzle throat. One was a ceramic fiber (aluminum, silicon oxides), mat-phenolic resin material with no filler in the resin and with an as-cured density of 0.90-1.0 g/cm^3. The other two were E-glass, fiber mat-phenolic resin materials with no filler in the resin, and with as-cured densities of 1.0 to 1.1 g/cm^3. All three of the insulation materials were processed into the nozzle components by the tape-wrap technique. Only one alternate material was tested as the structural overwrap component of the exit cone liner. It was a carbon fiber-epoxy material, using PAN-based carbon fibers, that was applied to the nozzle by the filament winding technique. It had an as-cured density of 1.55 g/cm^3.

From analyses and inspection of post-test nozzle sections from the subscale tests, it was concluded that a full-scale SRM nozzle can be successfully designed using materials tested in the program. The design would: (1) weigh less than the current qualified SRM nozzle assembly; (2) include PAN-based carbon cloth-phenolic material in the throat region to provide a 15 to 24 percent decreased erosion over that experienced with the baseline rayon-based carbon cloth-phenolic material; (3) employ lightweight PAN-based carbon cloth-phenolic material for the aft exit cone, fixed housing, and cowl; (4) use lightweight glass-phenolic material for all insulator components; and (5) have a PAN-based graphite fiber-epoxy filament wound exit cone overwrap. The alternate full-scale SRM nozzle assembly shown in Figure

55 would provide an increase in payload capability, a multiple supply source, and a cost reduction due to the lower cost of raw materials. (B. Powers/EP25/205-453-4739)

Publication:

Kimmel, N. A., "Alternate Nozzle Materials Program," JPL Report No. 84-58, in press.

1	2	3	4	5	6	7	8	9	10	11	12
K411 SPUN PAN STACKPOLE	K411 SPUN PAN STACKPOLE	K411A SPUN PAN POLYCARB	FM5074 SPUN PAN STACKPOLE	MX4960 LD MAT E GLASS	FMS034A SPUN PAN POLYCARB	K411 SPUN PAN STACKPOLE	MX134LD LD PAN (3K) PLAIN WVE	FX475R21 GRPH EPXY AS4/902	FMS908 LD PAN (6K) LENO WVE	MX4967 LD PAN (3K) LENO W /E	FMS908A LD PAN (3K) PLAIN WVE
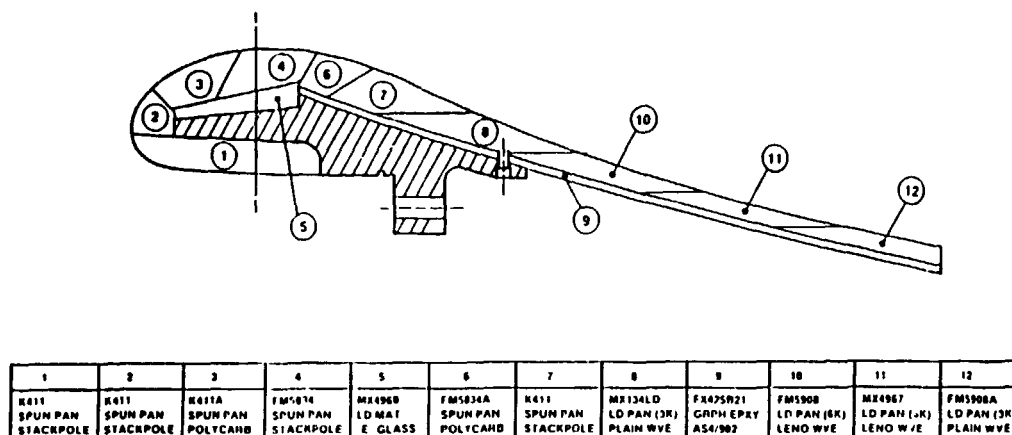
Figure 54. Alternate Ablatives Subscale Test Nozzle.

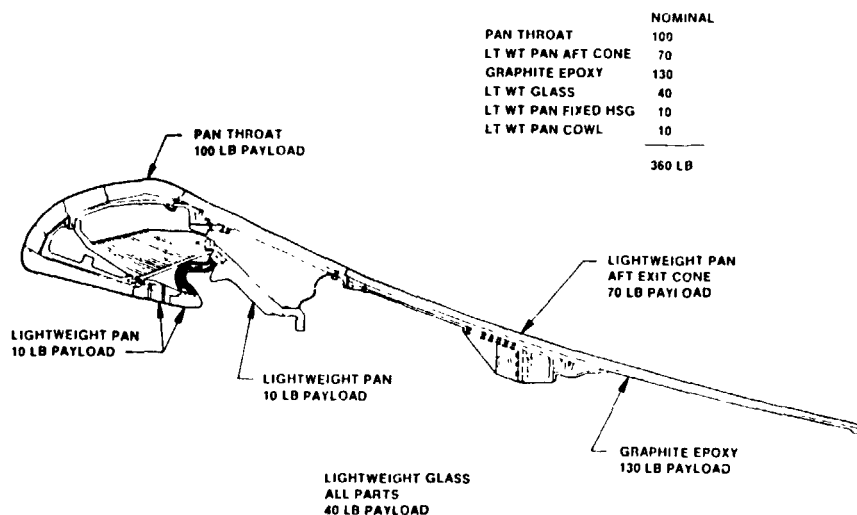|	NOMINAL
PAN THROAT	100
LT WT PAN AFT CONE	70
GRAPHITE EPOXY	130
LT WT GLASS	40
LT WT PAN FIXED HSG	10
LT WT PAN COWL	10
	360 LB

Figure 55. Full-Scale Alternate Ablatives SRM Nozzle.

High-Speed Cryogenic Turbomachinery Main Shaft Bearing Research, Technology, and Modeling

The objective of this effort is to advance the state-of-the-art in bearing technology, primarily cryogenic turbomachinery bearing technology, by exploring the life and performance effects under various loads of design, materials, manufacturing, and lubrication system changes; to compare each new variation against the current bearing design in full-scale cryogenic tests; and to utilize test data to verify thermal and mechanical cryogenic bearing models. Many of the SSME turbomachinery failures and life problems can be attributed to their rotor support bearings and the loads and speeds being imposed upon them. Bearing life and load carrying capacity improvements are required.

At MSFC, an in-house bearing tester and hazardous test facility have been designed and built such that full-scale cryogenic turbopump tests can be made utilizing liquid nitrogen or oxygen. Future plans are to expand the facility to permit liquid hydrogen, full-scale bearing tests. The present facility can accommodate lox bearing bore sizes from 45 to 85 mm and shaft speeds to 42,000 r/min. The tester and facility will be utilized to test various new bearing materials, including new alloys and some powder metallurgy materials. Concepts being planned or being designed and manufactured out-of-house include powder metallurgy ball bearings (three different alloys), roller bearing designs (three different alloys and/or designs), and various bearing alloys which have been surface-altered with different ion implantation or ion plating processes. A magnetically levitated bearing is being studied. Various lubrication scheme studies and tests are also planned. Out-of-house feasibility contracts which culminate with the manufacture of bearings are intended to supply the bearing tester with test articles. All concepts, designs, and materials will be tested in direct comparison to the standard 440C angular contact bearings currently being utilized. An out-of-house contract was also let for a study of available bearing computer programs and the analysis of data being generated by the bearing tester. The intent is to have mechanical and thermal bearing computer programs generated and adjusted to predict thermal performance, cryogenic bearing life, and other pertinent turbopump bearing design parameters.

A lumped-node thermal network model of the SSME lox turbopump turbine end bearing has been developed. This model represents the bearing elements, the shaft, carrier, housing, and cryogenic fluid flow. The two-phase heat transfer characteristics of the cryogen are modeled to account for the various regimes of forced convection boiling. Typical results show that for specific loading conditions there is a thermal mechanical coupling that can cause loss of operating clearances (due to thermal growth of the bearing), increased loading, and heat generation, subsequently causing premature bearing failure. It has also been found that the bearing contacts operate at temperatures well above the local saturation temperature of the cryogenic fluid and are, therefore, operating in vapor rather than liquid. Consequently, any fluid lubrication or benefits that might be expected from fluid film separation of the contacts do not occur at those conditions.

This information provides visibility into potentially different failure modes for these operating conditions. Elevated temperatures can reduce lubrication, increase surface friction and shear, and reduce surface hardness. These conditions support a surface failure mode rather than the traditional subsurface fatigue experienced by conventionally operated rolling bearings. The modeling techniques developed are vital in the assessment of new materials for high-speed bearings operating in cryogenics due to the strong influence of material properties on contact temperatures and thermal gradients. In addition, these modeling methods have extended the capability for analytical evaluation of the thermal and mechanical operating characteristics of high-speed rolling bearings in cryogenics. Figures 56 through 60 show indepth explanations of the features of this bearing thermal model. (F. Dolan/EH14/205-453-1504)
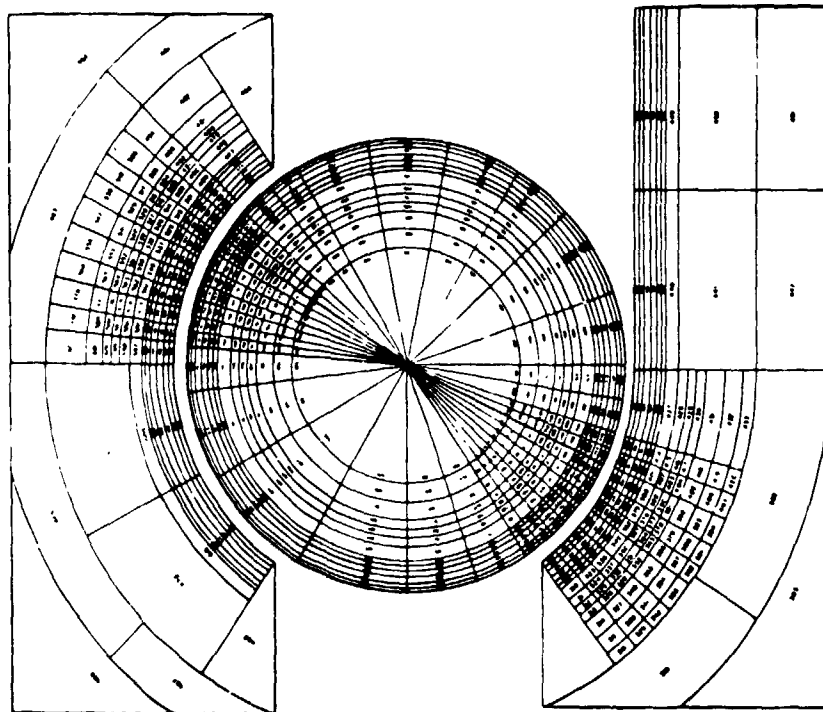
Figure 56. Finite Element Representation, 57 mm Bearing. The inner race, ball, and outer race are shown. There are 642 nodes in the model. Surface nodes are connected by the appropriate thermal resistors to the cryogenic fluid. Techniques have been developed to adjust these resistors, as the surface temperature of the node changes, to represent the various regimes of fluid boiling.
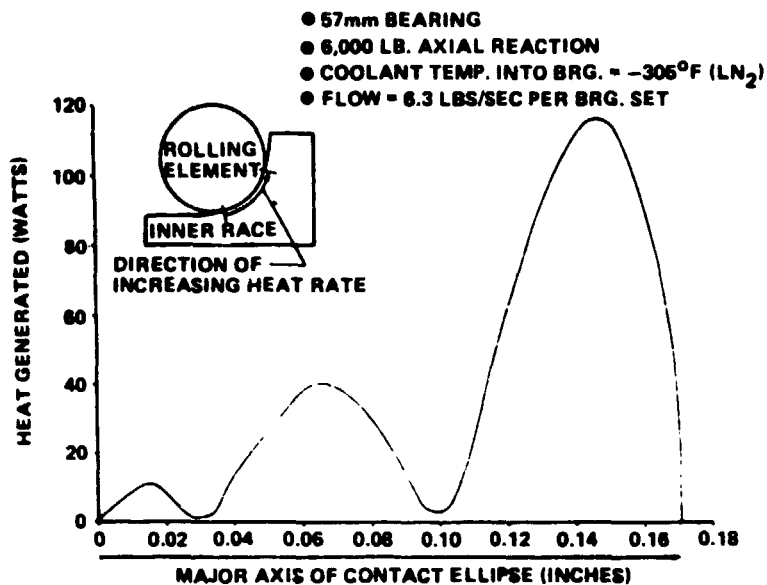
Figure 57. Inner Race Heat Generated at Contact Ellipse. An estimate of the frictional heat generated across the inner race/ball contact for the indicated operating conditions is shown. This distribution accounts for the friction generated due to ball sliding and spinning in the contact. The minimum values represent the areas of relative rolling. The maximum value at the inner race shoulder is due to the large relative velocity caused by ball spin. The outer race neat distribution is obtained in a similar manner, and these values are input to the bearing thermal model. This permits a detailed representation of the surface temperature in the bearing contacts.

(TEMPERATURES IN DEGREES FARENHEIT)
AXIAL REACTION = 6000 LB.
FLOW RATE = 6.3 LBS/SEC PER BRG. SET
COOLANT TEMP. INTO BRG. SET = -305°F (LN$_2$)

TRACK NODES
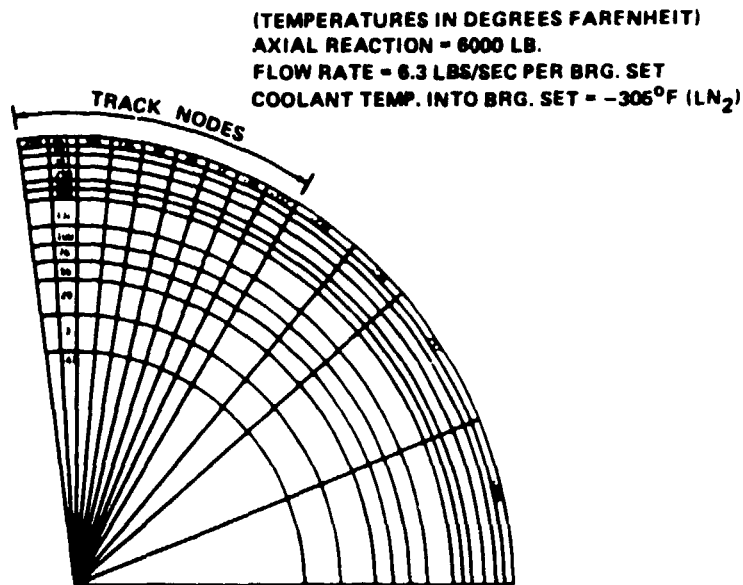
Figure 58. Rolling Element Temperature Distribution for Lox Pump Turbine End Bearing. These temperatures were based on the load and environment conditions. Notice that the contact temperatures are well above the local saturation temperature (-241 °F) of the LN$_2$ coolant.

- 57mm BEARING
- 30,000 RPM SHAFT SPEED
- 6,000 LB AXIAL REACTION
- COOLANT INLET TEMP (°F) (LN$_2$)
- f = 0.2 ──── -285
          ──── -305

Figure 59. Average Bearing Component Temperature Versus Coolant Flow. The component temperatures become increasingly nonlinear as the flow is reduced due to the increased rate of clearance reduction caused by thermal growth.

100
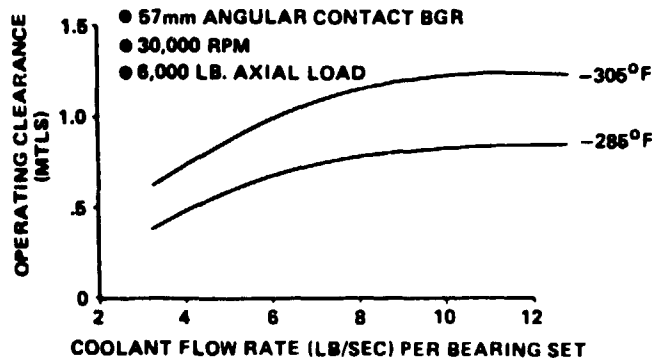
Figure 60. Operating Clearances Versus Coolant Flow. The reduction in operating clearances as the coolant flow is reduced causes an increase in heat generation, bearing thermal gradient, thermal growth, and contact loads.

Effects of Sodium on Processing and Properties of Carbon/Phenolic Nozzle Materials

A systematic evaluation has been completed on effects of sodium on the resin chemistry, and, therefore, the processability and cure of the resin, and on the mechanical and thermal oxidative properties of carbon/phenolic composite materials used as an ablative liner in the solid rocket motor nozzle of the space shuttle. The results show that an increasing sodium level has the following effects on processing and cure of the resin: increased moisture pickup by the B-stage resin; lowering of the polymerization onset temperature; and an increase in resin cure kinetics. Mechanical properties show a plasticizing effect due to increasing sodium level; i.e., increased shear strength and lower flexural strength. Thermal oxidative stability is lowered by increasing sodium levels, and thermal expansion and water vapor absorption are increased. This work was performed at MSFC through funding from the Shuttle Solid Rocket Booste Projec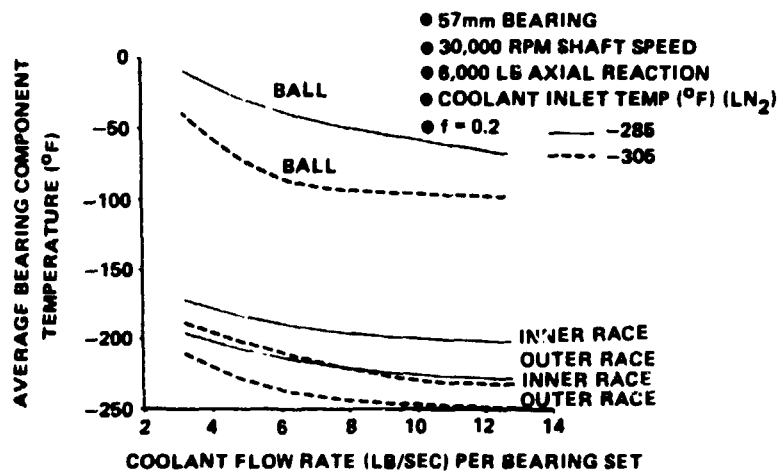t Office. The results provide the most comprehensive data set available on the impact of impurity sodium in this class of materials and a basis for the proper specification of materials for flight motor nozzles. (B. Goldberg/EH34/ 205-453-1227)

Powder Metallurgy Techniques

State-of-the-art 440C bearings are currently used in the space shuttle main engine turbopumps. However, these bearings have a relatively short life in the high pressure oxidizer turbopump. The problems are high wear rates and spalling by rolling contact fatigue. To alleviate these problems, improved bearing materials are being developed which have greater resistance to wear and spalling. These new materials are prepared by powder metallurgy (PM) techniques. The main advantage of PM techniques lies in the ability to control the volume percent and size of carbides. The microstructures show uniform distribution of fine carbides, which helps to improve the rolling contact fatigue life. Higher volume percent of

carbides tends to increase the hardness and hence, the wear resistance of bearing material. Hot isostatic pressing is used to obtain 100 percent density.

Several promising candidate materials (some having rolling contact fatigue lives 5 to 10 times the standard 440C) have been identified. These materials are being further characterized for fracture toughness and corrosion resistance. In addition, bearing balls will be manufactured and tested in a five-ball tester. Based on the results of tests, three most promising candidates will be selected for manufacturing full-scale bearings. (B. N. Bhat/EH23/205-453-5509)

SSME Internal Flow Process Modeling

The Space Shuttle Main Engine (SSME) Computational Fluid Dynamics Team of the Systems Dynamics Laboratory's Fluid Dynamics Branch continued its activities toward the development of a strong MSFC in-house capability for gaining a better physical and quantitative understanding of factors governing physical and chemical processes in SSME internal flows and characterizing such environments by suitable mathematical models and computer codes. Preliminary studies on the preburner fuel/oxidizer mixing and hot gas manifold flows, together with a two-dimensional (axisymmetric) turbulent flow and heat transfer of three configurations of the turnaround duct, have been completed along with a three-dimensional analysis of the hot gas manifold system using a constant eddy-viscosity turbulence model. An in-house code for transient flow conditions is being developed using the method of lines. Analysis of turbulent flow and heat transfer in SSME turnaround ducts will be published in the Journal of Propulsion and Power. (N. C. Costes/ED42/205-453-0946)

Effects of Geometry on Linear Shaped Charges (LSC's)

The loss of two Solid Rocket Boosters (SRB's) during the STS-4 mission in June 1982 prompted an investigation of LSC's and the shock they produce. A project was initiated to evaluate the effects of geometrical variations of LSC's, the effects of chevron irregularities, and the variation in the shock response spectra (SRS) produced by the firing of LSC's from the same production lot.

Geometrical variations have been investigated with each of the three vendors of the LSC's that are used on MSFC space shuttle programs. This investigation involved a physical measurement of the chevron shape and an inspection of the liner area for any visible irregularities. At least 50 samples from each vendor were inspected. Most of the observed irregularities were introduced during the forming process. They were found to have been caused by defects in the rolling wheels such as chips caused by repeated usage, foreign material embedded in the wheels, or poorly manufactured wheels. The most serious type of irregularity observed is a curvature in one or both surfaces of the liner (Figure 61). This curvature is an indication of a separation of the liner from the explosive and occurs when the liner springs back after the forming process. This condition is usually caused by an insufficient number of forming operations. A survey

of the literature documenting the pyrotechnic shock associated with the firing of an LSC has been completed. Most of this literature was generated in the late 1960's and the early 1970's. An investigation of the topic proposed for this study was not found.

The testing program to identify the variation in SRS for LSC's from the same production lot has been defined. Explosive Technology has been awarded a contract to perform this testing beginning in October 1984. (J. L. Smith/ED23/205-453-2521)

LINEAR SHAPED CHARGE
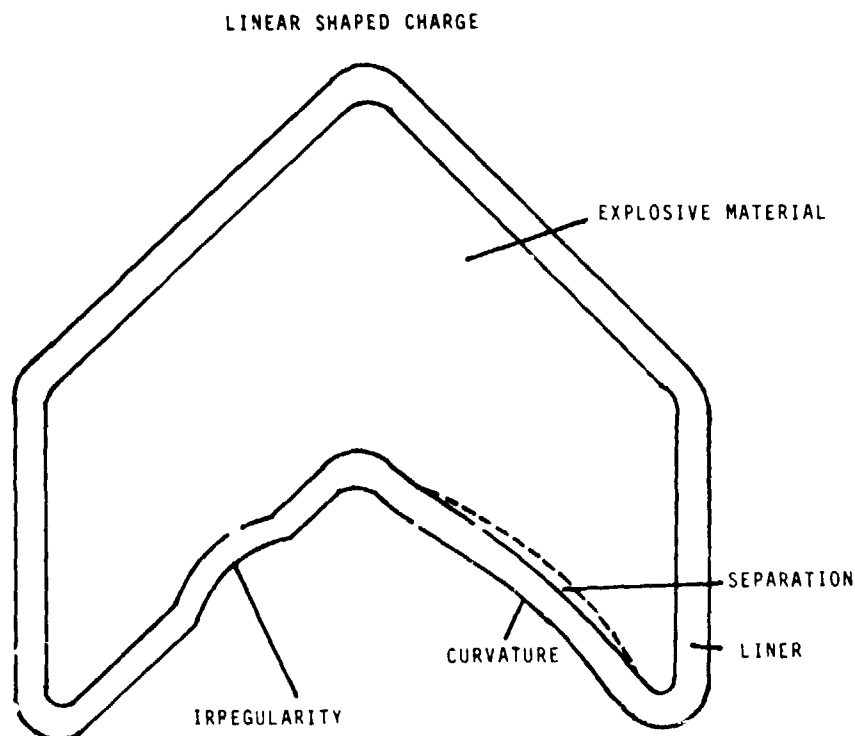
Figure 61. Types of Geometrical Variations Affecting LSC's.

Development of Dynamic Coefficients for Turbopump Seals

During the early phase of the Space Shuttle Main Engine (SSME) development program, both the High Pressure Fuel Turbopump (HPFTP) and the High Pressure Oxidizer Turbopump (HPOTP) experienced severe vibration problems which limited their operations considerably. Both pumps exhibited tendencies to subsynchronous whirl with large amplitude motions at speeds below the SSME Rated Power Level (RPL). Stable and reliable operation at RPL was made possible by changes which included use of annular seals in place of labyrinth seals in the HPFTP pump interstage and the HPOTP turbine interstage. The annular seals provided increased stiffness and damping forces at those locations, while providing reduced tangential destabilizing forces which are inherently large in labyrinth seals. The seal design was based on theoretical calculations which were experimentally verified only by water

tests at relatively low Reynolds numbers. Dynamic analysis and test data obtained subsequently indicated the pumps were marginally stable at power levels above RPL to Full Power Level (FPL). Due to lack of instrumentation internal to the pumps, their stability margins could not be ascertained.

A research program was undertaken which provided a high Reynolds number seal data base for calculating rotor dynamic coefficients of annular seals. A reasonable correlation between experimental data and analytical prediction was established. This formed the basis for a modified analytical prediction technique with improved accuracy. The investigation findings also indicate that annular seals with optimum characteristics, depending on the specific application, are feasible. From a performance viewpoint, minimum leakage is desired. For rotor dynamic consic rations, maximum effective damping is desirable, but the preference for effective stiffness may vary. Some applications may benefit from seals with moderate stiffness; whereas, for other applications, maximum stiffness may be preferred. The desired characteristics can be achieved by applying a specific degree of roughness on the stationary surface of the seal.

Table 1 is a summary of the findings of this investigation. It is shown that tapered smooth seals have approximately twice the effective stiffness and effective damping of comparable stepped smooth seals with the same leakage. The effective stiffness and added mass terms derived from measured data are much larger than predicted. Also, a comparison of the relative merits of the seal roughness configuration indicates the round pocket configuration is preferable. These findings strongly support the use of the tapered smooth seal configuration in the HPFTP pump interstage seal and the roughened stator seal configuration for the HPOTP seals.
(F. Garcia//EP23/205-453-3812)

Publication:

Childs, D. W., "SSME Interstage Seal Research Progress Report," Report No. RD-1-84 (Turbomachinery Laboratory, Mechanical Engineering Department, Texas A&M University, College Station, Texas), 1984.

Table 1. Comparison of Annular Seal Test Results

Stepped vs. Tapered	$\dfrac{K_{EF}}{K_{EF}(REF)}$	$\dfrac{C_{EF}}{C_{EF}(REF)}$	$\dfrac{C_L}{C_L(REF)}$
Smooth Stepped Seal	1.00	1.00	1.00
Smooth Tapered Seal	2.04	2.45	1.07

Experimental vs. Theory	$K_{EF}(\tfrac{EX}{TH})$	$C_{EF}(\tfrac{EX}{TH})$	$M_{EF}(\tfrac{EX}{TH})$
Smooth Stator/Smooth Rotor	1.5-2.0	~1.0	1.0-1.5
Rough Stator/Smooth Rotor	1.5-2.0	~1.0	1.0-2.0

Smooth Stator vs. Roughened Stator	$\dfrac{K_{EF}}{K_{EF}(MAX)}$	$\dfrac{C_{EF}}{C_{EF}(MAX)}$	$\dfrac{C_L}{C_L(MAX)}$
Smooth	0.82	0.86	1.00
Diamond Pockets	1.00	0.86	0.73
Round Pockets	0.80	1.00	0.63

Nomenclature: K_{EF} = Effective Stiffness

C_{EF} = Effective Damping

M_{EF} = Effective Added Mass

C_L = Leakage Coefficient

EX = Experimental

TH = Theoretical

105

Effect of Trace Impurities on Reactivity of Materials in Hydrazine

The fuel isolation valve from the Solid Rocket Booster Auxiliary Power Unit on STS-11 showed signs of a white material on the cog and shaft. Analysis of this material indicated a high chloride content. An investigation led to the possibility that hydrazine could have reacted with traces of chlorinated solvents used in cleaning operations.

Trace amounts of Freon TF were added to hydrazine and placed under a steam bath to evaporate to dryness. It was found that hydrazine reacts with Freon to form hydrazine monohydrochloride. This salt is highly acidic and corrosive to metals. Analysis of the corrosion products by energy dispersive x-ray fluorescence and energy dispersive analysis by x rays indicated a high chloride content as well as the presence of iron, chromium, and molybdenum.

Further investigations are underway to ascertain whether other reaction products were formed and whether the hydrazine-Freon TF combination has a deleterious metallurgical effect on steel components. (R. T. Congo/ EH32/205-453-1286)

Influence of Variations in Gravity on the Microstructure of MAR-M246(Hf)

MAR-M246(Hf) was directionally solidified in a high temperature furnace with a water-cooled quench block while onboard NASA's KC-135 aircraft. This aircraft flies a series of parabolas during which the experiments and personnel experience up to 30 seconds of low-gravity time (10^2 g) and up to 1.5 minutes of pullout and climb (up to 1.7 g). Therefore, a sample which is being solidified experiences a repetitive sequence of low- and high-gravity forces. Growth rates of 1.0 and 1.6 cm/min were selected for the alloy since these produced excellent dendritic structure in the laboratory and would enable around 5 mm of sample to be solidified during the low-gravity periods. Ground-based control samples were solidified in the same furnace under identical conditions excepting the gravity force variation.

Secondary dendrite arm spacing measurements and volume fraction carbide measurements were taken along each ingot length. In each instance, secondary arm spacings increased in low gravity and decreased in high gravity. The primary arm spacings were also larger for the low gravity than for the high-gravity sections. There is a distinct difference in the amount of interdendritic phase present. The low gravity has significantly less than the high-gravity section, an effect that is paralleled by the carbides. However, a microprobe trace along the sample indicates that there is no gross difference in the constituents in the two regions. The volume fraction of carbides also decreases with decreasing gravity force, but it lags the change in dendrite arm spacing. The ground-based samples did not show any variations in dendrite arm spacings or segregation of constituents as a function of distance along the axis.

Variation in gravity force during directional solidification of the superalloy MAR-M246(Hf) produces a concomitant variation in microstructure

and microsegregation. Both primary and secondary dendrite arms spacings are larger in the low-gravity portion, the latter being due to an increased coarsening rate. The amount of interdendritic constituents and carbides decreases with decreasing gravity and is an effect generally seen when arm spacings increase. Although the overall homogeneity of the sample remained constant, the actual composition of the carbides and interdendritic eutectic was found to vary with gravity level. (M. H. Johnston/EH22/205-453-5510)

MATERIALS

Electrochemical Studies of Hydrogen Uptake and Elimination by Bare and Gold-Plated Waspaloy

Electrochemical studies, using samples charged with high pressure hydrogen (5000 psi), of hydrogen uptake by bare Waspaloy at room temperature have indicated that such hydrogen is contained in the interstitial solid solution of the metal. This result was obtained using a new method for the analysis of hydrogen desorption proposed by Zakroczymski, which distinguishes between fast hydrogen and hydrogen desorption controlled by the diffusion process. The result for high pressure hydrogen charging is in contrast to that for electrolytically charged samples, where the hydrogen is in the form of surface and subsurface hydrodes which are unstable at room temperature and which represent the so-called fast hydrogen. The fact that the rate of elimination for electrolytically charged samples is faster than that for samples charged at high pressure was verified in this study by measuring the rates of elimination of hydrogen for both methods of charging. The rate constant for electrolytically charged samples was greater by over a factor of 2.

Studies of hydrogen uptake by gold-plated samples were also made. The breakthrough point for samples charged at high pressure for a period of 1 hour was determmined to lie between 0.0005 and 0.001 inch of gold plate. Although hydrogen penetrated 0.0005 inch of gold plate at 5000 psi, the reverse process (diffusion of hydrogen out of the sample after removal of the sample from the charging chamber) was prevented by the gold plate. The gold plate, therefore, traps the hydrogen which enters under high pressure conditions.

The effect of electropolishing the Waspaloy metal surface was also determined. It was found that electropolishing drastically reduces the amount of hydrogen absorbed by the metal sample when charged under the same conditions at high pressure. This observation is in agreement with other studies, using different techniques, of the effect of electropolishing on hydrogen uptake by metals under high pressure conditions.

The electrochemical methods themselves were studied and evaluated as part of this study. The electrochemical method is a powerful means for determining hydrogen concentrations in metals where the hydrogen concentrations are small. It was determined that hydrogen concentrations, measured using the Cottrell equation, are high when dealing with electrolytically charged samples because of the fast hydrogen. It is implicit in the Cottrell equation that all hydrogen elimination is controlled by diffusion, a condition not satisfied by the electrolytically charged samples, where the rate of elimination is much faster than could be accounted for by the diffusion process. In the case of samples charged at high pressure, the Cottrell equation holds quite well, since the hydrogen is contained interstitially, and elimination is controlled by diffusion. The Zakroczymski method provides an accurate and reliable means for determining hydrogen concentrations on an absolute basis for samples charged at high pressure and for electrolytically charged samples, allowing the percent contribution of interstitial hydrogen and surface hydrogen to be obtained.
(M. D. Danford/EH24/205-453-5872)

Cure Studies of High Molecular Weight Silphenylene-Siloxane (SPS) Polymers

The need to develop high temperature elastomers that will perform in extreme thermo-oxidative environments is widely recognized. Long-term thermal, hydrolytic, and oxidative stability as well as retention of mechanical properties are sought for these materials. A logical starting point for this development is the silicone polymers with their inherent thermal/oxidative stability. Substantial research in the laboratory has been directed toward a class of aryl-modified siloxane polymers designated as silphenylene-siloxane.

The initial goal of development of polymerization methodology for SPS polymers with molecular weights approaching 10^6 was met. The multistage polymerization methodology involving preparation/isolation of a silanol-terminated prepolymer and subsequent chain extension with additional aminosilane monomer proved to be an effective route to the formation of ultrahigh molecular weight polymer. Scale-up to 100-gram quantities with retention of high $\bar{M}_w$ was demonstrated.

The SPS polymers were structurally modified to incorporate vinyl groups, and the resulting gum stock was successfully cured to a thermoset elastomer via peroxide vulcanization. Tensile properties of the cured SPS polymer appear at least as good as the comparably formulated commercial dimethylsilicone polymer with a considerable increase in thermal stability over the commercial product. (N. H. Hundley/EH33/205-453-1231)

Cure Monitoring Methodology for Advanced Composite Materials

Two methods of dielectric cure monitoring have been investigated which have potential application to shuttle solid rocket motor nozzle and filament wound case processing: parallel plate electrodes (Audrey) and microchip monoprobe (Micromet). While evidencing potential viability for low conductivity epoxy resin monitoring, the Audrey system with current electrodes appears to be incompatible with phenolic composite materials. Further work is necessary to determine whether these incompatibilities are inherent Audrey limitations or electrode-induced limitations.

The Micromet system II appears to be a viable means for cure monitoring of both epoxies and phenolic materials. While initial cure monitoring data for phenolic composite materials display reproducible events, further work is necessary to determine data significance. Further promise is added to the mic probe monitoring technique by corroboration with dynamic mechanical analysis data. It must be noted that, as yet, no data exist to indicate the applicability of the Micromet system to feedback control.

Finally, an additional conductivity-related term has been indicated f. the dielectric permittivity, ε'. This unreported term becomes important when boundary layer effects and subsequent electrode shielding are noted. Initial investigations indicate that this term should be diffusion controlled. (M. L. Semmel/EH33/205-453-1229)

Mechanics of Granular Materials at Low Intergranular Stresses

A Phase A/B study, recently completed by MSFC's Program Development Office, established that the performance of this microgravity experiment in the Orbiter middeck is feasible and resulted in the preliminary design of a flight apparatus. This experiment which has been proposed by the University of Colorado, Boulder (Stein Sture) and MSFC is sponsored by the Physics and Chemistry Experiments in Space (PACE) program. The purpose of the experiment is to determine the stress-deformation characteristics and failure modes of dry, granular materials at very low intergranular stresses. Such information cannot be obtained on Earth because of gravity-induced stress gradients and the inability of test specimens to sustain their own weight. The experimental results are expected to provide a better scientific understanding of the extent to which the following factors control the bulk frictional resistance to deformation of dry granular materials at very low confining pressures: dilatancy (coupling of shear stresses with volumetric changes), particle interlocking, gravity-induced stress inhomogeneity, kinematic aspects of stress paths (stress history), gravity-induced material inhomogeneity and anisotropy in laboratory test specimens, and local and global stability conditions. A Conceptual Design Review (CDR) of the experiment by scientific and engineering peer groups is scheduled during the fall of 1984. (N. C. Costes/ED42/205-453-0946)

Thin Film Research

Concepts and techniques proposed in 1975 for a Long-Duration Exposure Facility (LDEF) experiment and hardware developed for the Induced Environment Contamination Monitor (IECM) were combined with new hardware to investigate the fundamental processes occurring when orbiting surfaces interact with ambient atomic oxygen. Various thin film coating and measurement techniques acquired for earlier R&T programs (Gravity Probe-B, superconducting instrumentation, IECM, and LDEF) were effectively utilized to investigate the accommodation, reaction, and recombination of atomic oxygen on orbiting surfaces.

The formation of volatile and degrading oxides of certain metals and other materials leading to destructive effects on films and materials was reported which has influenced the design, fabrication, and experimental procedures involved with hardware already flown and much of the subsequent hardware.

The lack of full accommodation on a representative surface has been shown. The fact that only a relatively small fraction of the atoms reacts with most surfaces has been determined, and very accurate etch rates have been measured. Most atoms interacting with a representative carbon surface were reflected as active oxygen (probably atoms), suggesting recombination scarcely occurs. Unexpected activation energies associated with the etching of certain surfaces were discovered and measured.

Surprising topological structures produced by etching have been observed, but not yet satisfactorily explained.

An absence of effects of solar radiation and ions on the etching of carbon was measured, and the large effect of very small quantities of certain contaminants on etch rate and other effects was discovered. The protective nature of the contaminants indicates that very thin coatings can be developed to protect future hardware.

These atomic oxygen studies were a collaborative effort involving the Marshall Space Flight Center, the University of Alabama-Huntsville, and the University of Alabama (Tuscaloosa) directly, and Johnson Space Center and numerous other groups indirectly. (P. N. Peters/ES63/205-453-5134)

Publications:

Peters, P. N., R. C. Linton, and E. R. Miller, "Results of Apparent Atomic Oxygen Reactions on Ag, C, and Os Exposed During the Shuttle STS-4 Orbits," Geophys. Res. Lett., 10, 569 (1983).

Peters, P. N., J. C. Gregory, and J. Swann, "An Investigation of the Accommodation, Reaction, and Recombination of Atomic Oxygen on an Orbiting Carbon Surface," Journal of Chemical Physics, in preparation.

PROCESSES

Weld Modeling

Heat applied to a metal surface by an electrical beam or a welding arc liquifies the metal out to the melting isotherm of the temperature distribution produced by the power source.

MSFC has assembled and made frequent use of a minicomputer weld heat flow model. The model computes the melting isotherm of a combined moving point and line heat source. Matching the model isotherm to the crown and root widths of a real weld permits an estimation of model power input to the welding device and provides a means of estimating process efficiency. Given the correct power parameters, the model computes the power needed to produce a given weld, the temperature/time histories of various sites in the vicinity of the weld, and weld puddle cross sections.

It is observed that identical power applied to identical metal does not necessarily produce identical melting isotherms; i.e., weld puddle shapes. It is now understood that fluid currents in the weld puddle have an important effect on the weld puddle shape. Important fluid flows are driven by magnetic pumping, which depends on electrical current, and by variation of surface tension with temperature.

Quadrupoles (as well as dipoles representing the effect of the latent heat of phase transitions at the melt zone interface) have been added to the MSFC minicomputer weld model. Use of the quadrupole representation permits the analysis of weld phenomena which have either been previously ignored or which have only been dealt with in a qualitative manner. It is anticipated that this analytical tool will lead to new discoveries and will advance the understanding of the control of welding processes.

Weld model software incorporating thermal dipoles and quadrupoles is being forwarded to the University of Georgia/NASA Computer Software Management and Information Center.

One use for the weld model, which is contemplated for the immediate future, is to assess the capability for estimating weld penetration from temperature distributions measured on the workpiece surface adjacent to the weld puddle and, if it appears feasible, to determine an algorithm to perform the estimate. (A. C. Nunes/EH42/205-453-0012)

Large Weld Tooling Technology Development

A full-scale assembly tool simulating the Martin Marietta 5019 Major H_2 Tank Weld Fixture has been designed, fabricated, and installed in the structural tower of building 4707. Hardware installed in the tool are barrels 3 and 4 that are surplus External Tank (ET) heavyweight number 7. This installation is utilized to determine the production impact of tooling and assembly improvements for the ET. Additionally, this installation is used to develop welding parameters and process controls for charge over of the 5019 tool from Tungsten Inert Gas (TIG) welding to Variable Polarity Plasma Arc (VPPA) welding. The new welding process and tooling improvements currently under investigation will significantly reduce manpower and

flow time in the 5019 fixture at the New Orleans Michoud Assembly Facility. To date, two innovations in assembly tooling have been developed and are in the process of implementation at the Michoud Shuttle ET Assembly Facility. These are greatly simplified internal and external clamping tools that offer greater ease in jigging for welding and improvements in peaking and mismatch for the welded joints. In addition, a true track system for separating welded joints has been developed that has application for production. Work continues on weld process parameter development/ refinement and on other tooling developments for the ET. Figures 62 through 64 show various installations of the ET barrel assembly prior to initial welding. (J. H. Ehl/EH44/205-453-1520)
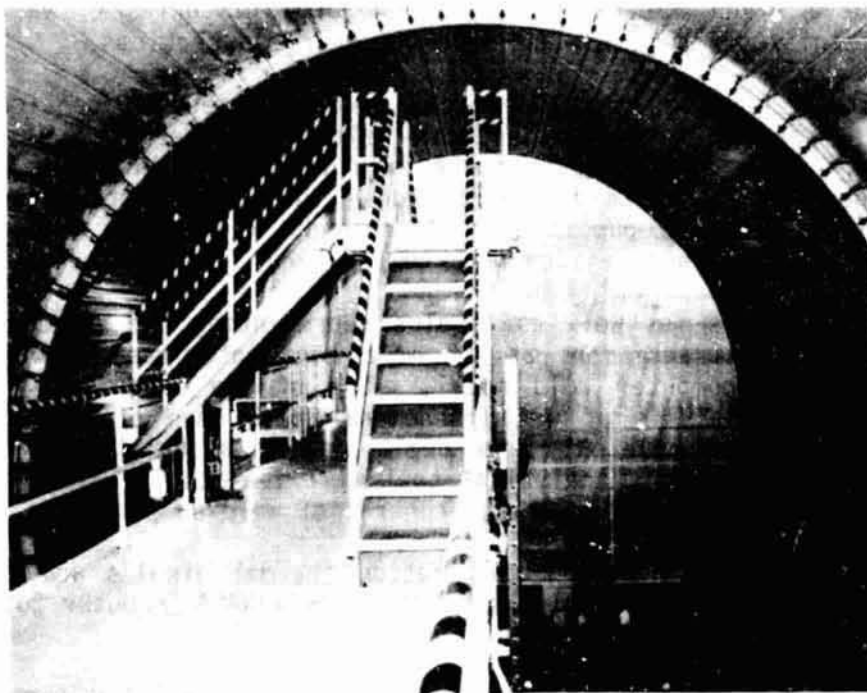

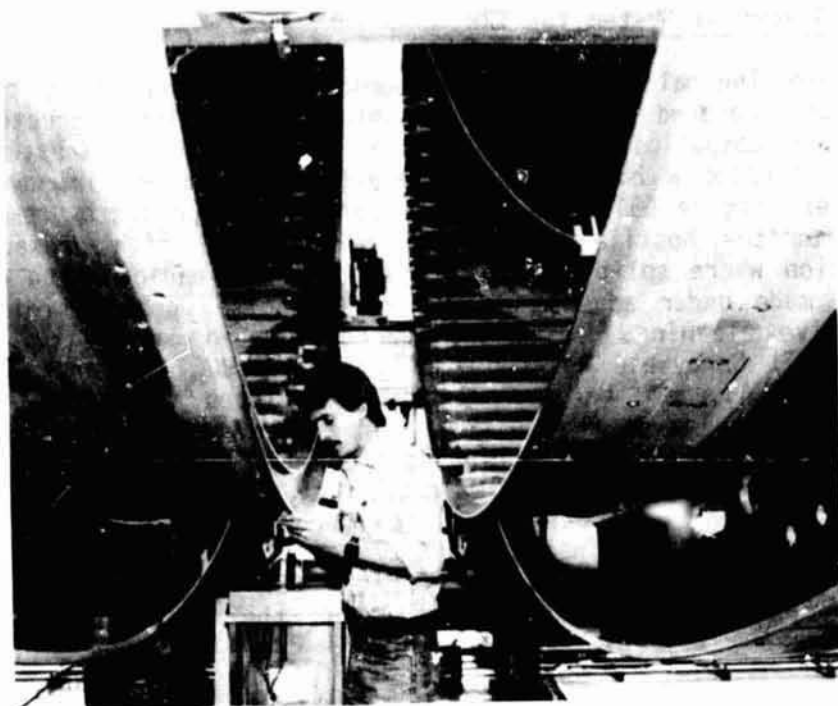Figure 62. Internal View of ET Barrel Assembly with Weld Attachment Clamps Installed.

114

Figure 63. Pre-Installation Inspection of ET Barrel Assembly Tooling Aids.

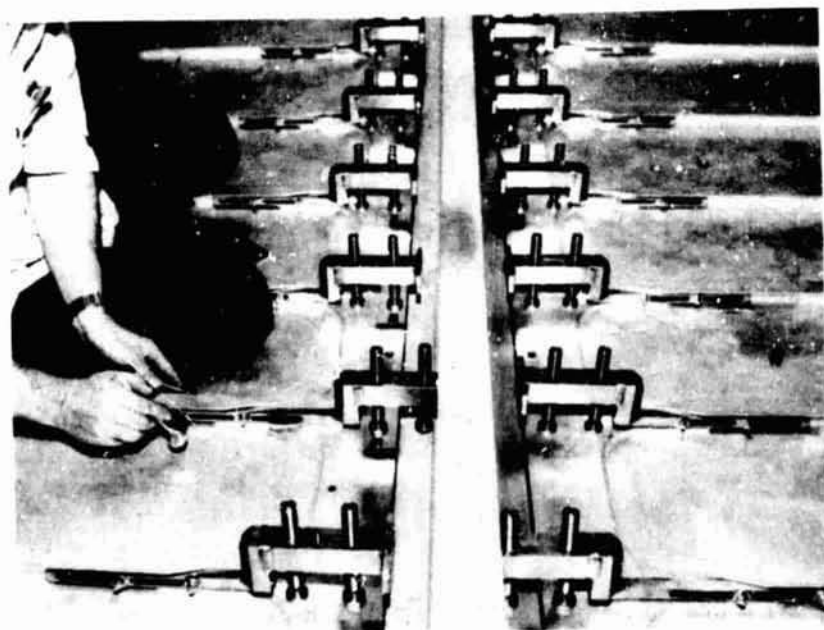Figure 64. Installation of ET Barrel Assembly Weld Alignment Clamps.

Automated TPS Removal System for SRB

To remove Thermal Protection Systems (TPS's) and other protective coatings from recovered Solid Rocket Booster (SRB) flight structures at a turnaround time compatible with anticipated shuttle launch rates, it became necessary to develop a high-speed computerized system and improved stripping processes (Figure 65). Operational safety is improved by removing the personnel from the hostile environment of a manual high pressure water blast operation where split-second decisions in the manipulation of a hand gun must be made under adverse conditions of noise, poor visibility, and wet restrictive clothing. With this new automated capability, the TPS, whether Marshall Sprayable Ablator (MSA), cork, K5NA, or Marshall Trowelable Ablator (MTA), may be preferentially stripped to the white Bostik epoxy paint. This leaves the substrate in a condition most desirable for refurbishment with TPS. After stripping the TPS, if there is paint damage, the white paint may be stripped. Walnut hulls are injected into the water blast stream to remove the paint from the hardware to bare metal with the automated robotic system. This capability has already been demonstrated on test panels, the SRB Structural Test Article (STA) forward skirt (TPS and paint), the SRB STA aft skirt (paint), and the flight SRB nose cones (paint) (Figure 66).
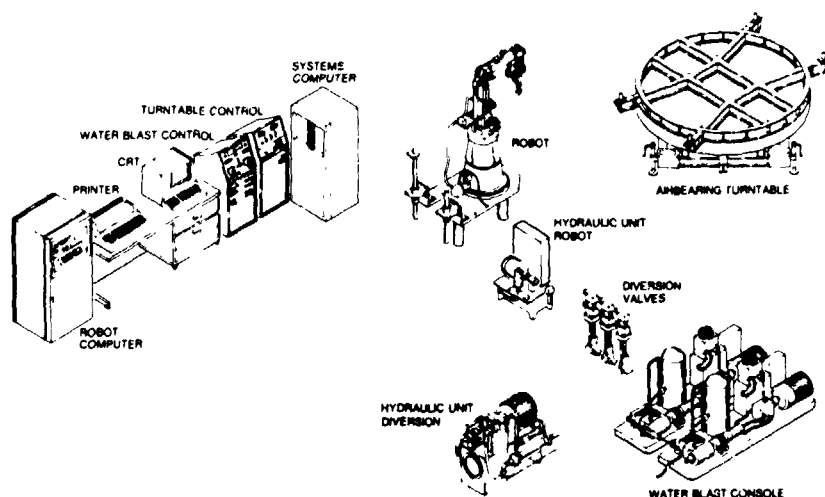

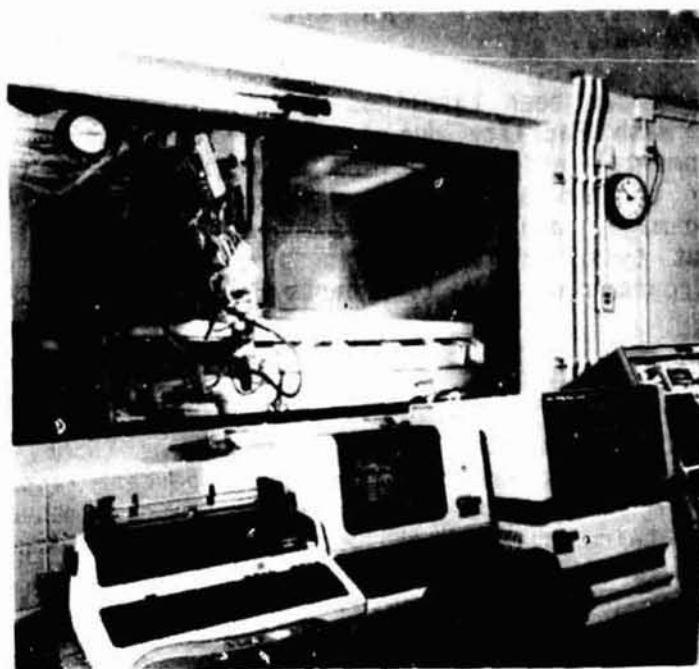Figure 65. SRB Automated TPS Removal System.

Figure 66. SSME Robotic Welding Work Cell.

A master computer integrates and controls the equipment which consists of a high pressure pump forcing water at supersonic speeds through a robot-manipulated nozzle to blast TPS from SRB hardware positioned by an air bearing turntable. The high pressure water blast pumping system consists of two 200 hp electric motors driving two 5-plunger, positive displacement pumps through hydraulic drives which are infinitely variable between 50 and 400 r/min. The robot used to manipulate the blast nozzle over the SRB hardware is a computerized, six-axis, 25 hp waterproofed industrial robot able to withstand the 225 pounds of reaction force and still maintain an accuracy of 0.050 inch. The turntable provides the seventh axis of rotation for the system and has the ability, under direction from the system computer, to rotate the SRB hardware past the blast nozzle. Air bearings are provided to support the table platen during rotation and also to move the loaded turntable on the floor to accommodate various hardware sizes and to move hardware into and out of the blast area. Retractable wheels are used for over-the-road transport. Powered by two 9 hp electric motors, the turntable platen has an angular positioning accuracy of 0.05 degree under the control of the system computer. The system computer is a PDP 11/23+ with RS232 interface to monitor and control the process parameters such as turntable location, position, and speed; blast water pressure, flow rate, and pump r/min; and robot program uploading and downloading.

This system offers several advantages over the present manual system. These include expeditious hardware flow with increased removal rate and improved operating safety for personnel and hardware; reduced follow-on refurbishment operations by stripping to selected levels and leaving the surface ready for topcoat reapplication; reduced costs ($53,000 for the first vehicle, or $8 million for the total program); and reduced labor costs (serial time work hours: one-tenth the time for automation

117

versus manual; trigger time on equipment: one-thirtieth the time for automation versus manual).

This system has been baselined for installation at KSC in the High Pressure East Wash Facility due to start construction in January 1986. Future developmental efforts include optical scanning for automated reprogramming of touchup and automated assessment of removal effectiveness and coating damage, and off-line computer programming to make program changes without tying up the facility and/or flight hardware for manual manipulative programming. (M. L. Roberts/EH43/205-453-0643)

SSME Robotic Weld System

Fabrication of the Space Shuttle Main Engine (SSME) requires approximately 23,000 inches of welding, of which 60 percent is performed by automatic equipment. The remainder of the welds are made manually, at a cost rate more than twice that of the automated welds. Application of conventional automatic welding equipment to the welds (presently done manually) is not practical since they are relatively inaccessible, impractical to tool for automation, or require compensation for fitup beyond their capability.

The SSME robotic welding system being developed by the Marshall Space Flight Center (MSFC) represents a distinct improvement over conventional welding automation because of the extensive positioning capability of its five-axis torch manipulator as well as the ability to tilt and rotate the part as it is welded. In addition, the robot can be programmed to perform welds on any number of different parts with the program stored on magnetic cassette tapes. The robot controller also programs the operation of all the welding process equipment to a degree of repeatability unattainable by its human counterparts. This system is equipped with a computer interface to a vision-based welding sensor that can compensate for variations in seam alignment and puddle size as the weld is being made. The interface will allow the sensor to offset the welding path and velocity, as well as process parameters, while the weld is being made.

Rocketdyne welding engineers are working closely with MSFC to characterize the critical parameters necessary to develop equipment and processes for SSME hardware. A penetration control sensor being developed by Rocketdyne shows great promise to allow optimal control of the welds.

The robot has been installed in the Process Engineering Division's Producibility Enhancement Center at MSFC, and representative parts are being welded to determine the capabilities and limitations of the robot as they apply to joining SSME parts. The vision-based welding system developed by Ohio State University has been interfaced to the control system of the robot. The vision system has demonstrated its ability to track the weld joint and compensate for varying gaps by modifying the wire feed rate. Development work is continuing to allow tracking on a greater variety of weld joints and control the welding current as a function of weld puddle size. Other work underway includes the downloading of programs for the robot from a computer-aided design/computer-aided manufacturing data base. Figure 67 shows the major components of the robotic weld system.
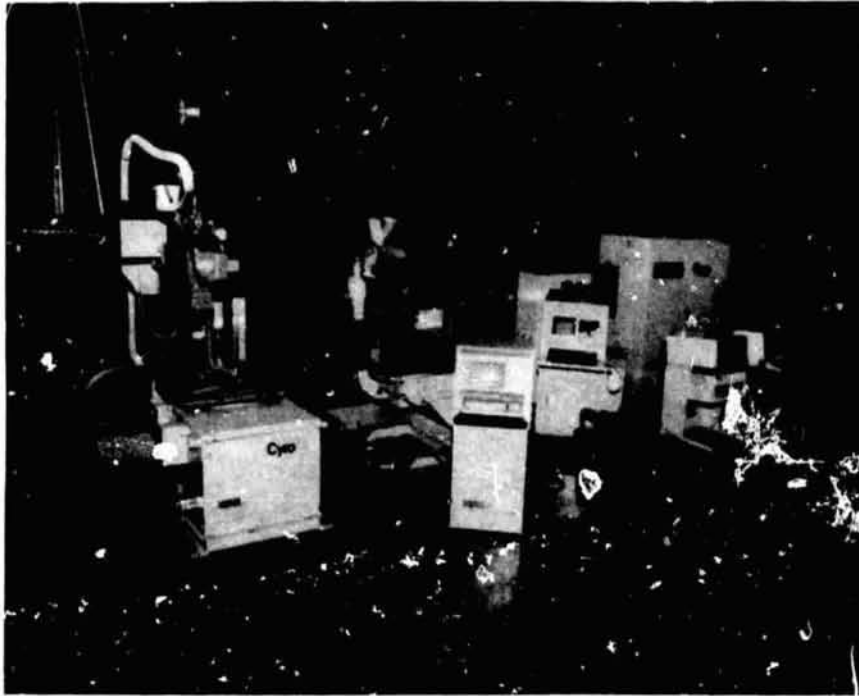(C. S. Jones/EH42/205-453-0012)

Figure 67. SSME Robotic Weld System.

Variable Polarity Plasma Arc (VPPA) Welding on the Space Shuttle External Tank

Two additional major External Tank (ET) weld fixtures were converted to the VPPA welding process during 1984. Excellent quality welds are being obtained from this relatively new aluminum welding process (process development work began at MSFC in 1979) with over 40,000 inches of hardware welded without any internal defects (Figure 68). The entire welding system, controlled by a computer, has proven so reliable that welding schedules developed at MSFC can be transferred to identical welding systems at the Michoud Assembly Facility (MAF) and used on ET hardware with only minor adjustments.

Reduced cleaning requirements, peaking, repairs, eventual reduction in the 100 percent radiographic requirements, and improved weld quality are the benefits gained by implementing the VPPA process on all major welding tools at MAF. Five additional fixtures are being planned for implementation during 1985.

A significantly improved VPPA welding torch, which uses hermetic sealing in lieu of O-rings to separate the cooling water and shielding gas, was conceived by MSFC and fabricated by B&B Machine under contract to MSFC (Figure 69). The new torch is being introduced into ET production at MAF to reduce setup time and eliminate weld interruption associated with the operational breakdown of the present commercial torch. (E. O. Bayless/ EH42/205-453-0011)
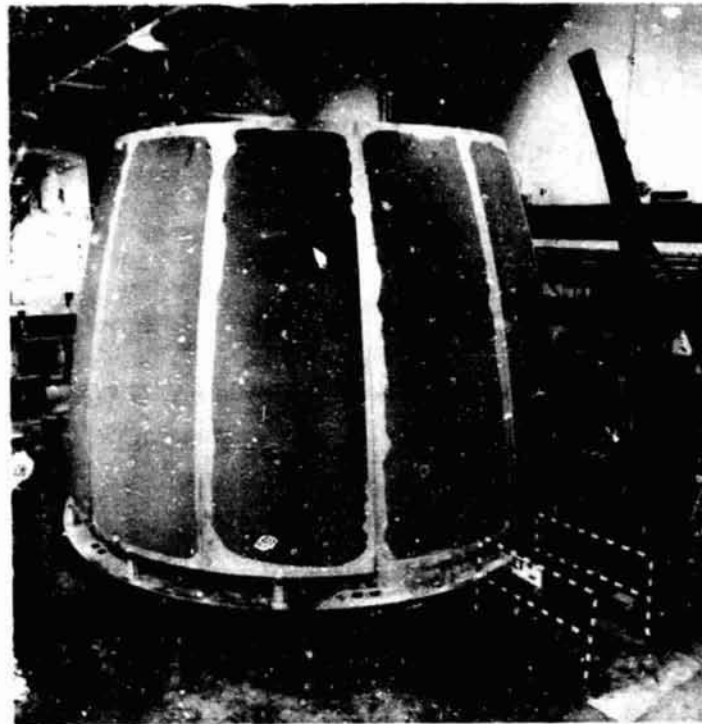
119

Figure 68. Ogive Welded by VPPA Process at Michoud on Fixture 5014.

Figure 69. MSFC Plasma Torch.

120

SPACE POWER

Miniature Cassegrainian Concentrator Solar Array

Development of the miniature Cassegrainian concentrator solar array has been ongoing for several years. Experimental and analytical evaluation has indicated that this solar array concept shows significant promise for reducing both solar array cost and area. The miniaturization of the element allows it to operate in low-Earth orbit at a temperature of about 85 °C utilizing only passive, radiative cooling. The efficiency of the element's GaAs cell at this temperature is near 20 percent. Each element is approximately 50 mm in diameter and uses a GaAs solar cell which is only 4 mm in diameter.

Most of the past effort has been directed at design, fabrication, and testing of the solar cells and individual elements. The emphasis has begun to shift more toward the development of a structure to which the individual elements are attached in order to produce a solar array.

Because of the high concentration ratio of the element, it is sensitive to off-pointing error. Therefore, a high degree of planarity must be maintained by the structure. Graphite epoxy was selected as the structure material. Graphite epoxy panels of the design depicted in Figure 70 had not previously been produced. In FY-84, 25- by 28-inch panels were successfully fabricated and elements installed for testing. (M. R. Carruth/ EB12/205-453-4275)

Publication:

Patterson, R., "A Miniature Cassegrainian Concentrator Solar Array for High Power Space Application," presented 21st Space Congress, Cocoa Beach, Florida, April 1984.
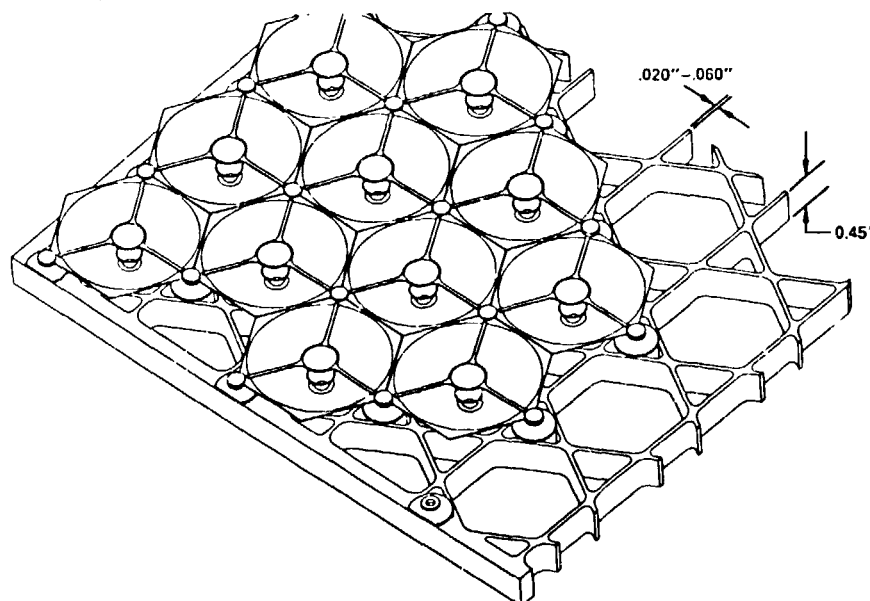

Figure 70. Miniature Cassegrainian Concentrator Solar Array Elements in Graphite Epoxy Panel Structure.

121

Programmable Power Processor (P^3)

The Programmable Power Processor (P^3) has been employed as a power source regulator and power source charger for several years at the Marshall Space Flight and Johnson Space Centers. In FY-84, the versatility of the P^3 was further demonstrated in a significant manner. By simply changing the P^3 software to support a Space Telescope battery test, the P^3 simulated the Space Telescope charge current control, solar array degradation and off-normal operation, constant power load to test battery with resistive load, and the six-battery configuration with only the one battery. Flexibility of the P^3 kept battery test setup time and costs to a minimum. Figure 71 shows a simplified block diagram of the P^3. (J. R. Bush/EB12/ 205-453-4952)

Publication:

Bush, J. R., Jr., "A High Voltage Electrical Power System for Low Earth Orbit Applications," NASA Technical Memorandum TM-86453, Marshall Space Flight Center, Alabama, June 1984.
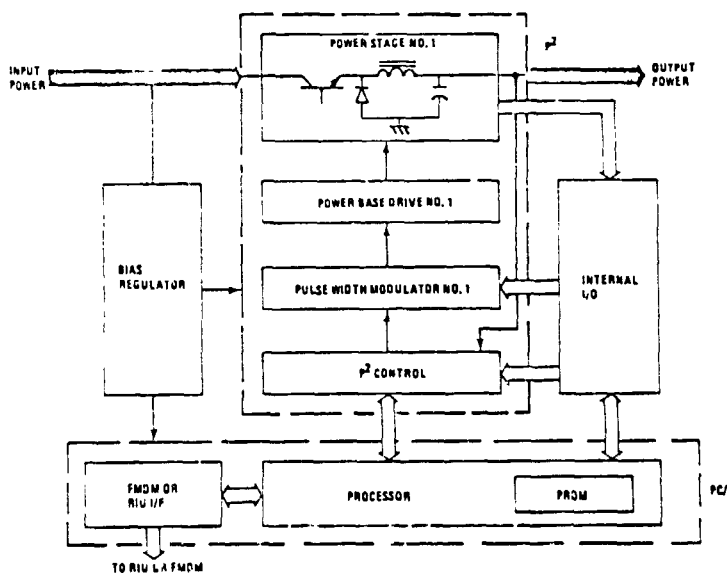

Figure 71. P^3 Simplified Block Diagram.

Battery Protection and Reconditioning Circuit (BPRC)

The BPRC development and testing has been underway for several years at MSFC, culminating in a flight design in FY-84 for the Space Telescope (Figure 72). On the Space Telescope battery test, the BPRC reconditioned the battery in 2 days versus 9 days required by the reconditioning system proposed by the contractor.

Capable of protecting up to 120 cells in one or more batteries, the BPRC protects weak cells from cell reversal during the discharge cycle,

protects low-capacity cells from cell reversal during battery reconditioning, and allows battery discharge to less than 0.5 volt per cell for reconditioning. (L. F. Lollar/EB12/205-453-2510)
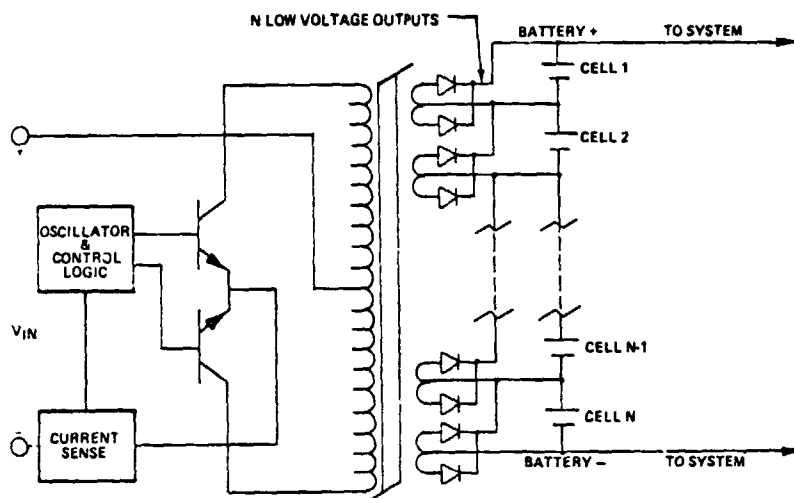

Figure 72. Simplified Battery Protection and Reconditioning Circuit.

Programmable Transformer Coupled Converter (PTCC)

Development of a PTCC has been underway at MSFC for 2 years, resulting in a successful breadboard model in FY-84. This converter is a promising candidate to interface existing 28 Vdc power systems such as the space shuttle with higher voltage distribution systems of future spacecraft. Another application would be to interface high-voltage equipment (120 Vdc) requiring regulated power with direct energy transfer distribution systems whose bus voltage is battery-regulated up to 270 Vdc.

Featuring programmable microprocessor control, the PTCC outputs 5.4 kW with 93 to 94 percent efficiency. Utilizing Cuk magnetics, the PTCC provides source-to-bus isolation and minimum electromagnetic interference emissions at regulator unit and output terminals. Figure 73 gives an illustration of the PTCC concept. (K. E. Kapustka/EB12/205-453-4952)

Publication:

Kapustka, R. E., "A Programmable Transformer Coupled Converter for High Power Space Applications," presented IEEE 15th Power Electronics Specialists Conference, Gaithersburg, Maryland, June 1984.
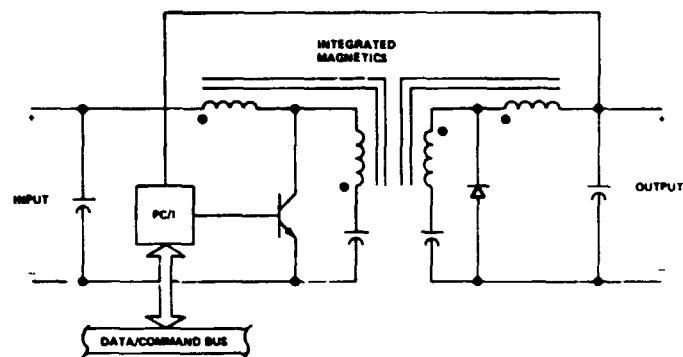
Figure 73.   Illustration of Programmable Transformer
Coupled Converter Concept.

TELEOPERATIONS AND ROBOTICS

The focus of technology investigations in teleoperations and robotics at MSFC is systems-oriented. The investigative approach emphasizes ground-based experimental and simulation techniques, using an appropriate blend of hardware and software techniques. Special test and simulation systems are a key ingredient in this approach, and in FY-84 major enhancements and augmentation of simulation systems were completed. A new simulation system was completed which utilizes a remotely controlled mobility vehicle on an air bearing floor to realistically simulate free-flying teleoperators. A remote manipulation test system was completed which involves the Proto-flight Manipulator Arm (PFMA), a flexibly reconfigurable control station, video system, computational system, and control software.

During FY-84, several significant technology milestones were achieved. The static and dynamic characteristics of a space-capable manipulator arm (the PFMA) were investigated to enable comparison of physical and software simulation of manipulator systems. An analysis of algorithms for control of manipulator arms resulted in the selection of three algorithms for more detailed study in robotic simulations. A concept was developed to permit interchangeable and effector/tools to be used by a space manipulation system, thus greatly increasing flexibility and dexterity. A contracted study (Martin Marietta Aerospace Corporation) to identify teleoperator human factor issues/options and define tests/experiments/analyses required for their resolution was completed.
(W. O. Frost/EB01/205-453-1413)

Publications:

Teah, W., "A Simplified Mathematical Model of the Orbital Maneuvering Vehicle," University of Alabama-Huntsville, Research Report No. 407, August 1984.

Cooper, T. W., D. L. Miller, and A. K. Wildgen, "Teleoperator Human Factors Study," Martin Marietta Aerospace Corporation Report No. MCR 84-511 (issues 1 through 4), Contract NAS8-35184, 1984.

INFORMATION SYSTEMS

Data Base Management System/Mass Memory Assembly (DBMS/MMA)

The need for data base management and archival systems that can accept data at high rates and archive it in large volumes has been apparent for some time. The DBMS/MMA represents elements of new technology that have been integrated into a system that addressed the requirements for handling high data rates, archiving large volumes of data, and making the archived data available to a large network of users in a short period of time.

The system is configured around a passive star coupler fiber optic data bus that has seven data ports (can be expanded to sixteen) to which computer systems can be interfaced. Each port consists of logic to convert electrical signals to light and the light back to electrical for transmission onto and off of the fiber optic bus. The light signal is transmitted on a 50-μ-diameter graded index fiber by an avalanche laser diode at a rate of 100 million bits/sec. Data entering the system through one port are broadcast to all other ports simultaneously. Only the port(s) that have a need for the data will capture it. Five of the ports have computer subsystems interfaced to them. They are: three VAX 11/780's, an SEL 32/2750, and a laser optical disk. One of the VAX 11/780 computers is the user gateway into the system. Through this VAX, a network of users can query the data base directory to see what data are in the archive and request data from the archive. Source data to be archived enter the system through a high-speed port (50 million bits/sec) in a packet format. A directory of the packets is being created at the same time the data are being archived.

The MMA is a laser optical disk which is interfaced to a port on the fiber optic bus. All data entering the DBMS/MMA will be received at one of the ports and transmitted over the fiber optic bus to the MMA to be archived. The MMA uses a 300 mW Argon laser to record the data on a 14-inch tellurium-coated disk. A bit of data recorded on the disk by the laser is a 0.5-μ-diameter pit on the disk surface. A track of data is recorded as a concentric circle at a rate of 100 million bits/sec. Spacing between each bit is 1.25 micron. One disk has a capacity of 0.8×10^{11} bits, and the system has 128 disks on line for a total capacity of 10^{13} bits. The projected archival life of the data is 12-15 years with no degradation in the data quality. The MMA is internally controlled by two 68,000 microprocessors that can drive the MMA to access any data archived in the system in a worse case time of 6.5 sec.

In addition to the new technology involved in the MMA archive and the use of a fiber optic bus for high-speed local data communication, the overall system design itself represents a new approach to high-speed data handling. When packetized data enter the system via one of the fiber optic ports, the data are transmitted on the bus to the MMA and archived without ever having gone through the memory or the data bus structure of any computer. This allows the data to be moved at rates of 50-100 million bits/sec. By the use of fiber optics, the data rates could be increased up to 500 million bits/sec. (D. T. Thomas/EB32/205-453-0677)

PRECEDING PAGE BLANK NOT FILMED

127

DYNAMICS/FLUID MECHANICS

SAFE Dynamic Augmentation Experiment (DAE)

The Solar Array Flight Experiment (SAFE) DAE flew on space shuttle mission 41-D in August 1984. The objectives of the DAE were to provide a qualified mechanism and technique for on-orbit test definitions of Space Station and large space structures dynamic characteristics and to demonstrate the success of the hardware and technique by test definitions of SAFE dynamic characteristics.

The DAE sensor uses laser diodes that illuminate reflective targets and a device that detects the motion of those targets. The targets are made of reflective tape placed on small aluminum tents at 16 locations on the back hinge folds of the blanket. As the blanket flattens out during deployment, these targets stand off the blanket surface to provide a better reflective angle. There are seven additional targets (4 on the mast, 2 on the containment box cover, and 1 on the tip fitting of the mast), for a total of 23. All the targets are proportioned to appear equal in size to the sensor. The motions of these targets are optically sensed by a solid-state device (a field tracker) similar to some new TV cameras.

The laser diodes and the solid-state field tracker sensor are housed in the DAE sensor head. The sensor head is mounted to the mission support structure by means of a special support structure.

An electronics package supporting the experiment is located on top of the support structure and includes a recorder to tape the sensor and some engineering data.

Experiment operations were conducted on the nightside of orbits to reduce background sunlight. Data during flight were taken on all prescribed tests, and several additional tests were completed.

Although data are not available at this time, the housekeeping data on the SAFE/DAE indicate that the hardware system functioned normally. (R. Schock/ED24/205-453-2561)

Fluid Interface and Bubble Experiment (FIBEX)

Equilibrium-free surface behavior of a liquid in a low-gravity environment plays a key role in fuel tank design and fluid management systems. The FIBEX was constructed to investigate this phenomenon in the low-gravity environment on NASA's KC-135 aircraft. Interest in this area was initially motivated by the Gravity Probe-B liquid helium management problem in which the superfluid must be distributed in such a manner that it is gravitationally symmetric about a fixed proof mass. This problem is complicated by the fact that the only forces available to control the liquid are surface tension and centrifugal forces. The dynamic characteristics of the spacecraft are such that these two forces are of the same order of magnitude and compete in distributing the fluid. Equations for the shape of the free surface were derived and solved numerically by computer. These results showed that for low rotation rates compared with the

129

surface tension, the free surface becomes unstable; a closed bubble forms whose position is less predictable. FIBEX has been flown on the KC-135, and experimental results are in qualitative agreement with the theories, but quantitative comparisons await further analysis of the data. (F. W. Leslie/ED42/205-453-2047)

APPLICATIONS

Advanced Firefighting Equipment Applications

Technology derived from investigation of low vapor pressure liquid flow into rocket engine turbopumps has been applied in the development of a high-flow, high-suction-lift 5000 gal/min pump, which is used in a small, light-weight, helicopter portable firefighting module. The module, shown in Figure 74, is self-contained and consists of a pump, gas turbine engine, control system, priming system, and water discharge system. Its normal mode of operation is drafting water from any available body of water through three 8-inch flexible suction hoses and discharging through three 5-inch firehoses. The physical dimensions are 4 feet by 8 feet by 6 feet, and it weighs 2700 pounds. The gas turbine is a free turbine design, which allows the compressor and gasifier turbine to rotate up to ignition speed with little rotation of the power turbine and pump during start sequence. The pump requires 550 horsepower to produce 5000 gal/min at a 150 psi discharge pressure with a 20-foot suction lift. The module will operate at this condition for 3 hours without refueling. Operation is simplified by an electronic controller which provides automatic start and automatic shutdown in the event specific preset operating conditions are violated. A two-stage mixed flow pump, with inducer, was designed specifically for this application. The second stage impeller shaft is driven directly by the gas turbine engine. A small internally mounted planetary gear train, driven by the second stage shaft, then drives the first stage impeller and inducer at reduced speed to enhance suction lift performance by minimizing the net positive suction head required.

The unit (Figure 75) was delivered by NASA to the Navy in the spring of 1984 and is presently being demonstrated in various applications. The unit can be flown by helicopter sling into remote areas for firefighting, dewatering, flood control, emergency pumping, and other applications.

This effort was funded by and initiated at the request of the U.S. Navy Facilities Engineering Command. (R. Burns/EP33/205-453-2711)

Figure 74. Module Block Diagram.

Figure 75. Advanced Firefighting Module.